# *C. elegans* Apoptosis: CED-4 Translocation and Involvement in a Model of Mucolipidosis Type IV Human Lysosomal Storage Disorder

by
Bradley Michael Hersh

A. B.
Kenyon College, 1994

Submitted to the Department of Biology in partial fulfillment of the requirements for the degree of

DOCTOR OF PHILOSOPHY

at the
MASSACHUSETTS INSTITUTE OF TECHNOLOGY

February 2002



Signature of Author: _____
Department of Biology
December 7, 2001

Certified by: _____
H. Robert Horvitz
Professor of Biology
Thesis Supervisor

Accepted by: _____
Alan Grossman
Chairman of the Graduate Committee
Department of Biology

# *C. elegans* Apoptosis: CED-4 Translocation and Involvement in a Model of Mucolipidosis Type IV Human Lysosomal Storage Disorder

Bradley M. Hersh

**ABSTRACT**

The process of programmed cell death is important in the development and homeostasis of multicellular organisms. The conserved morphological events of this process have been termed apoptosis. The molecular mechanisms of apoptosis execution are also conserved. We have investigated the behavior of these shared components during programmed cell death in the nematode *Caenorhabditis elegans*. We have found that the CED-9 protein, an anti-apoptotic member of the Bcl-2 family of apoptotic regulators, is required for the sequestering of the CED-4 cell-death activator to mitochondria. In the absence of CED-9 in *C. elegans* embryos, we found that CED-4 protein translocates to the nuclear membrane. In addition, inducing excess programmed cell death by expression of the EGL-1 cell-death activator triggers the translocation of CED-4 from mitochondria to the nuclear membrane. We performed a genetic screen for mutations that trigger programmed cell death in *ced-9* gain-of-function animals where cell death is blocked. We identified a mutation in *cup-5*, the *C. elegans* homolog of the human mucolipidosis type IV gene, which is mutated in a lysosomal storage disorder. We found that *cup-5* is required for viability and that excess lysosomes accumulate in *cup-5* mutants. In addition, *cup-5* mutants contain excess programmed cell deaths, suggesting that apoptosis may play a role in the pathology of mucolipidosis type IV.

Thesis Supervisor: H. Robert Horvitz
Title: Professor of Biology

## ACKNOWLEDGMENTS

I would like to thank Bob Horvitz for fostering a lab environment that teaches not only how to effectively perform science, but also how to effectively communicate that science to others. I would like to thank my thesis committee members over the years—Hermann Steller, Richard Hynes, Paul Garrity, Chris Kaiser, Terry Orr-Weaver, and Gary Ruvkun—for their suggestions, insights, and interest in this work.

Many members of the Horvitz lab have made my stay here more productive and more enjoyable. Sander van den Heuvel taught me the basics and endured all my early questions. Na An and Beth Castor always treated me like family. I will not soon forget Ho-Yon Hwang's Petri plate cityscapes, sporting goods store, or his tireless efforts to teach me patience. Jeff Thomas, Mark Metzstein, Gillian Stanfield, Zheng Zhou, Barbara Conradt, Ewa Davison, Craig Ceol, Peter Reddien, and Eric Miska provided friendship, insights, and interesting conversations.

Giving me reasons to spend time outside of lab doing interesting things were my classmates—Chris Armstrong, Josh Gamse, Anna Lau, Doug Menke, Brad Smith, Charles Tilford, and Garth Wiens—and those non-scientists who provided balance—Rob Rogers, Jason Creux, Stephanie Hartman, Amanda Mason, and Carice Pingenot.

Finally, I thank my family for their support and encouragement.

TABLE OF CONTENTS

# Chapter 1

# Introduction
# Programmed Cell Death, Mitochondria, and Lysosomes

## INTRODUCTION TO PROGRAMMED CELL DEATH

The fate of all organisms is eventually to die, but within many metazoans a subset of cells contribute to the development of the organism through their own fated deaths. This process of programmed cell death is a carefully regulated, genetically controlled form of cellular suicide employed by multicellular organisms to eliminate cells in a variety of developmental and pathological contexts. Proper regulation of programmed cell death is essential for normal development (Jacobson et al., 1997), and misregulation of this process can disrupt the delicate balance of cell numbers maintained by the interplay of cell death and cell proliferation (Evan and Vousden, 2001; Raff, 1992).

During development, programmed cell death can be used to sculpt the shape of tissues and organs (Jacobson et al., 1997). A developing organism often produces cells in excess, only to eliminate unwanted cells in order to reach the final functional product. For instance, during vertebrate development, the cells that comprise the interdigital webbing may survive (as in ducks) or may be eliminated by programmed cell death to generate well-separated digits (as in chickens). In addition, cavitation, the process by which the hollow embryonic cavity is formed within the initially solid blastula, occurs by programmed cell death (Coucouvanis and Martin, 1995).

Programmed cell death is also used to regulate cell numbers in the developing nervous system. At least half of the cells originally generated in the nervous system are eliminated by programmed cell death (Burek and Oppenheim, 1999), and connections in the developing nervous system may be refined by competition of neurons for limited target-derived neurotrophic survival factors (Raff et al., 1993). This competition may serve to optimize synaptic connections and remove excess neurons that have failed to find suitable targets.

The immune system also contains numerous examples of programmed cell death (Cohen et al., 1992; Krammer, 2000). Only a fraction of B and T cells successfully rearrange their antigen receptor genes to produce full-length, functional receptors. Cells without productively rearranged receptors are useless in immune responses and are removed from the pool of immune cells, likely because they do not receive required survival signals. Cells with high-affinity receptors for self proteins are eliminated by programmed cell death during the process of negative selection to prevent autoimmune responses. In addition, following the clonal expansion of an immune response and

subsequent elimination of the immunological challenge, most lymphocytes are eliminated, leaving only a small pool of memory cells.

Given this diversity of developmental and homeostatic processes in which programmed cell death acts, it is not surprising that misregulation of programmed cell death can lead to a variety of pathological consequences (Thompson, 1995). Mutations that disrupt programmed cell death in the immune system of mice and humans lead to lymphoproliferative autoimmune disorders (Krammer, 2000) with symptoms similar to systemic lupus erythematosus. Suppression of programmed cell death can also lead to the survival and proliferation of tumor cells (Evan and Vousden, 2001), and is a primary cause of follicular lymphoma. In the opposite direction, too much cell death is associated with retinal degeneration (Davidson and Steller, 1998; Portera-Cailliau et al., 1994) and neurodegenerative diseases such as Alzheimer's disease, Huntington's disease, and amyotrophic lateral sclerosis (Nijhawan et al., 2000). Ischemic injuries, such as heart attack or stroke, also result in increased levels of programmed cell death.

**Morphological features of programmed cell death**

The most widely recognized form of programmed cell death is apoptosis. Apoptosis was defined almost 30 years ago (Kerr et al., 1972), and refers to a common set of morphological features displayed by dying cells (Wyllie et al., 1980). It is also partly defined in contrast to the unregulated, accidental, injury-induced cell death referred to as necrosis. Necrotic dying cells and the organelles within them swell in size and burst, releasing cellular contents and potentially provoking an inflammatory response. Apoptotic cells, by contrast, maintain intact organelles, shrink in cytoplasmic and nuclear volume, undergo chromatin condensation, and break apart into smaller, membrane-bound vesicles. Apoptotic cells are eventually recognized and engulfed by phagocytic cells, where final digestion of the dying cells' contents is accomplished.

One of the major biochemical events of the apoptotic process is degradation of the genomic DNA. Endonucleases cleave the DNA in the linker region between nucleosomes, generating a nucleosomal ladder of ~180 base pair fragments that can be visualized on an agarose gel (Wyllie, 1980). In addition, apoptotic cells can be detected *in situ* by labeling of 3'-hydroxyl groups on the ends of cleaved DNA fragments (Gavrieli et al., 1992), a technique also referred to as TUNEL (TdT-mediated dUTP nick-end labeling).

Though programmed cell death and apoptosis have come to be used synonymously, it is apparent that some physiological cell deaths do not display the classical morphological features of apoptosis (Kitanaka and Kuchino, 1999; Zakeri et al., 1995). In these type 2 physiological cell deaths, nuclear condensation is rare and DNA fragmentation occurs late in the process, the cytoplasm fills with large vacuoles, likely autophagic in nature, and engulfment of cellular fragments is slow. These differences in morphology may represent differences in the underlying molecular mechanisms or may reflect variations in the manner or magnitude by which common molecular mechanisms are employed. The extent to which molecular mechanisms overlap and which specific molecular characteristics are displayed by a dying cell are important factors in assessing how cell death impacts disease.

**Programmed cell death in *Caenorhabditis elegans***

Of the 1090 cells generated during somatic development of the *C. elegans* hermaphrodite, 131 undergo programmed cell death (Sulston and Horvitz, 1977; Sulston et al., 1983). These cell deaths occur at the same position in the lineage in essentially all animals, indicating that the deaths are specified as part of the developmental program of the animal. Some of these deaths are sex-specific (e.g., the death of the male-specific CEM neurons in hermaphrodites and the hermaphrodite-specific HSN neurons in males), but the functional role of many of these deaths is unclear, and mutants that have extra cells due to a defect in programmed cell death appear grossly normal in phenotype. In addition, it is estimated that over half of the cells in the hermaphrodite germline die by programmed cell death (Gumienny et al., 1999). These deaths are not specified by lineage, and environmental insults, including DNA-damaging agents (Gartner et al., 2000) and bacterial infection (Aballay and Ausubel, 2001), can trigger an increase in germline cell deaths. Thus, *C. elegans* provides a powerful system for studying both developmentally-regulated and externally-induced programmed cell death. Importantly, the programmed cell deaths in *C. elegans* display many of the characteristics associated with mammalian apoptosis. Dying cells in *C. elegans* undergo ultrastructural changes similar to mammalian cells as determined by electron microscopy (Robertson and Thomson, 1982). DNA condensation and degradation also occur (Hedgecock et al., 1983), though nucleosomal laddering has not been specifically observed. *C. elegans* does not have professional

phagocytes, so instead engulfment is performed by neighboring cells, including hypodermal cells and germ line sheath cells (Zhou et al., 2001).

Cells undergoing programmed cell death in *C. elegans* are easily visualized by differential interference contrast (DIC, Nomarski) microscopy as refractile, button-like cells in living animals. The combination of lineal specification and simple visualization of cell death has allowed the isolation of numerous mutants with altered programmed cell death. Mutations in at least eighteen genes, affecting various aspects of programmed cell death, have been identified (Metzstein et al., 1998). Such mutations can affect the life and death decision of a few specific cells or the execution of all programmed cell deaths in the animal. Other genes are required for proper timing of cell death, proper cell corpse morphology, engulfment of cell corpses, and degradation of corpse DNA. Most of the genes identified in the worm have counterparts that act in programmed cell death in other systems. Thus, these studies in *C. elegans* have proven instrumental in the identification of genes acting at multiple steps in the cell death pathway, from developmental specification, to execution of the death program, to engulfment of dying cells, to degradation of cellular contents. Additional genes, as yet unidentified, are likely to act in many of these steps, and *C. elegans* will continue to be important in the identification of these components of the cell death pathway.

**Neurodegenerative cell death in *C. elegans***

In addition to programmed cell deaths occurring during development or in the germline, aberrant cell death of neurons has also been characterized in *C. elegans* mutants. Dominant gain-of-function mutations in the genes *mec-4* (mechanosensory abnormal) or *deg-1* (degeneration) induce the degeneration of neurons involved in the detection of touch by the animal (Chalfie and Wolinsky, 1990; Royal and Driscoll, 1999). Morphologically, the cell deaths induced by these mutations are distinct from developmental cell deaths. Degenerating cells swell to several times their normal size (Chalfie and Wolinsky, 1990) and sometimes lyse, characteristics similar to morphological changes observed in mammalian necrotic cell death. Furthermore, abnormal cells contain tightly wrapped whorls of membrane that are internalized and coalesce into large electron-dense membranous structures (Hall et al., 1997).

Neurodegeneration induced by *mec-4(d)* and *deg-1(d)* is independent of the pathway for programmed cell death, as blocking programmed cell death by mutation

does not suppress the neurodegenerative phenotype (Chalfie and Wolinsky, 1990; Driscoll and Chalfie, 1991). However, proper removal of the necrotic cell corpses does require the activity of the same set of genes required for removal of developmental programmed cell deaths (Chung et al., 2000), indicating that both necrotic and apoptotic cell corpses may be eliminated through a common engulfment pathway. This result suggests that the characterization of necrosis as a process that necessarily culminates in cell lysis may not be entirely accurate.

The *mec-4* and *deg-1* genes both encode ions channels of the DEG/ENaC (degenerin/epithelial $Na^+$ channel) family (Mano and Driscoll, 1999). Members of this family have two hydrophobic transmembrane domains, one of which forms an amphipathic α-helix that lines the channel pore. The gain-of-function mutations in *mec-4* and *deg-1* both affect conserved alanine residues adjacent to this transmembrane domain, and it is postulated that substitution of larger amino acids in this position causes the channel to remain open inappropriately (Driscoll and Chalfie, 1991). Thus, neurodegenerative death is initiated by increased ion influx in a process that may be comparable to mammalian excitotoxic cell death of hyperstimulated neurons (Choi, 1992). Mutations that eliminate channel function can suppress degenerative death of the touch neurons (Chalfie and Wolinsky, 1990), confirming that cell death results from too much, rather than too little, channel activity.

Specifically, movement of $Ca^{2+}$ ions appears to be critical for neurodegenerative death. Mutations in calreticulin (*crt-1*), reduction of calnexin (*cnx-1*) activity, chelation of $Ca^{2+}$ by EGTA, or mutation of the ER $Ca^{2+}$ channels InsP3R (*itr-1*) or RyR (*unc-68*) are all capable of suppressing the degenerative death induced by *mec-4(d)* (Xu et al., 2001).

As inappropriate cell death is associated with neurodegenerative disorders (Nijhawan et al., 2000), it is important to determine whether these deaths are apoptotic or necrotic in nature, to what extent these two pathways for cell death overlap mechanistically, and how suppressors of one pathway may affect the other.

## REGULATION OF PROGRAMMED CELL DEATH EXECUTION

The initiation and execution of programmed cell death must be carefully regulated to prevent inappropriate activation that would destroy a healthy cell. In mammalian cells, multiple pathways interact with one another in a complex fashion to integrate cell death signals and either forestall or initiate the biochemical and

morphological events of programmed cell death. The execution of programmed cell death in *C. elegans* employs many of the same molecular mechanisms, but in a simpler form. This simple pathway first identified in the worm by genetic means led to the description and characterization of the more complex mammalian pathway.

**Cell death execution in *C. elegans***

The core pathway for programmed cell death execution in *C. elegans* consists of the four genes, *ced-3*, *ced-4*, *ced-9*, and *egl-1*. Loss-of-function mutations in *ced-3*, *ced-4*, and *egl-1* block programmed cell death in the worm, indicating that these genes are required for cell-killing activities (Conradt and Horvitz, 1998; Ellis and Horvitz, 1986). The gene *ced-9* acts in an opposite fashion, to prevent programmed cell death (Hengartner et al., 1992). A gain-of-function mutation in *ced-9* blocks programmed cell death (Hengartner and Horvitz, 1994a), whereas loss-of-function mutations in *ced-9* result in maternal-effect lethality due to excess ectopic programmed cell death in the embryo (Hengartner et al., 1992). The activities of *ced-4* and *ced-3* are required for this ectopic cell death, and mutations in *ced-3* and *ced-4* can suppress the lethality of *ced-9*(lf), indicating that these genes act downstream of *ced-9*. By contrast, loss of *egl-1* activity does not suppress *ced-9*(lf) lethality, indicating that *egl-1* acts genetically upstream of *ced-9* (Conradt and Horvitz, 1998). Further ordering of the genetic pathway by overexpression studies indicates that *ced-4* acts upstream of *ced-3* (Shaham and Horvitz, 1996). The ordered genetic pathway for programmed cell death execution in *C. elegans* starts with the cell-death activator *egl-1*, which inhibits *ced-9*. *ced-9*, in turn, negatively regulates *ced-4*, which activates *ced-3*. Thus, transcriptional activation of *egl-1* (Conradt and Horvitz, 1999) acts to relieve *ced-9* inhibition of *ced-4*, thereby unleashing *ced-3* activity to effect programmed cell death.

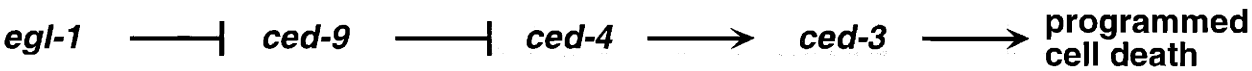


**Figure 1. The core genetic pathway for programmed cell death in *C. elegans***

Not surprisingly, the regulation of programmed cell death is not quite so simple, and a number of other genes appear to assist the core cell death pathway in completing its executory role. For instance, the engulfment genes, long thought to act only to remove the remains of already dead cells, also aid in the killing process, as mutations in engulfment genes enhance the cell death defect caused by weak loss-of-function

mutations in *ced-3*, *ced-4*, and *egl-1* (Hoeppner et al., 2001; Reddien et al., 2001). In addition, the *cps-6* gene, encoding a mitochondrial endonuclease, is important for cell killing, as it too can weakly enhance the cell death defect caused by weak *ced-3* mutations, and DNA degradation (Parrish et al., 2001). That downstream events, such as engulfment and DNA degradation, contribute in small measures to the life or death fate of a cell is consistent with the notion that cell death, like other cell fates, proceeds by the expansion of a few key effector activities into the actions of a multitude of target genes.

**Molecular characterization of core cell death pathway components**

***Caspases***

The position of the *ced-3* gene as the furthest genetically downstream gene required for all programmed cell deaths in *C. elegans* suggested a role as a key effector molecule in the cell death pathway. Cloning of the *ced-3* gene confirmed this role and indicated for the first time some of the molecular mechanisms behind specific biochemical events in programmed cell death (Yuan et al., 1993). CED-3 protein is one of the founding members of the family of caspases, cysteine proteases with aspartate specificity (Cryns and Yuan, 1998), and has a biochemically demonstrable protease activity (Xue et al., 1996).

Caspase-1, the first mammalian member of the family, was identified as the enzyme that proteolytically processes pro-interleukin-1β into its active form (Cerretti et al., 1992; Thornberry et al., 1992), and the similarity of CED-3 to this molecule was the first evidence for specific proteases involved in programmed cell death execution. Protease activity is critical for programmed cell death, as blocking caspase activity with peptide inhibitors (e.g., zVAD-fmk) or viral competitive inhibitors (e.g., p35, CrmA, IAPs) can block cell death (reviewed in Thornberry and Lazebnik, 1988). To date, the family of mammalian caspases has grown to fourteen members (Ahmad et al., 1998; Thornberry and Lazebnik, 1998). In addition, seven caspases have been identified in *Drosophila* (Kumar and Doumanis, 2000), including *dcp-1*, a gene required for larval viability and oocyte development (McCall and Steller, 1998; Song et al., 1997).

Caspases are synthesized as inactive zymogens, and these procaspases are processed by proteolytic cleavage into a small subunit (15 kD for CED-3), a large subunit (17 kD for CED-3), and an enzymatically nonessential N-terminal prodomain

(24 kD for CED-3). The cleavage sites for activation occur at specific aspartate residues, indicating that procaspases are themselves substrates for caspase cleavage. It is unclear whether all caspases have the capacity for autoproteolysis or whether they require activation by other caspases. Once cleaved, the enzymatically active form of caspases consists of a tetramer of two small subunits and two large subunits (Rotonda et al., 1996; Walker et al., 1994).

Beyond *ced-3*, the *C. elegans* genome contains genes for three additional caspases, *csp-1*, *csp-2*, and *csp-3* (Shaham, 1998). These genes produce multiple alternatively spliced transcripts, and at least one of the six protein products of these transcripts is capable of cleaving caspase substrates *in vitro*. CED-3 and CSP-1B proteases appear to differ in substrate specificity, and CSP-1B and CSP-2B have shorter prodomains than CED-3. These differences in substrate specificity and prodomain length may reflect differences in function *in vivo*, but roles for *csp-1*, *csp-2*, or *csp-3* in programmed cell death have not yet been demonstrated, either singly or in a redundant fashion with *ced-3* or each other.

Differences in substrate specificity and in the length of the N-terminal prodomain also characterize different categories within the mammalian caspases (Figure 2). Caspases are divided into three subgroups on the basis of prodomain length, substrate specificity, and functional role (Wang and Lenardo, 2000). Caspase-1 and caspase-11 do not play essential roles in programmed cell death, but instead act in processing of inflammatory cytokines. Mice in which caspase-1 has been eliminated lack mature interleukin-1β, but do not have significant defects in apoptosis (Kuida et al., 1995; Li et al., 1995). Caspase-$11^{-/-}$ mice are similar in phenotype to caspase-$1^{-/-}$ mice and have defects in activation of caspase-1 (Wang et al., 1998). The remaining caspases that have roles in programmed cell death can be divided into those with long prodomains and those with short prodomains. Caspases-2, -8, -9, –10, and -12 (as well as CED-3) have long prodomains, and caspases-3, -6, and –7 have short prodomains. Generally, caspases with long prodomains act as initiators of cell death, acting upstream to transduce cell death signals to the downstream short prodomain effector caspases via proteolytic cleavage and activation. Furthermore, the substrate specificity of many initiator caspases corresponds to known cleavage sequences in effector caspases (Thornberry et al., 1997), providing strong evidence for a proteolytic caspase cascade.

Caspase-3-deficient mice die shortly after birth, show profoundly abnormal brain development, and have reduced apoptosis in the central nervous system (Kuida et al., 1996). Loss of caspase-9 results in a similar, though more severe, neurological phenotype, suggesting that caspase-3 and other caspases act downstream of caspase-9 during brain development (Hakem et al., 1998; Kuida et al., 1998). Caspase-8-deficient mice die as embryos with defective heart muscle and hematopoietic cell development (Varfolomeev et al., 1998), and caspase-$8^{-/-}$ fibroblasts are resistant to tumor necrosis factor and Fas-induced apoptosis. That caspase deficiency can separately affect nervous system and hematopoietic development suggests that the proliferation of mammalian caspases may represent functional divergence of caspases and restriction of their activity to specific tissue types or the response to specific apoptotic stimuli.

Caspases with short prodomains, such as caspase-3, are considered to be the executors and effectors of programmed cell death, responsible for the biochemical events that result in morphological apoptosis (Thornberry and Lazebnik, 1998). More than 60 proteins have been demonstrated to be caspase substrates (Stroh and Schulze-Osthoff, 1998), but in few cases has caspase cleavage been directly linked to morphological changes associated with cell death. Two exceptions to this are the nuclear proteins lamin and ICAD. Lamins are intermediate filament proteins that form the major structural component of the nuclear lamina underlying the inner nuclear membrane, and function in part to organize chromatin (Gruenbaum et al., 2000). Lamin cleavage by caspases causes chromatin condensation (Lazebnik et al., 1995). Mutant lamin with an altered cleavage site is resistant to caspase cleavage *in vitro* and *in vivo*, causes a delay in the onset of apoptosis, and prevents normal chromatin condensation during programmed cell death (Rao et al., 1996). In the second case, the caspase-activated deoxyribonuclease (CAD) can degrade DNA during apoptosis to generate nucleosomal laddering, but its activation requires cleavage of its inhibitor, ICAD, by caspase-3 (Enari et al., 1998; Sakahira et al., 1998).

The long prodomains of caspases act as protein interaction modules, facilitating the oligomerization of caspases and their interaction with other cell death signaling molecules. One such interaction domain is the death effector domain (DED), present in caspase-8 and caspase-10. The DED of these caspases is able to interact with the DED in FADD/MORT1 (Fas-associated death domain), an adaptor protein recruited to ligand-bound receptors of the Fas/tumor necrosis factor (TNF) receptor family (Boldin et al.,

1995; Chinnaiyan et al., 1995; Chinnaiyan et al., 1996). Ligand binding of a death signal (e.g., Fas) leads to clustering of Fas/TNFR receptors, binding of the FADD adaptor molecule, the recruitment of procaspase-8 to this multiprotein complex (Boldin et al., 1996; Muzio et al., 1996), known as the death-inducing signaling complex (DISC), and finally activation of caspase-8 by proteolytic cleavage. Artificially induced oligomerization of procaspase-8 results in proteolytic autoactivation and execution of apoptosis (Martin et al., 1998; Muzio et al., 1998), suggesting a proximity-induced model for the activation of this initiator caspase.

The second type of interaction module found in caspase prodomains is the caspase recruitment domain (CARD). The important initiator caspase-9 contains this domain, and it mediates the interaction between procaspase-9 and Apaf-1 (apoptotic protease-activating factor 1) (Li et al., 1997; Zhou et al., 1999)--an interaction critical for the activation of cell death in response to a multitude of cell death signals, including UV-irradiation and staurosporine treatment.

*Apaf-1*

The cell death activator Apaf-1 was originally isolated biochemically from a cell-free extract capable of activating caspase-3 in the presence of dATP and cytochrome c (Liu et al., 1996; Zou et al., 1997). As intriguing as its biochemical activity, the molecular identity of Apaf-1 was at least as compelling—for here, finally, was the long-sought after mammalian counterpart to CED-4 (Yuan and Horvitz, 1992; Zou et al., 1997), the CED-3 caspase activator from *C. elegans*. Apaf-1 contains a CARD domain, followed by a 320 amino acid stretch of similarity to CED-4, including Walker A and B motifs involved in nucleotide binding. The C-terminal of Apaf-1 contains 12 WD-40 repeats that are not present in CED-4.

Unlike FADD, which serves as an adaptor to oligomerize and activate procaspase-8, Apaf-1 appears to contribute to caspase-9 activity in a more integral fashion. Upon cytochrome c binding and hydrolysis of either ATP or dATP, Apaf-1 oligomerizes (Saleh et al., 1999), and recruits procaspase-9 into the multimeric complex (Zou et al., 1999). The WD-40 repeats of Apaf-1 appear to inhibit oligomerization, as truncated Apaf-1 lacking this region can spontaneously oligomerize and activate procaspase-9 in the absence of cytochrome c and dATP (Srinivasula et al., 1998). Since CED-4 does not contain WD-40 repeats, its regulation of CED-3 activity may be

independent of cytochrome c, and this aspect of cell death regulation may differ between mammals and *C. elegans*. However, induced oligomerization of CED-4 is also capable of activating CED-3, so this basic mechanism of CED-4/Apaf-1 does seem to be conserved (Yang et al., 1995). Unlike in the case of FADD oligomerization, where active caspase-8 is released from the DISC complex, the multimeric Apaf-1/caspase-9 complex appears not to dissociate and acts as a very large (~700 kD) functional unit called the apoptosome (Cain et al., 2000; Cain et al., 1999; Rodriguez and Lazebnik, 1999). Processed caspase-9 released from the apoptosome is active, but much less so than caspase-9 retained in the complex (Rodriguez and Lazebnik, 1999). In addition, uncleaved procaspase-9 possesses measurable proteolytic activity, but only in the presence of cytochrome c, dATP, and cytosolic extract (Stennicke et al., 1999). These results suggest that caspase-9 is regulated by an allosteric interaction within the apoptosome, and not only autoactivation by proteolytic cleavage.

***The Bcl-2 family***

Both of the remaining genes in the *C. elegans* execution pathway, *ced-9* and *egl-1*, encode members of the Bcl-2 family of cell death regulators. CED-9 protein acts as an inhibitor of programmed cell death, and EGL-1 activates programmed cell death. Likewise, the mammalian members of the Bcl-2 family fall into classes of apoptotic activators and inhibitors. The *bcl-2* gene was originally identified at the t(14;18) chromosome translocation breakpoint in human B-cell lymphomas (Bakhshi et al., 1985; Cleary and Sklar, 1985; Tsujimoto et al., 1984), and was demonstrated to act as an oncogene by inappropriately promoting cell survival (Vaux et al., 1988), rather than directly affecting cell proliferation. The Bcl-2 family itself, however, has proliferated greatly since then, and consists of more than 20 members in mammals, worms, flies, and viruses (Chen and Abrams, 2000; Gross et al., 1999a).

Family members possess up to four short conserved Bcl-2 homology domains (BH1 to BH4) that form alpha-helical segments (Adams and Cory, 1998; Kelekar and Thompson, 1998). Anti-apoptotic members, including Bcl-2 itself, usually contain all four BH domains, while the pro-apoptotic members divide into two groups. Members of the Bax-like group possess the BH1, BH2, and BH3 domains, but lack the BH4 domain. The second group of pro-apoptotic molecules is highly variable, and members (such as Bad and Bid) share similarity only in the short BH3 domain (Huang and

Strasser, 2000). Anti-apoptotic CED-9 is most similar to the Bcl-2 anti-apoptotic class (Hengartner and Horvitz, 1994b), whereas EGL-1 is a member of the pro-apoptotic "BH3-only" class (Conradt and Horvitz, 1998).

The alpha-helical BH domains mediate protein-protein interactions between members of the Bcl-2 family, and association of the BH3 domain with a hydrophobic pocket formed by the BH1, BH2, and BH3 domains permits interaction between members of all three groups (Sattler et al., 1997). One simple model for the regulation of apoptosis by Bcl-2 family members postulates that homodimerization and heterodimerization between pro-apoptotic and anti-apoptotic molecules modulates the activity of these molecules, and that the relative levels of pro- and anti-apoptotic molecules will determine the apoptotic status of the cell. Consistent with this model, expression of pro-apoptotic Bcl-2 family members Bax and Noxa (a BH3-only protein) is induced by p53 (Miyashita and Reed, 1995; Oda et al., 2000), and an apoptotic stimulus of X-ray irradiation induces Noxa in a p53-dependent manner. However, a *bcl-2* transgene is capable of blocking apoptosis either in the presence or absence of *bax*, and *bax* can promote apoptosis in the absence of *bcl-2* (Knudson and Korsmeyer, 1997), suggesting that each can regulate apoptosis independently of one another. This independence may represent the activity of other competing family members, though such interactions were not detected in thymocytes from *bax*$^{-/-}$ mice (Knudson and Korsmeyer, 1997), or activities that are not affected by heterodimerization. Cells from *Bax bak* doubly-deficient mice are resistant to multiple apoptotic stimuli, and these genes are required for BH3 domain-only molecules to induce apoptosis (Cheng et al., 2001; Wei et al., 2001). Further, it has been proposed that the primary function of protective Bcl-2 and Bcl-$x_L$ is to sequester BH3-only molecules to prevent them from activating Bax or Bak (Cheng et al., 2001).

Ultimately, however, either the anti-apoptotic or the pro-apoptotic Bcl-2 family members must possess some intrinsic regulatory or biochemical activity for the other members to amplify or inhibit by heterodimerization. One possible such activity is that of an ion channel. The solution structure of Bcl-$x_L$ displays similarities to the pore-forming subunit of diphtheria toxin (Muchmore et al., 1996), and anti-apoptotic Bcl-$x_L$ and Bcl-2 and pro-apoptotic Bax can all form pH-sensitive, voltage-gated ion channels (Antonsson et al., 1997; Minn et al., 1997; Schendel et al., 1997; Schlesinger et al., 1997). Bcl-2 and Bcl-$x_L$ are cation selective whereas Bax is anion selective, but ion selectivity for

all three is fairly weak, and it is not apparent that these minor differences in ion selectivity could account for functional differences in apoptotic regulation.

**A molecular framework for cell death regulation**

On the basis of genetic studies in the worm and *in vitro* analyses of interactions between the worm proteins and their vertebrate counterparts, a relatively simple model for regulation of programmed cell death emerges. The Bcl-2-like CED-9 molecule physically interacts with Apaf-1-like CED-4 (Chinnaiyan et al., 1997; Spector et al., 1997; Wu et al., 1997), and CED-4 can physically interact with the CED-3 caspase (Chinnaiyan et al., 1997). The BH3 protein and cell death activator EGL-1 interacts with CED-9, and can displace CED-4 from CED-9 (Conradt and Horvitz, 1998; del Peso et al., 1998). Thus, CED-9 protects against cell death by sequestering CED-4 and preventing its activation of the CED-3 caspase, and EGL-1 activates cell death by triggering the release of CED-4 from CED-9 (Figure 3). This model has obtained *in vivo* support from the observation that CED-4 and CED-9 co-localize to mitochondria in *C. elegans* and that EGL-1 can disrupt this co-localization (Chen et al., 2000 and Chapter 2).

Aspects of this simple framework seem to hold true for mammalian cell death, as well. For instance, Apaf-1 is capable of binding to caspase-9, as well as caspase-1 and caspase-8 (Chinnaiyan et al., 1997; Li et al., 1997), indicating that the caspase-activating role of CED-4 and Apaf-1 appears to be similar. However, Apaf-1 interaction with Bcl-2 family members is more controversial. Whereas two groups demonstrated interactions between Bcl-$x_L$ and Apaf-1 in cell extracts (Hu et al., 1998; Pan et al., 1998), other studies have failed to detect the interaction of any Bcl-2 family member with Apaf-1 (Conus et al., 2000; Moriishi et al., 1999). In addition, the subcellular localization of Apaf-1 appears to be distinct from that of Bcl-2 or Bcl-$x_L$, limited to the cytosol and not the mitochondria (Hausmann et al., 2000). Therefore, current models of Bcl-2 family member function have focused on mitochondria. And though it is possible that other mammalian CED-4-like molecules that do regulate cell death by interaction with Bcl-2 family members remain to be discovered, or that CED-9 in the worm has additional functions beyond CED-4 sequestration, we will now consider mitochondrial models for programmed cell death.

**Mitochondria: where mechanisms meet**

The subcellular localization of Bcl-2 family members, together with various biochemical investigations of apoptosis, strongly implicate mitochondria as the site at which cell death stimuli and regulatory pathways interact with one another to generate an outcome of survival or death. Bcl-2 protein is localized to intracellular membranes, including the nuclear envelope, the endoplasmic reticulum, and the outer mitochondrial membrane (Akao et al., 1994; Hockenbery et al., 1990; Krajewski et al., 1993; Monaghan et al., 1992). A fraction enriched in mitochondria can stimulate apoptotic events in Xenopus egg extracts (Newmeyer et al., 1994), and cytochrome c, a key component in the activation of Apaf-1 (Liu et al., 1996; Zou et al., 1997), is a resident of the mitochondrial matrix. Furthermore, mitochondria undergo a number of major changes preceding and during apoptosis, including a major transition in ion permeability, and additional apoptotic molecules besides cytochrome c are released from mitochondria. The transformation of the mitochondria, the energy source of the cell, into its engine of destruction was unexpected and yet appropriate. It also appears that mitochondrial dysfunction and caspase activation, two major events in programmed cell death, regulate and are regulated by each other in an intertwined fashion, making it difficult to determine which is the irrevocable event that ultimately dooms a cell to death.

***Regulation of cytochrome c release by Bcl-2 family members***

The discovery that cytochrome c, an integral component of the mitochondrial oxidative phosphorylation pathway, was also a critical molecule for the activation of caspase-3 (Liu et al., 1996) provided an unexpected link between the cell's basic metabolic pathways and programmed cell death. Cytochrome c deficiency results in embryonic lethality, likely due to the defect in mitochodrial respiration (Li et al., 2000). However, cells derived from these embryos are resistant to serum starvation, staurosporine, and UV-induced cell death, but are still susceptible to TNFα (Li et al., 2000). This result indicates that caspase-3 dependent death involves cytochrome c, but cell death downstream of caspase-8 activation does not necessarily require cytochrome c. Cytochrome c is encoded in the nuclear genome, and apocytochrome c is transported across the outer mitochondrial membrane, where it gains a heme group to form the mature holocytochrome c molecule. Only holo-cytochrome c can trigger programmed

cell death and caspase activation (Yang et al., 1997), yet to do so, this mitochondrial matrix molecule must be released to the cytosol.

Two general models for the release of cytochrome c are possible. First, cytochrome c may be transported across the outer mitochondrial membrane by the specific action of a channel molecule or be released in a non-specific fashion following the opening of large mitochondrial pore complexes. Alternatively, major changes in mitochondrial permeability associated with programmed cell death may trigger rupturing of the outer mitochondrial membrane, allowing cytochrome c to leak out into the cytoplasm.

Bcl-2 family members can regulate cytochrome c release, and given their similarity to pore-forming diphtheria toxin, they are candidates to act as the cytochrome c channel themselves. Bcl-2 overexpression is capable of blocking cytochrome c release (Kluck et al., 1997; Yang et al., 1997), while Bax can trigger cytochrome c release from isolated mitochondria (Jurgensmeier et al., 1998). Indeed, Bax can support the release of cytochrome c in an artificial liposome system, and four Bax molecules are estimated to form a pore of approximately 22 Å, sufficient to pass the estimated 17 Å cytochrome c molecule (Saito et al., 2000).

Bax is normally localized in the cytosol, but translocates to the mitochondria upon receipt of death-inducing stimuli (Hsu et al., 1997; Wolter et al., 1997). Induced dimerization of Bax can also lead to its translocation to mitochondria, and triggers loss of mitochondrial membrane potential ($\Delta\Psi_m$) and apoptosis (Gross et al., 1998), but not cytochrome c release. Unlike in the pure liposome system, Bax release of cytochrome c in cells appears to involve the additional activity of the BH-3 only protein BID. BID induces a conformational change in Bax and Bak (a Bax-like Bcl-2 family member), allowing these molecules to oligomerize, insert into mitochondrial membranes, and trigger the release of cytochrome c (Desagher et al., 1999; Eskes et al., 2000; Wei et al., 2000). BID is unable to induce cytochrome c release in cells derived from *Bax Bak* doubly deficient mice, indicating that it acts through these Bcl-2 family members (Wei et al., 2001). The truncated form of BID (tBID) is the active molecule that induces cytochrome c release (Gross et al., 1999b), and tBID is derived from cytosolic p22 BID by caspase-8 cleavage (Li et al., 1998). Caspase-8 activation is dependent on Fas/TNFR signaling, but is independent of cytochrome c release, whereas caspase-3 activation depends on cytochrome c. The cleavage of tBID by caspase-8 therefore links Fas-

activated cell death to a pathway for mitochondrial amplification of caspase activation. *Bid*-deficient mice have defects in Fas-induced death in hepatocytes and reduced caspase activity in thymocytes (Yin et al., 1999), indicating that BID-mediated mitochondrial amplification is necessary for programmed cell death in specific cell types.

***The permeability transition pore and mitochondrial homeostasis***

The Bcl-2 family members need not act as the cytochrome c channel themselves, but could also regulate the activity of other mitochondrial channel molecules or the permeability of lipid membranes. For instance, both pro-apoptotic and anti-apoptotic members of the Bcl-2 family are able to bind the voltage-dependent anion channel (VDAC) and regulate its channel activity (Shimizu et al., 1999). However, the pore size of VDAC is too small for the release of cytochrome c, so either the binding of pro-apoptotic Bax or Bak induces a conformational change that increases pore size, or opening of the VDAC pore causes cytochrome c release indirectly.

This indirect mechanism of release may be related to the activity of the permeability transition (PT) pore. The PT pore is a mitochondrial megachannel of large conductance that when open creates a channel from the mitochondrial matrix to the cytoplasm through which molecules ≤1.5 kD may pass. The exact composition of the PT pore is unknown, but it is a complex of at least VDAC, the adenine nucleotide transporter (ANT), and cyclophilin D, and is localized to contact points between the inner and outer mitochondrial membranes (Crompton, 1999). PT pore opening can be triggered by $Ca^{2+}$ overload, low concentrations of adenine nucleotides, low $\Delta\Psi_m$, and Bax expression(Crompton, 1999; Marzo et al., 1998), and results in the equilibration of ions between the cytoplasm and mitochondrial matrix and complete dissipation of membrane potential. Because the matrix has a high solute concentration, PT pore opening also causes mitochondrial swelling, which can cause a physical disruption of the outer membrane. Alternatively, disruption of nucleotide transport has also been suggested to cause mitochondrial swelling and membrane rupture in the absence of PT pore opening (Vander Heiden et al., 1997). In either case, rupture of the outer mitochondrial membrane may be sufficient for the escape of cytochrome c.

Several observations suggest that PT opening may not be the cause, but rather the consequence of cytochrome c release. First, cytochrome c release can occur prior to

or in the absence of loss of $\Delta\Psi_m$ (Bossy-Wetzel et al., 1998; Kluck et al., 1997). Second, Bax and Bid can induce co-release of cytochrome c and other intermembrane molecules without inducing mitochondrial swelling (Finucane et al., 1999; Kluck et al., 1999; von Ahsen et al., 2000). Finally, caspase inhibition can block $\Delta\Psi_m$ disruption but not cytochrome c release (Bossy-Wetzel et al., 1998; Eskes et al., 1998), strongly arguing that loss of mitochondrial membrane potential and PT pore opening can not be causative in the release of cytochrome c. It has been proposed that the PT pore may flicker between closed and open states, producing transient swelling and cytochrome c release, without causing complete loss of $\Delta\Psi_m$ (Green and Kroemer, 1998), but such flickering has not been observed in apoptotic cells or cell-free systems.

*Smac/DIABLO*

Further confounding the primacy of caspases or mitochondria in the regulation of programmed cell death is another caspase regulator released from the mitochondria. This protein, alternatively known as Smac (second mitochondria-derived activator of caspases) (Du et al., 2000) or DIABLO (direct IAP-binding protein with low pI) (Verhagen et al., 2000), is released from mitochondria by an unknown mechanism, and activates caspase by counteracting the effects of a caspase inhibitor. The IAP (inhibitor of apoptosis) family has mammalian, viral, fly, and worm members, and several of these act as competitive inhibitors of caspases (Goyal, 2001). Smac/DIABLO sequesters IAP proteins, thereby relieving this potential inhibition of caspases. Since Smac/DIABLO release appears to require mitochondrial dysfunction, and mitochondrial dysfunction requires caspase activation, and full caspase activation requires Smac/DIABLO release, this system acts as a feedback loop to regulate the activation of cell death. When mitochondrial dysfunction is serious enough to allow Smac/DIABLO release the full death program can be activated, whereas the IAPs may restrain caspases in the event of minor insults to the cell.

*Protein translocation during programmed cell death*

As we have already seen for Bax, Bid, and cytochrome c, movement either to or from the mitochondria is an important event during the regulation of programmed cell

death. Such movements are not limited to these components, and numerous regulators and executors of cell death undergo changes in localization (Porter, 1999).

Yet another mitochondrial molecule released during apoptotic cell death is AIF, an apoptosis-inducing factor capable of triggering chromatin condensation and apoptotic morphology in isolated nuclei (Susin et al., 1999b). AIF is similar to bacterial oxidoreductases, and translocates to the nucleus upon release from mitochondria (Daugas et al., 2000). Nuclear translocation is independent of caspases and is not blocked by the caspase inhibitor zVAD-fmk. AIF-deficient mouse embryonic stem cells are resistant to growth factor deprivation and embryoid bodies derived from these cells fail to undergo cavitation (Joza et al., 2001). However, AIF is dispensible for cell death in response to staurosporine and ultraviolet irradiation. Its mechanism of action, what other molecules may mediate its effects, and its fundamental role in apoptotic cell death are still not well understood.

Caspases also undergo protein translocation during apoptosis. Pro-caspases-2, -3, and –9 are all found in the mitochondria, and translocate to the cytosol (all three) and nucleus (caspase-2 and caspase-3) during cell death (Mancini et al., 1998; Susin et al., 1999a; Zhivotovsky et al., 1999). Pro-caspase-7 translocates in the opposite direction, from the cytosol to the mitochondria (Chandler et al., 1998). Such differences in localization during cell death may reflect another level of regulation—caspases with similar specificities may cleave different substrates during apoptosis because distinct localizations may provide access to distinct sets of substrates. Caspase-3 localization to the nucleus, for instance, is likely to be critical for nuclear apoptotic events, as cleavage of ICAD in the nucleus is required for DNA fragmentation (Sakahira et al., 1998).

## LYSOSOMES IN PROGRAMMED CELL DEATH AND DISEASE

Lysosomes are acidified cytoplasmic organelles involved in the disposal of cellular contents. They contain numerous hydrolytic enzymes and are important for both the degradation of phagocytosed material and for autophagy (digestion of obsolete cellular organelles such as mitochondria or secretory vesicles). One mode of programmed cell death displaying non-apoptotic morphology is characterized by large vacuoles in the cytoplasm, and these vacuoles may represent lysosomal degradation of cellular material (Zakeri et al., 1995). In Chapter 3, we describe a screen for mutants with increased programmed cell death that identified a *C. elegans* counterpart to the

gene mutated in human mucolipidosis type IV, a disease in which lysosomes inappropriately store excess material. Therefore, we will explore the function and biogenesis of lysosomes, the disease consequences of lysosomal dysfunction, and a possible role for programmed cell death in such diseases.

**Lysosome function and biogenesis**

Lysosomes contain approximately 40 kinds of degradative enzymes, including glycosidases, lipases, phosphatases, sulfatases, and the cathepsin family of proteases (Lloyd and Mason, 1996). All of these enzymes require an acidic environment for optimal activity, and the lysosome maintains a pH of approximately 5. This acidic optimum protects cells from the dire consequences of accidental release of lysosomal hydrolases, as these enzymes will be non-functional in the slightly basic cytosol of most cells.

Lysosomes are generally considered the terminal compartment of the endocytic pathway, but are no longer thought of simply as the "trash can" of the cell, where a cell's refuse awaits disposal. Monomeric constituents of the macromolecules broken down by lysosomal enzymes are recycled for future use by the cell. Material is delivered to and transported away from lysosomes in a complex process of fusions and fissions with late endosomal compartments (Luzio et al., 2000; Storrie and Desjardins, 1996). Despite such complexity in the late steps, the general pathway of endocytosed material is a progression from early endosomes to late endosomes to lysosomes. The early endosome is a major sorting compartment in the endocytic pathway, and is where many ligands dissociate from their receptors, allowing the receptors to be recycled to the cell surface (Luzio et al., 2001). Early endosomes are tubular in shape, and are often localized near the plasma membrane. Late endosomes are more spherical and are positioned more closely to the nucleus. Lysosomes are variable in size, have electron-dense cores, and are enriched in acid phosphatases and acid-dependent hydrolases. Endosomes, by contrast, are not electron-dense, lack acid phosphatases, and contain mannose-6-phosphate receptors not present in lysosomes (Luzio et al., 2001).

Content mixing between late endosomes and lysosomes clearly indicates dynamic interactions between these two stages in the endocytic pathway. Three possible mechanisms have been proposed for these interactions. First, vesicular traffic between these compartments could be responsible for the transfer of contents from one

to another. Lack of evidence for vesicular transport suggests that one of two models for direct lysosome-endosome fusion is more likely to be correct. The "kiss and run" model suggests repeated transient fusions and fissions between late endosomes and lysosomes (Storrie and Desjardins, 1996). Diffusion of small soluble markers between compartments appears to be more rapid than for large molecules, consistent with transient fusion events. The third model, in some ways an extension of "kiss and run," proposes the direct and complete fusion of endosomes and lysosomes, followed by re-formation of lysosomes from the hybrid organelle (Luzio et al., 2000).

Hybrid organelles can be generated *in vitro* in a cell-free system, as an organelle with a density intermediate between late endosomes and lysosomes, and containing both the lysosomal protease cathepsin L and the endosomal mannose-6-phosphate receptor (Mullock et al., 1998). *In vivo* organelles with hybrid characteristics can be isolated from rat liver. Fusion *in vitro* requires ATP, NSF (N-ethylmaleimide sensitive factor), and SNAPs (soluble NSF attachment proteins), and is inhibitable by Rab-GDI (GDP dissociation inhibitor) (Mullock et al., 1998). These characteristics are consistent with regulation of lysosome-endosome fusion by SNARE (SNAP receptor) proteins, much like other fusion events in the secretory and endocytic pathways, but the specific SNAREs acting in lysosme-late endosome fusion have not been identified. Fusion between late endosomes and lysosomes *in vitro* is inhibited by the calcium chelator BAPTA, and this $Ca^{2+}$ requirement appears to involve calmodulin (Pryor et al., 2000). $Ca^{2+}$ is also required post-docking in yeast vacuole fusion (Peters and Mayer, 1998), and may be a common requirement for fusion events in the endocytic pathway.

**Lysosome dysfunction and human disease**

Because the major function of lysosomes is the degradation of biological macromolecules, the major defect when lysosome function is disrupted is the inappropriate accumulation of material. Over 40 human lysosomal storage diseases are known (Winchester et al., 2000). Most of these diseases are the result of a deficiency in a catabolic pathway involved in the degradation of particular macromolecules. The defective proteins may be hydrolases or activating cofactors. However, other diseases appear to be the result of inappropriate trafficking along the endocytic pathway (Chen et al., 1998; Liscum, 2000), rather than hydrolytic defects.

Lysosomal storage diseases cause the accumulation of several different classes of macromolecules, and are classified on the basis of the catabolic pathway affected. At least ten deficiencies affect degradation of mucopolysaccharides, five affect glycoprotein degradation, and eight disrupt sphingolipid degradation (Gieselmann, 1995). In addition, because lysosomal hydrolases often target terminal residues, rather than specific compounds, gangliosides and glycoproteins with identical terminal residues may in some cases both accumulate when a single enzyme is defective. Lysosomal storage disorders affecting either nucleic acid or protein degradation have not been described, suggesting primarily non-lysosomal routes or redundant lysosomal enzymes for the degradation of these macromolecules.

Degradation of glycosphingolipids (GSLs), major components of the plasma membrane, is commonly disrupted in lysosomal storage dieases. GSLs consist of a hydrophobic ceramide moeity linked to a wide range of hydophilic extracellular oligosaccharide chains. In the lysosome, sugar residues are cleaved sequentially to generate ceramide, which is then deacylated to sphingosine. Sphingosine can be further degraded or re-enter the biosynthetic pathway to generate new GSL molecules. Because degradation occurs in a stepwise fashion, loss of activity in any of 10 hydrolases or their associated activator proteins results in the accumulation of the corresponding lipid substrate in the lysosome.

***Tay-Sachs and Sandhoff disease***

The β-hexosaminidase enzyme is responsible for the removal of terminal β-D-N-acetylglucosamine or β-D-N-acetylgalactosamine moeities from glycolipids, glycoproteins, and glycosaminoglycans. Defects in three genes reduce hexosaminidase activity, causing the accumulation of GM2 gangliosides and leading to three clinically similar diseases. Mutations in the hexosaminidase α subunit cause Tay-Sachs disease; in the β subunit, Sandhoff disease; and in the GM2 activator, AB variant GM2 gangliosidosis (Mahuran, 1999). The GM2 activator protein is required as an enzyme co-factor to solubilize the lipid substrate molecule and allow cleavage by β-hexosaminidase.

Classical Tay-Sachs disease is an autosomal recessive disorder most prevalent in the Ashkenazi Jewish population. It is characterized by rapid, progressive neurological

degeneration leading to a vegetative state and death before the fourth year of life. Milder variants of the disease can have an adult onset and cause ataxia and muscle weakness. These milder variants are generally associated with missense mutations that lead to enzymes with residual activity, whereas the most common severe mutations are a 4 basepair insertion in Ashkenazi Jews and a 7.6 kb deletion in a high-incidence French Canadian group (Gieselmann, 1995). Sandhoff disease has a very similar clinical phenotype as Tay-Sachs, and also displays variable severity based on enzyme activity. The AB variant is rare, but is also pathologically similar to the severe form of Tay-Sachs disease.

Mouse models of both Tay-Sachs and Sandhoff disease have been generated by disruption of the hexosaminidase α- and β-chain genes, respectively (Kolter and Sandhoff, 1998). Interestingly, the Tay-Sachs mouse displays no clinical neurological phenotype, despite evidence of GM2 accumulation in the central nervous system. By contrast, Sandhoff mice develop severe neurological disorders, including muscle weakness, rigidity, tremor, ataxia, paralysis and the mice die within weeks of onset.

*Gaucher disease*

Gaucher disease is caused by deficiency of β-D-glucocerebrosidase, the enzyme responsible for the breakdown of glucosylceramide into glucose and ceramide (Gieselmann, 1995). Glucosylceramide accumulation occurs mainly in the bone marrow, spleen, and liver, resulting in bone lesions, anemia, and splenomegaly (type I disease). In the rarer type II disease, patients have accumulation in the central nervous system and display a variety of neuronal pathologies. Gaucher disease type I is the first lysosomal storage disease to be treated successfully by enzyme replacement (Winchester et al., 2000). Recombinant β-D-glucocerebrosidase is modified to contain terminal mannose residues on N-linked oligosaccharides. The terminal mannose is recognized by the mannose receptor on macrophages, triggering endocytosis and delivery of the enzyme to lysosomes. Though successful in this particular case, it is unclear whether such enzyme replacement therapies will be possible for disorders of the central nervous system due to the blood-brain barrier.

*Niemann-Pick disease*

Sphingomyelinase hydrolyzes sphingomyelin into ceramide and phosphorylcholine. In both type A and B Niemann-Pick disease, this enzyme is defective (Gieselmann, 1995). Type A is a severe infant disorder involving progressive psychomotor retardation and visceromegaly, and results in death by three years of age. Type B is characterized by visceromegaly, but does not dramatically affect the nervous system, and patients can survive into adulthood.

The clinically similar Niemann-Pick type C (NPC) disease does not involve a defect in sphingomyelinase activity. Patients exhibit an enlarged liver and spleen, as in type A and B, and undergo progressive loss of motor skills and dementia, indicating progressive degeneration in the central nervous system (Liscum, 2000). In NPC cells, increased levels of sphingomyelin and unesterified cholesterol are sequestered in lysosomes. Hydrolysis of cholesterol esters appears to be normal, but transport of cholesterol from the lysosome to the ER or the cell surface is dramatically delayed (Liscum, 2000). The NPC1 gene encodes a protein containing 16 transmembrane domains, a sterol-sensing domain, a leucine zipper, and a dileucine lysosomal targeting motif (Carstea et al., 1997; Loftus et al., 1997). It also displays extensive similarity to Patched, a membrane receptor that mediates Sonic hedgehog signaling. It is not clear yet how NPC1 directs or regulates cholesterol and sphingolipid transport. Fluid phase constituents of lysosomes also display abnormally efflux from late endosomes, indicating that NPC1 is involved in transporting additional molecules (Neufeld et al., 1999). NPC1 may in some way regulate retrograde trafficking, and improper recycling of cholesterol and sphingolipid from the plasma membrane may account for the accumulation defect.

*Mucolipidosis type IV*

Mucolipidosis type IV (MLIV) is a recessive autosomal disorder characterized by psychomotor retardation, corneal opacities, and retinal degeneration (Berman et al., 1974). Affected patients reach a maximal developmental level of 12-15 months in language and motor function, but little deterioration in condition is observed (Amir et al., 1987). The disease causes the accumulation of gangliosides, phospholipids, and mucopolysaccharides (Bargal and Bach, 1988; Bargal and Bach, 1989), and enlarged

lysosomes containing lamellar, membranous material are observed in virtually all cell types (Berman et al., 1974).

No defective lysosomal hydrolyase activity that could account for the observed accumulation in MLIV cells has been detected. Instead, similar to what is observed in NPC disease, the defect appears to be in the trafficking of lipid material, rather than its breakdown. Radiolabelled phosphatidylcholine accumulates to a higher level in MLIV cells than wild-type cells in a 24 hour pulse, but is degraded at the same rate in both samples during a chase period, indicating that accumulation occurs despite normal degradative capacity (Bargal and Bach, 1997). In addition, fluorescently labeled lactosylceramide (LacCer) accumulates in lysosomes despite the capacity of MLIV to produce lactyosylcermaide metabolites at the same rate as wild-type cells (Chen et al., 1998). These results suggest that ganglioside accumulation is due to abnormal transport or recycling, rather than defective degradation. The uptake of a fluid-phase marker, a plasma membrane lipid marker, and a marker for receptor-mediated endocytosis was identical in wild-type and MLIV cells, and recycling of the endocytic marker from the early endosome back to the plasma membrane occurred at identical rates (Chen et al., 1998). However, MLIV cells accumulate more labeled LacCer in dextran-labeled lysosomes than wild-type cells within 20 minutes following release from a block in the early endosome compartment, and LacCer is absent from the Golgi complex, where it could be found in wild-type cells (Chen et al., 1998). Therefore, lipid material appears to be inappropriately transported to lysosomes in MLIV cells downstream of the early sorting endosome.

MLIV may affect other aspects of lysosome trafficking, as well. First, the lysosomal pH in MLIV fibroblasts is elevated by almost a full pH unit (~5.2 in MLIV cells, versus 4.3-4.5 in wild-type cells) (Bach et al., 1999). This pH elevation is specific to MLIV, and was not observed in cultured NPC, Hunter, or Farber disease fibroblasts, which accumulate similar compounds. As pH-mediated receptor-ligand dissociation is required for the sorting of various proteins in the endocytic pathway, including the mannose-6-phosphate receptor and transferrin (van Weert et al., 1995), it is possible that pH also plays a role in the sorting of lipid material through this pathway, as well. Furthermore, stomach parietal cells in MLIV patients have lowered gastric acid output (Schiffmann et al., 1998), indicating that the lysosomal inclusion bodies in these cells can

also interfere with cell secretion. Thus, the MLIV defect may affect both endocytic and secretory functions in specific cells.

The gene mutated in human MLIV was recently identified (Bargal et al., 2000; Bassi et al., 2000). The predicted protein product, mucolipin-1, is 580 amino acids long, and contains at least six putative transmembrane domains in the C-terminal portion of the protein. In addition, this region of the protein displays some similarity to the transient receptor potential channel (TRPC) family of putative $Ca^{2+}$ channels. Polycystin-2, the product of the PKD2 gene involved in autosomal dominant polycystic kidney disease, also contains a TRPC domain (Mochizuki et al., 1996), and basolateral trafficking of proteins and lipids is disrupted in this disease (Charron et al., 2000). As $Ca^{2+}$ ions appear to play important roles in the fusion of endosomal vesicles, it is possible that both of these disease genes normally act to regulate some aspect of intracellular trafficking through modulation of $Ca^{2+}$.

**Programmed cell death and lysosomal storage disorders**

The *C. elegans* counterpart of the human MLIV gene was identified functionally in two different ways. First, a screen for mutations that affected the uptake of green fluorescent protein (GFP) in coelomocytes, cells of unknown function in the worm pseudocoelom, identified a single mutant that caused the accumulation of excess GFP (Fares and Greenwald, 2001a). The gene mutated in this strain, *cup-5*, was cloned and found to be similar to the human MLIV gene (Fares and Greenwald, 2001b). In addition, in Chapter 3, we describe the identification of mutations in the same gene from a screen for mutations affecting programmed cell death in the worm. The work described therein suggests that programmed cell death is increased in these mutants, and this work in turn implies that programmed cell death may play a role in MLIV and other human lysosomal storage disorders.

Further evidence of this possibility can be derived from mouse models of Tay-Sachs and Sandhoff disease. Symptomatic *Hexb*$^{-/-}$ (Sandhoff) mice display DNA laddering in central nervous system tissues, and brain stem and spinal cord sections contain apoptotic cells by *in situ* end labeling (Huang et al., 1997). In addition, *in situ* end labeling of human brain and spinal cord sections detected apoptotic cells in both Tay-Sachs and Sandhoff patients, but not in control samples (Huang et al., 1997). In both the mouse and human samples, the original cell type of the labeled cells was

impossible to determine, but surrounding surviving neurons were grossly abnormal in morphology and contained enlarged lysosomes. Thus, it is possible that the neurodegenerative phenotypes associated with these lysosomal storage disorders may be due to the removal of cells with aberrant lysosomes by programmed cell death, rather than to the primary defect of lipid accumulation.

## CONCLUSIONS

Though the principal molecules involved in programmed cell death regulation have been identified, the detailed course of events that unfolds in a dying cell has still not been fully described. Surely caspase activation and mitochondrial dysfunction play important roles in execution of the cell, but the complete set of regulatory interactions that affect these processes and the molecular events that are ultimately responsible at the biochemical level for the destruction of the cell and the generation of apoptotic morphology remain to be elucidated. Furthermore, despite evidence for the involvement of programmed cell death in specific diseases, its role as either consequence or causative agent must be carefully evaluated in the case of each new disease.

## REFERENCES


Aballay, A., and Ausubel, F. M. (2001). Programmed cell death mediated by *ced-3* and *ced-4* protects *Caenorhabditis elegans* from *Salmonella typhimurium*-mediated killing. Proc. Natl. Acad. Sci. USA *98*, 2735-9.

Adams, J. M., and Cory, S. (1998). The Bcl-2 protein family: arbiters of cell survival. Science *281*, 1322-6.

Ahmad, M., Srinivasula, S. M., Hegde, R., Mukattash, R., Fernandes-Alnemri, T., and Alnemri, E. S. (1998). Identification and characterization of murine caspase-14, a new member of the caspase family. Cancer Res. *58*, 5201-5.

Akao, Y., Otsuki, Y., Kataoka, S., Ito, Y., and Tsujimoto, Y. (1994). Multiple subcellular localization of bcl-2: detection in nuclear outer membrane, endoplasmic reticulum membrane, and mitochondrial membranes. Cancer Res. *54*, 2468-71.

Amir, N., Zlotogora, J., and Bach, G. (1987). Mucolipidosis type IV: clinical spectrum and natural history. Pediatrics *79*, 953-9.

Antonsson, B., Conti, F., Ciavatta, A., Montessuit, S., Lewis, S., Martinou, I., Bernasconi, L., Bernard, A., Mermod, J. J., Mazzei, G., *et al.* (1997). Inhibition of Bax channel-forming activity by Bcl-2. Science *277*, 370-2.

Bach, G., Chen, C. S., and Pagano, R. E. (1999). Elevated lysosomal pH in Mucolipidosis type IV cells. Clin. Chim. Acta *280*, 173-9.

Bakhshi, A., Jensen, J. P., Goldman, P., Wright, J. J., McBride, O. W., Epstein, A. L., and Korsmeyer, S. J. (1985). Cloning the chromosomal breakpoint of t(14;18) human lymphomas: clustering around JH on chromosome 14 and near a transcriptional unit on 18. Cell *41*, 899-906.

Bargal, R., Avidan, N., Ben-Asher, E., Olender, Z., Zeigler, M., Frumkin, A., Raas-Rothschild, A., Glusman, G., Lancet, D., and Bach, G. (2000). Identification of the gene causing mucolipidosis type IV. Nat. Genet. *26*, 118-23.

Bargal, R., and Bach, G. (1988). Phospholipids accumulation in mucolipidosis IV cultured fibroblasts. J. Inherit. Metab. Dis. *11*, 144-50.

Bargal, R., and Bach, G. (1989). Phosphatidylcholine storage in mucolipidosis IV. Clin. Chim. Acta *181*, 167-74.

Bargal, R., and Bach, G. (1997). Mucolipidosis type IV: abnormal transport of lipids to lysosomes. J. Inherit. Metab. Dis. *20*, 625-32.

Bassi, M. T., Manzoni, M., Monti, E., Pizzo, M. T., Ballabio, A., and Borsani, G. (2000). Cloning of the gene encoding a novel integral membrane protein, mucolipidin-and identification of the two major founder mutations causing mucolipidosis type IV. Am. J. Hum. Genet. *67*, 1110-20.

Berman, E. R., Livni, N., Shapira, E., Merin, S., and Levij, I. S. (1974). Congenital corneal clouding with abnormal systemic storage bodies: a new variant of mucolipidosis. J. Pediatr. *84*, 519-26.

Boldin, M. P., Goncharov, T. M., Goltsev, Y. V., and Wallach, D. (1996). Involvement of MACH, a novel MORT1/FADD-interacting protease, in Fas/APO-1- and TNF receptor-induced cell death. Cell *85*, 803-15.

Boldin, M. P., Varfolomeev, E. E., Pancer, Z., Mett, I. L., Camonis, J. H., and Wallach, D. (1995). A novel protein that interacts with the death domain of Fas/APO1 contains a sequence motif related to the death domain. J. Biol. Chem. *270*, 7795-8.

Bossy-Wetzel, E., Newmeyer, D. D., and Green, D. R. (1998). Mitochondrial cytochrome c release in apoptosis occurs upstream of DEVD- specific caspase activation and independently of mitochondrial transmembrane depolarization. EMBO J. *17*, 37-49.

Burek, M. J., and Oppenheim, R. W. (1999). Cellular interactions that regulate programmed cell death in the developing vertebrate nervous system. In *Cell Death and Diseases of the Nervous System*. V. E. Koliatsos, and R. R. Ratan, eds. (Totowa, Humana Press).

Cain, K., Bratton, S. B., Langlais, C., Walker, G., Brown, D. G., Sun, X. M., and Cohen, G. M. (2000). Apaf-1 oligomerizes into biologically active approximately 700-kDa and inactive approximately 1.4-MDa apoptosome complexes. J. Biol. Chem. *275*, 6067-70.

Cain, K., Brown, D. G., Langlais, C., and Cohen, G. M. (1999). Caspase activation involves the formation of the aposome, a large (approximately 700 kDa) caspase-activating complex. J. Biol. Chem. *274*, 22686-92.

Carstea, E. D., Morris, J. A., Coleman, K. G., Loftus, S. K., Zhang, D., Cummings, C., Gu, J., Rosenfeld, M. A., Pavan, W. J., Krizman, D. B., *et al.* (1997). Niemann-Pick C1 disease gene: homology to mediators of cholesterol homeostasis. Science *277*, 228-31.

Cerretti, D. P., Kozlosky, C. J., Mosley, B., Nelson, N., Van Ness, K., Greenstreet, T. A., March, C. J., Kronheim, S. R., Druck, T., Cannizzaro, L. A., and et al. (1992). Molecular cloning of the interleukin-1 beta converting enzyme. Science *256*, 97-100.

Chalfie, M., and Wolinsky, E. (1990). The identification and suppression of inherited neurodegeneration in *Caenorhabditis elegans*. Nature *345*, 410-6.

Chandler, J. M., Cohen, G. M., and MacFarlane, M. (1998). Different subcellular distribution of caspase-3 and caspase-7 following Fas-induced apoptosis in mouse liver. J. Biol. Chem. *273*, 10815-8.

Charron, A. J., Nakamura, S., Bacallao, R., and Wandinger-Ness, A. (2000). Compromised cytoarchitecture and polarized trafficking in autosomal dominant polycystic kidney disease cells. J. Cell. Biol. *149*, 111-24.

Chen, C. S., Bach, G., and Pagano, R. E. (1998). Abnormal transport along the lysosomal pathway in mucolipidosis, type IV disease. Proc. Natl. Acad. Sci. USA *95*, 6373-8.

Chen, F., Hersh, B. M., Conradt, B., Zhou, Z., Riemer, D., Gruenbaum, Y., and Horvitz, H. R. (2000). Translocation of *C. elegans* CED-4 to nuclear membranes during programmed cell death. Science *287*, 1485-9.

Chen, P., and Abrams, J. M. (2000). Drosophila apoptosis and Bcl-2 genes: outliers fly in. J. Cell. Biol. *148*, 625-7.

Cheng, E. H., Wei, M. C., Weiler, S., Flavell, R. A., Mak, T. W., Lindsten, T., and Korsmeyer, S. J. (2001). BCL-2, BCL-$X_L$ sequester BH3 domain-only molecules preventing BAX- and BAK-mediated mitochondrial apoptosis. Mol. Cell *8*, 705-11.

Chinnaiyan, A. M., O'Rourke, K., Lane, B. R., and Dixit, V. M. (1997). Interaction of CED-4 with CED-3 and CED-9: a molecular framework for cell death. Science *275*, 1122-6.

Chinnaiyan, A. M., O'Rourke, K., Tewari, M., and Dixit, V. M. (1995). FADD, a novel death domain-containing protein, interacts with the death domain of Fas and initiates apoptosis. Cell *81*, 505-12.

Chinnaiyan, A. M., Tepper, C. G., Seldin, M. F., O'Rourke, K., Kischkel, F. C., Hellbardt, S., Krammer, P. H., Peter, M. E., and Dixit, V. M. (1996). FADD/MORT1 is a common mediator of CD95 (Fas/APO-1) and tumor necrosis factor receptor-induced apoptosis. J. Biol. Chem. *271*, 4961-5.

Choi, D. W. (1992). Excitotoxic cell death. J Neurobiol *23*, 1261-76.

Chung, S., Gumienny, T. L., Hengartner, M. O., and Driscoll, M. (2000). A common set of engulfment genes mediates removal of both apoptotic and necrotic cell corpses in *C. elegans*. Nat. Cell Biol. *2*, 931-7.

Cleary, M. L., and Sklar, J. (1985). Nucleotide sequence of a t(14;18) chromosomal breakpoint in follicular lymphoma and demonstration of a breakpoint-cluster region near a transcriptionally active locus on chromosome 18. Proc. Natl. Acad. Sci. USA *82*, 7439-43.

Cohen, J. J., Duke, R. C., Fadok, V. A., and Sellins, K. S. (1992). Apoptosis and programmed cell death in immunity. Annu. Rev. Immunol. *10*, 267-93.

Conradt, B., and Horvitz, H. R. (1998). The *C. elegans* protein EGL-1 is required for programmed cell death and interacts with the Bcl-2-like protein CED-9. Cell *93*, 519-29.

Conradt, B., and Horvitz, H. R. (1999). The TRA-1A sex determination protein of *C. elegans* regulates sexually dimorphic cell deaths by repressing the *egl-1* cell death activator gene. Cell *98*, 317-27.

Conus, S., Rosse, T., and Borner, C. (2000). Failure of Bcl-2 family members to interact with Apaf-1 in normal and apoptotic cells. Cell Death Differ. *7*, 947-54.

Coucouvanis, E., and Martin, G. R. (1995). Signals for death and survival: a two-step mechanism for cavitation in the vertebrate embryo. Cell *83*, 279-87.

Crompton, M. (1999). The mitochondrial permeability transition pore and its role in cell death. Biochem. J. *341*, 233-49.

Cryns, V., and Yuan, J. (1998). Proteases to die for. Genes Dev. *12*, 1551-70.

Daugas, E., Susin, S. A., Zamzami, N., Ferri, K. F., Irinopoulou, T., Larochette, N., Prevost, M. C., Leber, B., Andrews, D., Penninger, J., and Kroemer, G. (2000). Mitochondrio-nuclear translocation of AIF in apoptosis and necrosis. FASEB J. *14*, 729-39.

Davidson, F. F., and Steller, H. (1998). Blocking apoptosis prevents blindness in Drosophila retinal degeneration mutants. Nature *391*, 587-91.

del Peso, L., Gonzalez, V. M., and Nunez, G. (1998). *Caenorhabditis elegans* EGL-1 disrupts the interaction of CED-9 with CED- 4 and promotes CED-3 activation. J. Biol. Chem. *273*, 33495-500.

Desagher, S., Osen-Sand, A., Nichols, A., Eskes, R., Montessuit, S., Lauper, S., Maundrell, K., Antonsson, B., and Martinou, J. C. (1999). Bid-induced conformational change of Bax is responsible for mitochondrial cytochrome c release during apoptosis. J. Cell. Biol. *144*, 891-901.

Driscoll, M., and Chalfie, M. (1991). The *mec-4* gene is a member of a family of *Caenorhabditis elegans* genes that can mutate to induce neuronal degeneration. Nature *349*, 588-93.

Du, C., Fang, M., Li, Y., Li, L., and Wang, X. (2000). Smac, a mitochondrial protein that promotes cytochrome c-dependent caspase activation by eliminating IAP inhibition. Cell *102*, 33-42.

Ellis, H. M., and Horvitz, H. R. (1986). Genetic control of programmed cell death in the nematode *C. elegans*. Cell *44*, 817-29.

Enari, M., Sakahira, H., Yokoyama, H., Okawa, K., Iwamatsu, A., and Nagata, S. (1998). A caspase-activated DNase that degrades DNA during apoptosis, and its inhibitor ICAD. Nature *391*, 43-50.

Eskes, R., Antonsson, B., Osen-Sand, A., Montessuit, S., Richter, C., Sadoul, R., Mazzei, G., Nichols, A., and Martinou, J. C. (1998). Bax-induced cytochrome c release from mitochondria is independent of the permeability transition pore but highly dependent on $Mg^{2+}$ ions. J. Cell. Biol. *143*, 217-24.

Eskes, R., Desagher, S., Antonsson, B., and Martinou, J. C. (2000). Bid induces the oligomerization and insertion of Bax into the outer mitochondrial membrane. Mol. Cell. Biol. *20*, 929-35.

Evan, G. I., and Vousden, K. H. (2001). Proliferation, cell cycle and apoptosis in cancer. Nature *411*, 342-8.

Fares, H., and Greenwald, I. (2001a). Genetic analysis of endocytosis in *Caenorhabditis elegans*. Coelomocyte uptake defective mutants. Genetics *159*, 133-45.

Fares, H., and Greenwald, I. (2001b). Regulation of endocytosis by CUP-5, the *Caenorhabditis elegans* mucolipin-1 homolog. Nat. Genet. *28*, 64-8.

Finucane, D. M., Bossy-Wetzel, E., Waterhouse, N. J., Cotter, T. G., and Green, D. R. (1999). Bax-induced caspase activation and apoptosis via cytochrome c release from mitochondria is inhibitable by Bcl-$x_L$. J. Biol. Chem. *274*, 2225-33.

Gartner, A., Milstein, S., Ahmed, S., Hodgkin, J., and Hengartner, M. O. (2000). A conserved checkpoint pathway mediates DNA damage--induced apoptosis and cell cycle arrest in *C. elegans*. Mol. Cell *5*, 435-43.

Gavrieli, Y., Sherman, Y., and Ben-Sasson, S. A. (1992). Identification of programmed cell death in situ via specific labeling of nuclear DNA fragmentation. J. Cell. Biol. *119*, 493-501.

Gieselmann, V. (1995). Lysosomal storage diseases. Biochim. Biophys. Acta *1270*, 103-36.

Goyal, L. (2001). Cell death inhibition: keeping caspases in check. Cell *104*, 805-8.

Green, D., and Kroemer, G. (1998). The central executioners of apoptosis: caspases or mitochondria? Trends Cell Biol. *8*, 267-71.

Gross, A., Jockel, J., Wei, M. C., and Korsmeyer, S. J. (1998). Enforced dimerization of BAX results in its translocation, mitochondrial dysfunction and apoptosis. EMBO J. *17*, 3878-85.

Gross, A., McDonnell, J. M., and Korsmeyer, S. J. (1999a). BCL-2 family members and the mitochondria in apoptosis. Genes Dev. *13*, 1899-911.

Gross, A., Yin, X. M., Wang, K., Wei, M. C., Jockel, J., Milliman, C., Erdjument-Bromage, H., Tempst, P., and Korsmeyer, S. J. (1999b). Caspase cleaved BID targets mitochondria and is required for cytochrome c release, while BCL-$X_L$ prevents this release but not tumor necrosis factor-R1/Fas death. J. Biol. Chem. *274*, 1156-63.

Gruenbaum, Y., Wilson, K. L., Harel, A., Goldberg, M., and Cohen, M. (2000). Review: nuclear lamins--structural proteins with fundamental functions. J. Struct. Biol. *129*, 313-323.

Gumienny, T. L., Lambie, E., Hartwieg, E., Horvitz, H. R., and Hengartner, M. O. (1999). Genetic control of programmed cell death in the *Caenorhabditis elegans* hermaphrodite germline. Development *126*, 1011-22.

Hakem, R., Hakem, A., Duncan, G. S., Henderson, J. T., Woo, M., Soengas, M. S., Elia, A., de la Pompa, J. L., Kagi, D., Khoo, W., *et al.* (1998). Differential requirement for caspase 9 in apoptotic pathways in vivo. Cell *94*, 339-52.

Hall, D. H., Gu, G., Garcia-Anoveros, J., Gong, L., Chalfie, M., and Driscoll, M. (1997). Neuropathology of degenerative cell death in *Caenorhabditis elegans*. J. Neurosci. *17*, 1033-45.

Hausmann, G., O'Reilly, L. A., van Driel, R., Beaumont, J. G., Strasser, A., Adams, J. M., and Huang, D. C. (2000). Pro-apoptotic apoptosis protease-activating factor 1 (Apaf-1) has a cytoplasmic localization distinct from Bcl-2 or Bcl-$x_L$. J. Cell. Biol. *149*, 623-34.

Hedgecock, E. M., Sulston, J. E., and Thomson, J. N. (1983). Mutations affecting programmed cell deaths in the nematode *Caenorhabditis elegans*. Science *220*, 1277-9.

Hengartner, M. O., Ellis, R. E., and Horvitz, H. R. (1992). *Caenorhabditis elegans* gene *ced-9* protects cells from programmed cell death. Nature *356*, 494-9.

Hengartner, M. O., and Horvitz, H. R. (1994a). Activation of *C. elegans* cell death protein CED-9 by an amino-acid substitution in a domain conserved in Bcl-2. Nature *369*, 318-20.

Hengartner, M. O., and Horvitz, H. R. (1994b). *C. elegans* cell survival gene *ced-9* encodes a functional homolog of the mammalian proto-oncogene *bcl-2*. Cell *76*, 665-76.

Hockenbery, D., Nunez, G., Milliman, C., Schreiber, R. D., and Korsmeyer, S. J. (1990). Bcl-2 is an inner mitochondrial membrane protein that blocks programmed cell death. Nature *348*, 334-6.

Hoeppner, D. J., Hengartner, M. O., and Schnabel, R. (2001). Engulfment genes cooperate with *ced-3* to promote cell death in *Caenorhabditis elegans*. Nature *412*, 202-6.

Hsu, Y. T., Wolter, K. G., and Youle, R. J. (1997). Cytosol-to-membrane redistribution of Bax and Bcl-X(L) during apoptosis. Proc. Natl. Acad. Sci. USA *94*, 3668-72.

Hu, Y., Benedict, M. A., Wu, D., Inohara, N., and Nunez, G. (1998). Bcl-$X_L$ interacts with Apaf-1 and inhibits Apaf-1-dependent caspase-9 activation. Proc. Natl. Acad. Sci. USA *95*, 4386-91.

Huang, D. C., and Strasser, A. (2000). BH3-Only proteins-essential initiators of apoptotic cell death. Cell *103*, 839-42.

Huang, J. Q., Trasler, J. M., Igdoura, S., Michaud, J., Hanal, N., and Gravel, R. A. (1997). Apoptotic cell death in mouse models of GM2 gangliosidosis and observations on human Tay-Sachs and Sandhoff diseases. Hum. Mol. Genet. *6*, 1879-85.

Jacobson, M. D., Weil, M., and Raff, M. C. (1997). Programmed cell death in animal development. Cell *88*, 347-54.

Joza, N., Susin, S. A., Daugas, E., Stanford, W. L., Cho, S. K., Li, C. Y., Sasaki, T., Elia, A. J., Cheng, H. Y., Ravagnan, L., *et al.* (2001). Essential role of the mitochondrial apoptosis-inducing factor in programmed cell death. Nature *410*, 549-54.

Jurgensmeier, J. M., Xie, Z., Deveraux, Q., Ellerby, L., Bredesen, D., and Reed, J. C. (1998). Bax directly induces release of cytochrome c from isolated mitochondria. Proc. Natl. Acad. Sci. USA *95*, 4997-5002.

Kelekar, A., and Thompson, C. B. (1998). Bcl-2-family proteins: the role of the BH3 domain in apoptosis. Trends Cell Biol. *8*, 324-30.

Kerr, J. F., Wyllie, A. H., and Currie, A. R. (1972). Apoptosis: a basic biological phenomenon with wide-ranging implications in tissue kinetics. Br. J. Cancer *26*, 239-57.

Kitanaka, C., and Kuchino, Y. (1999). Caspase-independent programmed cell death with necrotic morphology. Cell Death Differ. *6*, 508-15.

Kluck, R. M., Bossy-Wetzel, E., Green, D. R., and Newmeyer, D. D. (1997). The release of cytochrome c from mitochondria: a primary site for Bcl-2 regulation of apoptosis. Science *275*, 1132-6.

Kluck, R. M., Esposti, M. D., Perkins, G., Renken, C., Kuwana, T., Bossy-Wetzel, E., Goldberg, M., Allen, T., Barber, M. J., Green, D. R., and Newmeyer, D. D. (1999). The pro-apoptotic proteins, Bid and Bax, cause a limited permeabilization of the mitochondrial outer membrane that is enhanced by cytosol. J. Cell. Biol. *147*, 809-22.

Knudson, C. M., and Korsmeyer, S. J. (1997). Bcl-2 and Bax function independently to regulate cell death. Nat. Genet. *16*, 358-63.

Kolter, T., and Sandhoff, K. (1998). Glycosphingolipid degradation and animal models of GM2-gangliosidoses. J. Inherit. Metab. Dis. *21*, 548-63.

Krajewski, S., Tanaka, S., Takayama, S., Schibler, M. J., Fenton, W., and Reed, J. C. (1993). Investigation of the subcellular distribution of the bcl-2 oncoprotein: residence in the nuclear envelope, endoplasmic reticulum, and outer mitochondrial membranes. Cancer Res. *53*, 4701-14.

Krammer, P. H. (2000). CD95's deadly mission in the immune system. Nature *407*, 789-95.

Kuida, K., Haydar, T. F., Kuan, C. Y., Gu, Y., Taya, C., Karasuyama, H., Su, M. S., Rakic, P., and Flavell, R. A. (1998). Reduced apoptosis and cytochrome c-mediated caspase activation in mice lacking caspase 9. Cell *94*, 325-37.

Kuida, K., Lippke, J. A., Ku, G., Harding, M. W., Livingston, D. J., Su, M. S., and Flavell, R. A. (1995). Altered cytokine export and apoptosis in mice deficient in interleukin- 1 beta converting enzyme. Science *267*, 2000-3.

Kuida, K., Zheng, T. S., Na, S., Kuan, C., Yang, D., Karasuyama, H., Rakic, P., and Flavell, R. A. (1996). Decreased apoptosis in the brain and premature lethality in CPP32-deficient mice. Nature *384*, 368-72.

Kumar, S., and Doumanis, J. (2000). The fly caspases. Cell Death Differ. *7*, 1039-44.

Lazebnik, Y. A., Takahashi, A., Moir, R. D., Goldman, R. D., Poirier, G. G., Kaufmann, S. H., and Earnshaw, W. C. (1995). Studies of the lamin proteinase reveal multiple parallel biochemical pathways during apoptotic execution. Proc. Natl. Acad. Sci. USA *92*, 9042-6.

Li, H., Zhu, H., Xu, C. J., and Yuan, J. (1998). Cleavage of BID by caspase 8 mediates the mitochondrial damage in the Fas pathway of apoptosis. Cell *94*, 491-501.

Li, K., Li, Y., Shelton, J. M., Richardson, J. A., Spencer, E., Chen, Z. J., Wang, X., and Williams, R. S. (2000). Cytochrome c deficiency causes embryonic lethality and attenuates stress-induced apoptosis. Cell *101*, 389-99.

Li, P., Allen, H., Banerjee, S., Franklin, S., Herzog, L., Johnston, C., McDowell, J., Paskind, M., Rodman, L., Salfeld, J., and et al. (1995). Mice deficient in IL-1 beta-converting enzyme are defective in production of mature IL-1 beta and resistant to endotoxic shock. Cell *80*, 401-11.

Li, P., Nijhawan, D., Budihardjo, I., Srinivasula, S. M., Ahmad, M., Alnemri, E. S., and Wang, X. (1997). Cytochrome c and dATP-dependent formation of Apaf-1/caspase-9 complex initiates an apoptotic protease cascade. Cell *91*, 479-89.

Liscum, L. (2000). Niemann-Pick type C mutations cause lipid traffic jam. Traffic *1*, 218-25.

Liu, X., Kim, C. N., Yang, J., Jemmerson, R., and Wang, X. (1996). Induction of apoptotic program in cell-free extracts: requirement for dATP and cytochrome c. Cell *86*, 147-57.

Lloyd, J. B., and Mason, R. W. (1996). Biology of the Lysosome. Vol 27 (New York, Plenum Press).

Loftus, S. K., Morris, J. A., Carstea, E. D., Gu, J. Z., Cummings, C., Brown, A., Ellison, J., Ohno, K., Rosenfeld, M. A., Tagle, D. A., *et al.* (1997). Murine model of Niemann-Pick C disease: mutation in a cholesterol homeostasis gene. Science *277*, 232-5.

Luzio, J. P., Mullock, B. M., Pryor, P. R., Lindsay, M. R., James, D. E., and Piper, R. C. (2001). Relationship between endosomes and lysosomes. Biochem. Soc. Trans. *29*, 476-80.

Luzio, J. P., Rous, B. A., Bright, N. A., Pryor, P. R., Mullock, B. M., and Piper, R. C. (2000). Lysosome-endosome fusion and lysosome biogenesis. J. Cell. Sci. *113*, 1515-24.

Mahuran, D. J. (1999). Biochemical consequences of mutations causing the GM2 gangliosidoses. Biochim. Biophys. Acta *1455*, 105-38.

Mancini, M., Nicholson, D. W., Roy, S., Thornberry, N. A., Peterson, E. P., Casciola-Rosen, L. A., and Rosen, A. (1998). The caspase-3 precursor has a cytosolic and mitochondrial distribution: implications for apoptotic signaling. J. Cell. Biol. *140*, 1485-95.

Mano, I., and Driscoll, M. (1999). DEG/ENaC channels: a touchy superfamily that watches its salt. Bioessays *21*, 568-78.

Martin, D. A., Siegel, R. M., Zheng, L., and Lenardo, M. J. (1998). Membrane oligomerization and cleavage activates the caspase-8 (FLICE/MACHα1) death signal. J. Biol. Chem. *273*, 4345-9.

Marzo, I., Brenner, C., Zamzami, N., Jurgensmeier, J. M., Susin, S. A., Vieira, H. L., Prevost, M. C., Xie, Z., Matsuyama, S., Reed, J. C., and Kroemer, G. (1998). Bax and adenine nucleotide translocator cooperate in the mitochondrial control of apoptosis. Science *281*, 2027-31.

McCall, K., and Steller, H. (1998). Requirement for DCP-1 caspase during Drosophila oogenesis. Science *279*, 230-4.

Metzstein, M. M., Stanfield, G. M., and Horvitz, H. R. (1998). Genetics of programmed cell death in *C. elegans*: past, present and future. Trends Genet. *14*, 410-6.

Minn, A. J., Velez, P., Schendel, S. L., Liang, H., Muchmore, S. W., Fesik, S. W., Fill, M., and Thompson, C. B. (1997). Bcl-$x_L$ forms an ion channel in synthetic lipid membranes. Nature *385*, 353-7.

Miyashita, T., and Reed, J. C. (1995). Tumor suppressor p53 is a direct transcriptional activator of the human bax gene. Cell *80*, 293-9.

Mochizuki, T., Wu, G., Hayashi, T., Xenophontos, S. L., Veldhuisen, B., Saris, J. J., Reynolds, D. M., Cai, Y., Gabow, P. A., Pierides, A., *et al.* (1996). PKD2, a gene for polycystic kidney disease that encodes an integral membrane protein. Science *272*, 1339-42.

Monaghan, P., Robertson, D., Amos, T. A., Dyer, M. J., Mason, D. Y., and Greaves, M. F. (1992). Ultrastructural localization of bcl-2 protein. J. Histochem. Cytochem. *40*, 1819-25.

Moriishi, K., Huang, D. C., Cory, S., and Adams, J. M. (1999). Bcl-2 family members do not inhibit apoptosis by binding the caspase activator Apaf-1. Proc. Natl. Acad. Sci. USA *96*, 9683-8.

Muchmore, S. W., Sattler, M., Liang, H., Meadows, R. P., Harlan, J. E., Yoon, H. S., Nettesheim, D., Chang, B. S., Thompson, C. B., Wong, S. L., *et al.* (1996). X-ray and NMR structure of human Bcl-$x_L$, an inhibitor of programmed cell death. Nature *381*, 335-41.

Mullock, B. M., Bright, N. A., Fearon, C. W., Gray, S. R., and Luzio, J. P. (1998). Fusion of lysosomes with late endosomes produces a hybrid organelle of intermediate density and is NSF dependent. J. Cell. Biol. *140*, 591-601.

Muzio, M., Chinnaiyan, A. M., Kischkel, F. C., O'Rourke, K., Shevchenko, A., Ni, J., Scaffidi, C., Bretz, J. D., Zhang, M., Gentz, R., *et al.* (1996). FLICE, a novel FADD-homologous ICE/CED-3-like protease, is recruited to the CD95 (Fas/APO-1) death--inducing signaling complex. Cell *85*, 817-27.

Muzio, M., Stockwell, B. R., Stennicke, H. R., Salvesen, G. S., and Dixit, V. M. (1998). An induced proximity model for caspase-8 activation. J. Biol. Chem. *273*, 2926-30.

Neufeld, E. B., Wastney, M., Patel, S., Suresh, S., Cooney, A. M., Dwyer, N. K., Roff, C. F., Ohno, K., Morris, J. A., Carstea, E. D., *et al.* (1999). The Niemann-Pick C1 protein resides in a vesicular compartment linked to retrograde transport of multiple lysosomal cargo. J. Biol. Chem. *274*, 9627-35.

Newmeyer, D. D., Farschon, D. M., and Reed, J. C. (1994). Cell-free apoptosis in Xenopus egg extracts: inhibition by Bcl-2 and requirement for an organelle fraction enriched in mitochondria. Cell *79*, 353-64.

Nijhawan, D., Honarpour, N., and Wang, X. (2000). Apoptosis in neural development and disease. Annu. Rev. Neurosci. *23*, 73-87.

Oda, E., Ohki, R., Murasawa, H., Nemoto, J., Shibue, T., Yamashita, T., Tokino, T., Taniguchi, T., and Tanaka, N. (2000). Noxa, a BH3-only member of the Bcl-2 family and candidate mediator of p53-induced apoptosis. Science *288*, 1053-8.

Pan, G., O'Rourke, K., and Dixit, V. M. (1998). Caspase-9, Bcl-$X_L$, and Apaf-1 form a ternary complex. J. Biol. Chem. *273*, 5841-5.

Parrish, J., Li, L., Klotz, K., Ledwich, D., Wang, X., and Xue, D. (2001). Mitochondrial endonuclease G is important for apoptosis in *C. elegans*. Nature *412*, 90-4.

Peters, C., and Mayer, A. (1998). $Ca^{2+}$/calmodulin signals the completion of docking and triggers a late step of vacuole fusion. Nature *396*, 575-80.

Porter, A. G. (1999). Protein translocation in apoptosis. Trends Cell Biol. *9*, 394-401.

Portera-Cailliau, C., Sung, C. H., Nathans, J., and Adler, R. (1994). Apoptotic photoreceptor cell death in mouse models of retinitis pigmentosa. Proc. Natl. Acad. Sci. USA *91*, 974-8.

Pryor, P. R., Mullock, B. M., Bright, N. A., Gray, S. R., and Luzio, J. P. (2000). The role of intraorganellar $Ca^{2+}$ in late endosome-lysosome heterotypic fusion and in the reformation of lysosomes from hybrid organelles. J. Cell. Biol. *149*, 1053-62.

Raff, M. C. (1992). Social controls on cell survival and cell death. Nature *356*, 397-400.

Raff, M. C., Barres, B. A., Burne, J. F., Coles, H. S., Ishizaki, Y., and Jacobson, M. D. (1993). Programmed cell death and the control of cell survival: lessons from the nervous system. Science *262*, 695-700.

Rao, L., Perez, D., and White, E. (1996). Lamin proteolysis facilitates nuclear events during apoptosis. J. Cell. Biol. *135*, 1441-55.

Reddien, P. W., Cameron, S., and Horvitz, H. R. (2001). Phagocytosis promotes programmed cell death in *C. elegans*. Nature *412*, 198-202.

Robertson, A. M. G., and Thomson, J. G. (1982). Morphology of programmed cell death in the ventral nerve cord of *Caenorhabditis elegans* larvae. J. Embryol. Exp. Morph. *67*, 89-100.

Rodriguez, J., and Lazebnik, Y. (1999). Caspase-9 and APAF-1 form an active holoenzyme. Genes Dev. *13*, 3179-84.

Rotonda, J., Nicholson, D. W., Fazil, K. M., Gallant, M., Gareau, Y., Labelle, M., Peterson, E. P., Rasper, D. M., Ruel, R., Vaillancourt, J. P., *et al.* (1996). The three-dimensional structure of apopain/CPP32, a key mediator of apoptosis. Nat. Struct. Biol. *3*, 619-25.

Royal, D., and Driscoll, M. (1999). Neuronal cell death in *C. elegans*. In *Cell Death and Diseases of the Nervous System*. V. E. Koliatsos, and R. R. Ratan, eds. (Totowa, Humana Press).

Saito, M., Korsmeyer, S. J., and Schlesinger, P. H. (2000). BAX-dependent transport of cytochrome c reconstituted in pure liposomes. Nat. Cell Biol. *2*, 553-5.

Sakahira, H., Enari, M., and Nagata, S. (1998). Cleavage of CAD inhibitor in CAD activation and DNA degradation during apoptosis. Nature *391*, 96-9.

Saleh, A., Srinivasula, S. M., Acharya, S., Fishel, R., and Alnemri, E. S. (1999). Cytochrome c and dATP-mediated oligomerization of Apaf-1 is a prerequisite for procaspase-9 activation. J. Biol. Chem. *274*, 17941-5.

Sattler, M., Liang, H., Nettesheim, D., Meadows, R. P., Harlan, J. E., Eberstadt, M., Yoon, H. S., Shuker, S. B., Chang, B. S., Minn, A. J., *et al.* (1997). Structure of Bcl-$x_L$-Bak peptide complex: recognition between regulators of apoptosis. Science *275*, 983-6.

Schendel, S. L., Xie, Z., Montal, M. O., Matsuyama, S., Montal, M., and Reed, J. C. (1997). Channel formation by antiapoptotic protein Bcl-2. Proc. Natl. Acad. Sci. USA *94*, 5113-8.

Schiffmann, R., Dwyer, N. K., Lubensky, I. A., Tsokos, M., Sutliff, V. E., Latimer, J. S., Frei, K. P., Brady, R. O., Barton, N. W., Blanchette-Mackie, E. J., and Goldin, E. (1998). Constitutive achlorhydria in mucolipidosis type IV. Proc. Natl. Acad. Sci. USA *95*, 1207-12.

Schlesinger, P. H., Gross, A., Yin, X. M., Yamamoto, K., Saito, M., Waksman, G., and Korsmeyer, S. J. (1997). Comparison of the ion channel characteristics of proapoptotic BAX and antiapoptotic BCL-2. Proc. Natl. Acad. Sci. USA *94*, 11357-62.

Shaham, S. (1998). Identification of multiple *Caenorhabditis elegans* caspases and their potential roles in proteolytic cascades. J. Biol. Chem. *273*, 35109-17.

Shaham, S., and Horvitz, H. R. (1996). Developing *Caenorhabditis elegans* neurons may contain both cell-death protective and killer activities. Genes Dev. *10*, 578-91.

Shimizu, S., Narita, M., and Tsujimoto, Y. (1999). Bcl-2 family proteins regulate the release of apoptogenic cytochrome c by the mitochondrial channel VDAC. Nature *399*, 483-7.

Song, Z., McCall, K., and Steller, H. (1997). DCP-1, a Drosophila cell death protease essential for development. Science *275*, 536-40.

Spector, M. S., Desnoyers, S., Hoeppner, D. J., and Hengartner, M. O. (1997). Interaction between the C. *elegans* cell-death regulators CED-9 and CED- 4. Nature *385*, 653-6.

Srinivasula, S. M., Ahmad, M., Fernandes-Alnemri, T., and Alnemri, E. S. (1998). Autoactivation of procaspase-9 by Apaf-1-mediated oligomerization. Mol. Cell *1*, 949-57.

Stennicke, H. R., Deveraux, Q. L., Humke, E. W., Reed, J. C., Dixit, V. M., and Salvesen, G. S. (1999). Caspase-9 can be activated without proteolytic processing. J. Biol. Chem. *274*, 8359-62.

Storrie, B., and Desjardins, M. (1996). The biogenesis of lysosomes: is it a kiss and run, continuous fusion and fission process? Bioessays *18*, 895-903.

Stroh, C., and Schulze-Osthoff, K. (1998). Death by a thousand cuts: an ever increasing list of caspase substrates. Cell Death Differ. *5*, 997-1000.

Sulston, J. E., and Horvitz, H. R. (1977). Post-embryonic cell lineages of the nematode, *Caenorhabditis elegans*. Dev. Biol. *56*, 110-56.

Sulston, J. E., Schierenberg, E., White, J. G., and Thomson, J. N. (1983). The embryonic cell lineage of the nematode *Caenorhabditis elegans*. Dev. Biol. *100*, 64-119.

Susin, S. A., Lorenzo, H. K., Zamzami, N., Marzo, I., Brenner, C., Larochette, N., Prevost, M. C., Alzari, P. M., and Kroemer, G. (1999a). Mitochondrial release of caspase-2 and -9 during the apoptotic process. J. Exp. Med. *189*, 381-94.

Susin, S. A., Lorenzo, H. K., Zamzami, N., Marzo, I., Snow, B. E., Brothers, G. M., Mangion, J., Jacotot, E., Costantini, P., Loeffler, M., *et al.* (1999b). Molecular characterization of mitochondrial apoptosis-inducing factor. Nature *397*, 441-6.

Thompson, C. B. (1995). Apoptosis in the pathogenesis and treatment of disease. Science *267*, 1456-62.

Thornberry, N. A., Bull, H. G., Calaycay, J. R., Chapman, K. T., Howard, A. D., Kostura, M. J., Miller, D. K., Molineaux, S. M., Weidner, J. R., Aunins, J., and et al. (1992). A novel heterodimeric cysteine protease is required for interleukin-1 beta processing in monocytes. Nature *356*, 768-74.

Thornberry, N. A., and Lazebnik, Y. (1998). Caspases: enemies within. Science *281*, 1312-6.

Thornberry, N. A., Rano, T. A., Peterson, E. P., Rasper, D. M., Timkey, T., Garcia-Calvo, M., Houtzager, V. M., Nordstrom, P. A., Roy, S., Vaillancourt, J. P., *et al.* (1997). A combinatorial approach defines specificities of members of the caspase family and granzyme B. Functional relationships established for key mediators of apoptosis. J. Biol. Chem. *272*, 17907-11.

Tsujimoto, Y., Finger, L. R., Yunis, J., Nowell, P. C., and Croce, C. M. (1984). Cloning of the chromosome breakpoint of neoplastic B cells with the t(14;18) chromosome translocation. Science *226*, 1097-9.

van Weert, A. W., Dunn, K. W., Gueze, H. J., Maxfield, F. R., and Stoorvogel, W. (1995). Transport from late endosomes to lysosomes, but not sorting of integral membrane proteins in endosomes, depends on the vacuolar proton pump. J. Cell. Biol. *130*, 821-34.

Vander Heiden, M. G., Chandel, N. S., Williamson, E. K., Schumacker, P. T., and Thompson, C. B. (1997). Bcl-$x_L$ regulates the membrane potential and volume homeostasis of mitochondria. Cell *91*, 627-37.

Varfolomeev, E. E., Schuchmann, M., Luria, V., Chiannilkulchai, N., Beckmann, J. S., Mett, I. L., Rebrikov, D., Brodianski, V. M., Kemper, O. C., Kollet, O., *et al.* (1998). Targeted disruption of the mouse caspase 8 gene ablates cell death induction by the TNF receptors, Fas/Apo1, and DR3 and is lethal prenatally. Immunity *9*, 267-76.

Vaux, D. L., Cory, S., and Adams, J. M. (1988). Bcl-2 gene promotes haemopoietic cell survival and cooperates with c- myc to immortalize pre-B cells. Nature *335*, 440-2.

Verhagen, A. M., Ekert, P. G., Pakusch, M., Silke, J., Connolly, L. M., Reid, G. E., Moritz, R. L., Simpson, R. J., and Vaux, D. L. (2000). Identification of DIABLO, a mammalian protein that promotes apoptosis by binding to and antagonizing IAP proteins. Cell *102*, 43-53.

von Ahsen, O., Renken, C., Perkins, G., Kluck, R. M., Bossy-Wetzel, E., and Newmeyer, D. D. (2000). Preservation of mitochondrial structure and function after Bid- or Bax-mediated cytochrome c release. J. Cell. Biol. *150*, 1027-36.

Walker, N. P., Talanian, R. V., Brady, K. D., Dang, L. C., Bump, N. J., Ferenz, C. R., Franklin, S., Ghayur, T., Hackett, M. C., Hammill, L. D., and et al. (1994). Crystal structure of the cysteine protease interleukin-1 beta- converting enzyme: a (p20/p10)2 homodimer. Cell *78*, 343-52.

Wang, J., and Lenardo, M. J. (2000). Roles of caspases in apoptosis, development, and cytokine maturation revealed by homozygous gene deficiencies. J. Cell. Sci. *113*, 753-7.

Wang, S., Miura, M., Jung, Y. K., Zhu, H., Li, E., and Yuan, J. (1998). Murine caspase-11, an ICE-interacting protease, is essential for the activation of ICE. Cell *92*, 501-9.

Wei, M. C., Lindsten, T., Mootha, V. K., Weiler, S., Gross, A., Ashiya, M., Thompson, C. B., and Korsmeyer, S. J. (2000). tBID, a membrane-targeted death ligand, oligomerizes BAK to release cytochrome c. Genes Dev. *14*, 2060-71.

Wei, M. C., Zong, W. X., Cheng, E. H., Lindsten, T., Panoutsakopoulou, V., Ross, A. J., Roth, K. A., MacGregor, G. R., Thompson, C. B., and Korsmeyer, S. J. (2001). Proapoptotic BAX and BAK: a requisite gateway to mitochondrial dysfunction and death. Science *292*, 727-30.

Winchester, B., Vellodi, A., and Young, E. (2000). The molecular basis of lysosomal storage diseases and their treatment. Biochem. Soc. Trans. *28*, 150-4.

Wolter, K. G., Hsu, Y. T., Smith, C. L., Nechushtan, A., Xi, X. G., and Youle, R. J. (1997). Movement of Bax from the cytosol to mitochondria during apoptosis. J. Cell. Biol. *139*, 1281-92.

Wu, D., Wallen, H. D., and Nunez, G. (1997). Interaction and regulation of subcellular localization of CED-4 by CED- 9. Science *275*, 1126-9.

Wyllie, A. H. (1980). Glucocorticoid-induced thymocyte apoptosis is associated with endogenous endonuclease activation. Nature *284*, 555-6.

Wyllie, A. H., Kerr, J. F., and Currie, A. R. (1980). Cell death: the significance of apoptosis. Int. Rev. Cytol. *68*, 251-306.

Xu, K., Tavernarakis, N., and Driscoll, M. (2001). Necrotic cell death in *C. elegans* requires the function of calreticulin and regulators of $Ca^{2+}$ release from the endoplasmic reticulum. Neuron *31*, 957-71.

Xue, D., Shaham, S., and Horvitz, H. R. (1996). The *Caenorhabditis elegans* cell-death protein CED-3 is a cysteine protease with substrate specificities similar to those of the human CPP32 protease. Genes Dev. *10*, 1073-83.

Yang, E., Zha, J., Jockel, J., Boise, L. H., Thompson, C. B., and Korsmeyer, S. J. (1995). Bad, a heterodimeric partner for Bcl-XL and Bcl-2, displaces Bax and promotes cell death. Cell *80*, 285-91.

Yang, J., Liu, X., Bhalla, K., Kim, C. N., Ibrado, A. M., Cai, J., Peng, T. I., Jones, D. P., and Wang, X. (1997). Prevention of apoptosis by Bcl-2: release of cytochrome c from mitochondria blocked. Science *275*, 1129-32.

Yin, X. M., Wang, K., Gross, A., Zhao, Y., Zinkel, S., Klocke, B., Roth, K. A., and Korsmeyer, S. J. (1999). Bid-deficient mice are resistant to Fas-induced hepatocellular apoptosis. Nature *400*, 886-91.

Yuan, J., and Horvitz, H. R. (1992). The *Caenorhabditis elegans* cell death gene *ced-4* encodes a novel protein and is expressed during the period of extensive programmed cell death. Development *116*, 309-20.

Yuan, J., Shaham, S., Ledoux, S., Ellis, H. M., and Horvitz, H. R. (1993). The *C. elegans* cell death gene *ced-3* encodes a protein similar to mammalian interleukin-1 beta-converting enzyme. Cell *75*, 641-52.

Zakeri, Z., Bursch, W., Tenniswood, M., and Lockshin, R. A. (1995). Cell death: programmed, apoptosis, necrosis, or other? Cell Death Differ. *2*, 87-96.

Zhivotovsky, B., Samali, A., Gahm, A., and Orrenius, S. (1999). Caspases: their intracellular localization and translocation during apoptosis. Cell Death Differ. *6*, 644-51.

Zhou, P., Chou, J., Olea, R. S., Yuan, J., and Wagner, G. (1999). Solution structure of Apaf-1 CARD and its interaction with caspase-9 CARD: a structural basis for specific adaptor/caspase interaction. Proc. Natl. Acad. Sci. USA *96*, 11265-70.

Zhou, Z., Hartwieg, E., and Horvitz, H. R. (2001). CED-1 is a transmembrane receptor that mediates cell corpse engulfment in *C. elegans*. Cell *104*, 43-56.

Zou, H., Henzel, W. J., Liu, X., Lutschg, A., and Wang, X. (1997). Apaf-1, a human protein homologous to *C. elegans* CED-4, participates in cytochrome c-dependent activation of caspase-3. Cell *90*, 405-13.

Zou, H., Li, Y., Liu, X., and Wang, X. (1999). An APAF-1•cytochrome c multimeric complex is a functional apoptosome that activates procaspase-9. J. Biol. Chem. *274*, 11549-56.

## FIGURES

**Figure 2. Caspase structure and function**

Caspases are divided into three subgroups based on structure and functional role. The generalized structure of a caspase zymogen consists of a prodomain, a large subunit, and a small subunit. Caspase processing produces an active enzyme consisting of two large subunits and two small subunits.

The ICE/caspase-1 subfamily consists of caspases involved in inflammatory responses, but not apoptosis. Short prodomain caspases appear to function as effectors of apoptosis, whereas long prodomain caspases generally act as initiators of a caspase cascade. CED-3, the only *C. elegans* caspase known to function in programmed cell death has a long prodomain but may act as both an initiator and effector of programmed cell death. Similarly, caspase-2 appears to have a role as both initiator and effector.

Figure 2

## Generalized Structure of Caspases

| prodomain (3-24 kDa) | large subunit (17-21 kDa) | small subunit (10-15 kDa) |
|---|---|---|

## Caspase subfamilies

***Inflammation***

caspase-1
caspase-4
caspase-5
caspase-11

***Programmed cell death***

*Effectors, short prodomain*

caspase-3
caspase-6
caspase-7

*Initiators, long prodomain*

caspase-2
caspase-8
caspase-9
caspase-10
caspase-12
CED-3

**Figure 3. Model for regulation of programmed cell death in *C. elegans***
In living cells, CED-9 sequesters CED-4 to mitochondria. Programmed cell death is activated when EGL-1 displaces CED-4 from CED-9. CED-4 translocates to the nuclear membrane and promotes activation of the CED-3 caspase. Inactive proCED-3 is processed into its active form by proteolytic cleavage. CED-3 may be complexed with CED-4 either at mitochondria or the nuclear membrane, but the subcellular localization for both inactive and active forms is currently unknown. Figure adapted from Metzstein et al., 1998.

Figure 3

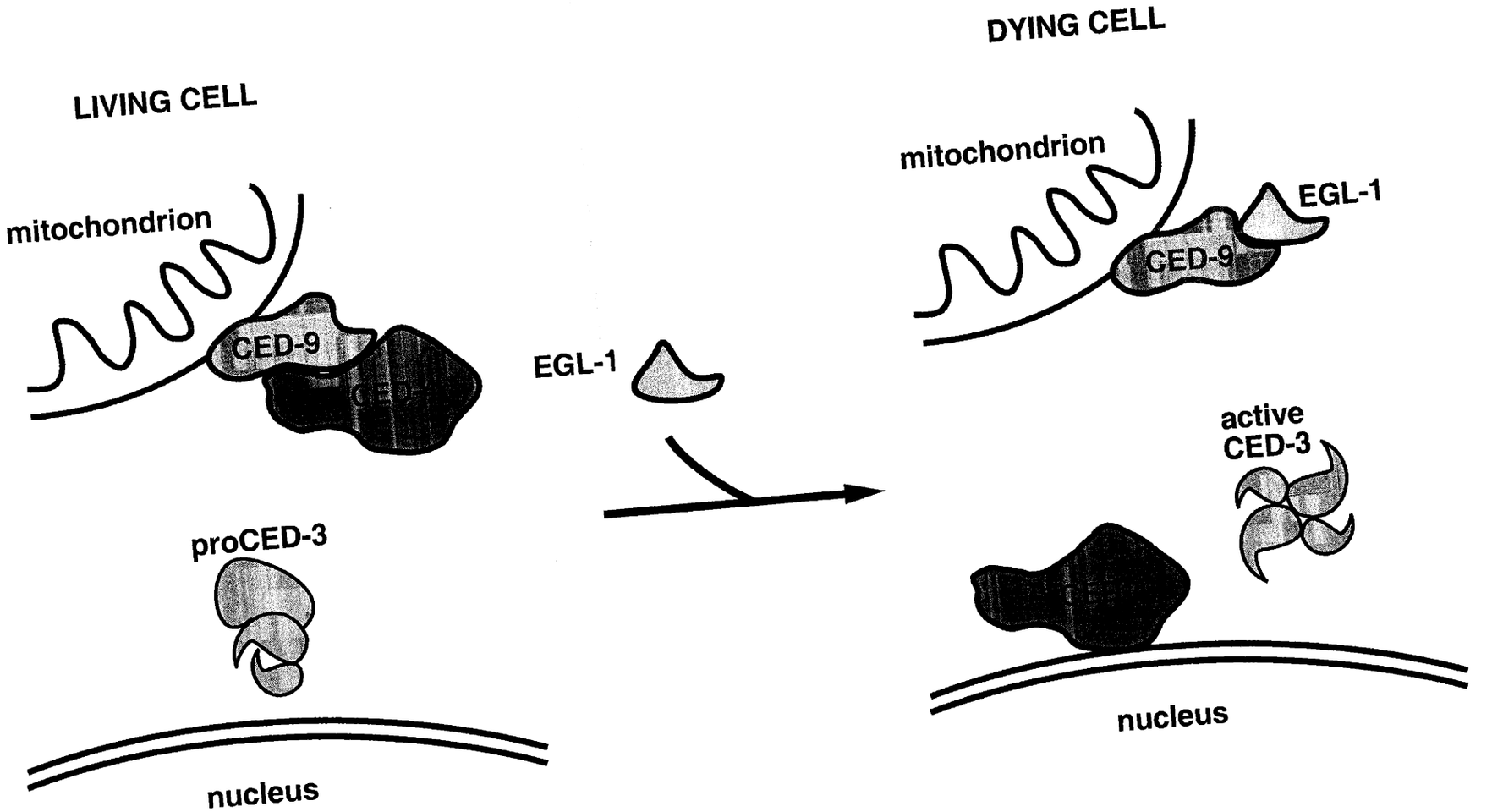
LIVING CELL
mitochondrion
CED-9
proCED-3
nucleus
EGL-1
DYING CELL
mitochondrion
EGL-1
CED-9
active
CED-3
nucleus

# Chapter 2
# Translocation of *C. elegans* CED-4 to Nuclear Membranes during Programmed Cell Death

Fangli Chen*, Bradley M. Hersh*, Barbara Conradt, Zheng Zhou,
Dieter Riemer, Yosef Gruenbaum, and H. R. Horvitz

* co-first authors

Published as Chen et al. (2000), Science 287: 1485-9. Zheng Zhou generated the anti-CED-4 antibody, Fangli Chen first performed CED-4 staining of embryos and first observed nuclear localization of CED-4, and Barbara Conradt performed cell corpse counts following EGL-1 overexpression. Dieter Riemer and Yosef Gruenbaum provided lamin antibody. I generated anti-CED-9 antibody, developed the Mitotracker staining protocol for *C. elegans*, performed the co-localization experiments with lamin antibody, and performed all confocal microscopy.

## SUMMARY

The *Caenorhabditis elegans* Bcl-2-like protein CED-9 prevents programmed cell death by antagonizing the Apaf-1-like cell-death activator CED-4. Endogenous CED-9 and CED-4 proteins localized to mitochondria in wild-type embryos, in which the majority of cells survive. By contrast, in embryos in which cells had been induced to die, CED-4 assumed a perinuclear localization. CED-4 translocation induced by the cell-death activator EGL-1 was blocked by a gain-of-function mutation in *ced-9* but was not dependent on *ced-3* function, suggesting that CED-4 translocation precedes caspase activation and the execution phase of programmed cell death. Thus, a change in the subcellular localization of CED-4 may drive programmed cell death.

Programmed cell death is important in regulating cell number and cell connections and for sculpting tissues during metazoan development (*1*). When misregulated, programmed cell death can contribute to various disease states, including cancer, autoimmune disease, and neurodegenerative disease (*2*). Many of the central components of the cell death machinery have been identified through genetic studies of the nematode *Caenorhabditis elegans* (*3*). Loss-of-function mutations in any of the genes *egl-1*, *ced-3*, or *ced-4* or a gain-of-function mutation in the gene *ced-9* block programmed cell death. Loss-of function mutations in *ced-9* cause sterility and maternal-effect lethality as a consequence of ectopic cell death and can be suppressed by *ced-3* and *ced-4* mutations but not by *egl-1* mutations, suggesting that *ced-9* acts upstream of *ced-3* and *ced-4* and downstream of *egl-1*. CED-9 is a member of the Bcl-2 family of cell-death regulators (*4*), and the EGL-1 protein contains a BH3 (Bcl-2 homology) domain and can physically interact with CED-9 (*5*). *ced-3* encodes a caspase (*6*), while CED-4 is similar to mammalian Apaf-1, an activator of caspases (*7*). CED-4 can bind CED-9 and CED-3 *in vitro*, in yeast, and in mammalian cells (*8*), and the interaction of CED-9 and EGL-1 may influence CED-4 activity (*9*). These observations suggest a model (*3*) in which CED-3 causes programmed cell death; CED-4 activates CED-3; CED-4 is directly inhibited by CED-9 (*10*); and EGL-1 initiates cell death by directly inhibiting CED-9. To determine when and where these cell-death proteins act, we have explored physical interactions among them using immunohistochemistry.

To study the expression and subcellular localization of CED-9 and CED-4 in *C. elegans*, we generated polyclonal antibodies that recognize these proteins (*11*). Affinity-purified antibodies to CED-9 specifically recognized bacterially-expressed CED-9 and a 32-kD protein corresponding to CED-9 on a western blot of wild-type (N2) embryo lysates; this protein was absent in *ced-9(n2812)* embryo lysates (*12,13*). The *ced-9(n2812)* allele contains an amber stop mutation at codon 46 and is probably a molecular and genetic null allele (*4*). Fixed embryos stained with anti-CED-9 revealed that CED-9 was present in all cells during *C. elegans* embryogenesis (Fig. 1A), beginning as early as the 2-cell stage. CED-9 levels peaked at approximately the 200-cell stage and slowly diminished, becoming undetectable around the time of hatching. CED-9 protein was not observed in larvae or adults. On the subcellular level, CED-9 exhibited a web-like, cytoplasmic staining pattern. CED-9 staining was highly similar to the staining of Mitotracker Red (*14*), which specifically labels mitochondria (Fig. 1).

Antibodies to CED-4 recognized bacterially-expressed CED-4 and detected a 63-kD protein on western blots of N2 embryo lysates; this protein was absent in *ced-4(n1162)* embryo lysates (*12*). The *ced-4(n1162)* allele contains an ochre stop mutation at codon 79 and is probably a molecular and genetic null allele (*15*). Embryos stained with anti-CED-4 displayed a web-like pattern in all cells (Fig. 1D), very similar to the patterns of CED-9 and Mitotracker Red. CED-4 staining appeared at approximately the 100-cell stage, prior to the first programmed cell death, persisted through embryogenesis, and like CED-9, was not detected in larvae and adults. Of the 131 developmental cell deaths in *C. elegans* hermaphrodites, 113 occur during embryogenesis and the remainder occur during larval development. Although we have not detected CED-4 or CED-9 in larvae, *ced-4* and *ced-9* mutants are defective in larval programmed cell deaths, suggesting that the CED-4 and CED-9 proteins act postembryonically.

We examined whether the expression and localization of CED-9 and CED-4 were affected by mutations that disrupt programmed cell death. Loss-of-function mutations in *ced-3*, *ced-4*, and *egl-1*, genes required for programmed cell death, did not affect either the expression pattern or mitochondrial localization of CED-9 protein. The expression and localization of CED-4 protein was also unaffected by loss-of-function mutations in *ced-3* and *egl-1*. To determine the expression pattern and localization of CED-4 in the absence of functional CED-9 protein, we stained *ced-9(n2812); ced-3(n717)* double mutant embryos with antibodies to CED-4. We observed that *ced-9(n2812)* embryos derived from homozygous *ced-9(n2812)* hermaphrodites arrested before the appearance of visibly recognizable corpses and before CED-4 expression, so these embryos could not be studied directly for CED-4 localization. Because *ced-3(n717)* did not affect the localization of CED-4 but does suppress the lethality of *ced-9(n2812)*, we used this double mutant to analyze CED-4 in the absence of CED-9. In *ced-9(n2812); ced-3(n717)* embryos, CED-4 was not localized to mitochondria but rather was associated with nuclear membranes (Fig. 2), as visualized by double-staining embryos with antibodies to CED-4 and antibodies directed against *C. elegans* lamin (*16*). We obtained similar results using the *ced-9* loss-of-function alleles *n1950 n2161* or *n1950 n2077* in combination with *ced-3(n717)*. Mitotracker Red staining was not altered in *ced-9(n2812); ced-3(n717)* embryos, indicating that the shift in CED-4 localization represents a

movement of CED-4 protein rather than a change in the morphology and/or localization of mitochondria (*17*).

To confirm this localization of CED-4 protein to nuclear membranes in *ced-9(lf)* embryos, we performed subcellular fractionations of embryo lysates (*18*). Both CED-9 and CED-4 were present predominantly in the organelle and membrane fraction, which includes the mitochondria [for example, (*19*)], in wild-type embryos (Fig. 3). By contrast CED-4 was present almost exclusively in the nuclear fraction in *ced-9(n2812); ced-3(n717)* embryos. Thus, in wild-type embryos, in which most cells survive, both CED-9 and CED-4 appeared to be predominantly mitochondrial. However, in *ced-9(n2812); ced-3(n717)* embryos, in which ectopic cell death was presumably initiated but blocked by the *ced-3* mutation, CED-4 was redistributed from mitochondria to nuclei. Thus, CED-9 protein is necessary to localize CED-4 to mitochondria.

These data suggest that stimuli that induce programmed cell death would induce a redistribution of CED-4 to nuclear membranes and that it might be possible to block programmed cell death by blocking CED-4 relocalization. We tested these predictions by ectopically inducing programmed cell death in embryos.

The binding of EGL-1 protein to CED-9 may directly inhibit CED-9 function and trigger programmed cell death by releasing CED-4 from a CED-9--CED-4 complex (*5,9*). To determine whether EGL-1 protein can affect the localization of CED-9 or CED-4, we expressed EGL-1 protein globally from an *egl-1* cDNA under the control of two *C. elegans* heat-shock promoters ($P_{hsp}$*egl-1*) (*20*) in the presence of the *ced-1(e1735)* mutation, which reduces cell-corpse engulfment and allows the quantification of cells that have undergone programmed cell death (*21*). Animals carrying heat-shock vectors without the *egl-1* cDNA insert developed normally, but transgenic animals carrying $P_{hsp}$*egl-1* arrested during embryogenesis following heat-shock treatment. The few hatched L1 larvae contained many more cell corpses than vector-only animals, indicating extensive programmed cell death (Table 1). Localization of CED-9 was unaffected in these animals. By contrast, overexpressed EGL-1 triggered the translocation of CED-4 from mitochondria to nuclei (Fig. 4A).

We next introduced the extrachromosomal array carrying $P_{hsp}$*egl-1* into two strains in which programmed cell death is blocked. The *ced-3(n717)* mutation suppressed programmed cell death induced by EGL-1 overexpression (Table 1) but did not affect CED-4 translocation from mitochondria to nuclear membrane (*22*). This

observation supports the idea that the release of CED-4 is not merely a consequence of cell death but rather precedes the execution of programmed cell death. Like *ced-3(n717)*, the *ced-9(n1950)* gain-of-function mutation blocked the ectopic death induced by *egl-1* overexpression (Table 1). However, unlike *ced-3(n717)*, *ced-9(n1950)* also blocked the translocation of CED-4 (Fig. 4B), suggesting this mutant form of CED-9 either is unable to interact with EGL-1 or is unable to release CED-4. We tested the interaction of CED-9(G169E) protein, which is encoded by the *ced-9(n1950)* mutation, with EGL-1 protein both *in vitro* and in yeast two-hybrid experiments and were unable to detect any difference between the interactions of the CED-9 and CED-9(G169E) proteins with the EGL-1 protein (*23*). It is possible that these *in vitro* studies failed to reveal a defect in the interaction between EGL-1 and CED-9 sufficient to produce the gain-of-function phenotype observed *in vivo* in *ced-9(n1950)* animals. Alternatively, in *ced-9(n1950)* animals EGL-1 may form a ternary complex with CED-9 and CED-4 without causing the release of CED-4. We also generated an *egl-1* heat-shock construct bearing the *egl-1(n3082)* mutation, which results in a truncated EGL-1 protein, a disruption of CED-9 binding and a strong cell-death defective phenotype. Transgenic animals carrying this construct had significantly fewer corpses than animals bearing the wild-type *egl-1* construct (Table 1). CED-4 localization was for the most part mitochondrial, but in occasional animals a few cells displayed nuclear CED-4 localization. Thus, overexpression of this *egl-1(n3082)* gene resulted in a weak partial induction of both programmed cell death and CED-4 translocation.

Overexpression of *egl-1* was sufficient to trigger both cell death and CED-4 translocation. Is *egl-1* necessary for the CED-4 translocation that occurs in the absence of CED-9? We stained *ced-9(n2812); ced-3(n717); egl-1(n1084 n3082)* embryos and determined that CED-4 protein was nuclear, just as in the *ced-9(n2812); ced-3(n717)* embryos. Thus, in the absence of CED-9 protein, EGL-1 is not required to release CED-4 from mitochondria to nuclei, indicating that EGL-1 promotes CED-4 translocation by antagonizing the activity of CED-9.

Thus, we observed that CED-4 was mitochondrial in living cells and nuclear in cells that had initiated programmed cell death, so that the subcellular localization of CED-4 appeared to correlate with the cell-death status of a cell. We next studied the localization of CED-4 in six *ced-4* missense mutants: *n2860, n2879, n3040, n3043, n3100, n3141*. In five of the six mutants, CED-4 was mitochondrially localized in the presence

of CED-9 and was associated with the nuclear membrane in the absence of CED-9, as in the wildtype. In *ced-4(n3040)* embryos, however, CED-4 displayed a diffuse, cytoplasmic localization both in the presence and in the absence of CED-9 (Fig. 4C), distinct from the web-like mitochondrial pattern of wild-type CED-4. *ced-4(n3040)*, which causes a proline-to-leucine substitution at amino acid 23, in a region that lacks any known protein motifs, results in as strong a cell-death defect as does *ced-4(n1162)*, which contains an early ochre nonsense mutation. This P23L substitution reduces the interaction between CED-9 and CED-4 by about 75% in the yeast two-hybrid assay (*24*). The failure of CED-4(P23L) to associate with either mitochondria or the nuclear membrane suggests that CED-4 is actively recruited not only to mitochondria (presumably through interaction with CED-9) but also to the nucleus. Alternatively, CED-4 may first have to interact with CED-9 to be competent to translocate to nuclear membranes. That wild-type CED-4 associated with nuclear membranes in the absence of CED-9 argues against this latter model.

CED-9 localization to mitochondria in *C. elegans* embryos is not surprising, since the mammalian CED-9-like cell-death protectors Bcl-2 and Bcl-$X_L$ both localize to mitochondria (*25*). Although Bcl-$X_L$ and the CED-4-like protein Apaf-1 have been reported to physically interact (*26*), Moriishi *et al.* (*27*) recently reported that they could find no interaction between Apaf-1 and any known anti-apoptotic Bcl-2 family member. Furthermore, there is no evidence for the localization of Apaf-1 to mitochondria. Apaf-1 was isolated as a cytosolic activator of caspases (*7*), and overexpressed CED-4 is cytosolic in mammalian cells (*8*). Therefore, the mitochondrial localization of CED-4 is unexpected.

Our data suggest a model in which the activity of CED-4 is regulated by its subcellular localization. Specifically, we propose that in living cells CED-9 prevents CED-4 activity by sequestering CED-4 to mitochondria. In cells triggered to undergo programmed cell death, EGL-1 binding to CED-9, possibly as a consequence of increased *egl-1* transcription (*28*), causes CED-4 release from CED-9 and allows the translocation of CED-4 to the nuclear region. There CED-4 activates the CED-3 procaspase, thereby causing programmed cell death.

How might we reconcile our finding with the report of Moriishi *et al.* (*27*) concerning their failure to detect interactions between Apaf-1 and Bcl-2 family members? One possibility is that CED-9 has anti-apoptotic activity independent of its

interaction with CED-4 and that this activity corresponds to the anti-apoptotic activity of Bcl-2 and Bcl-$X_L$. For example, CED-9 can directly inhibit the CED-3 caspase (*29*), although it has not been shown that this inhibition acts physiologically, and the region of CED-9 involved is not present in Bcl-2 or Bcl-$X_L$. Furthermore, at least some CED-4 is localized to the nuclear membrane at the permissive temperature in *ced-9*(*n1653*ts) embryos (*22*), suggesting that this mutant CED-9 protein can protect against cell death even when CED-4 is localized to the nucleus; however, we suspect that the level of nuclear CED-4 in these embryos is lower than in cells that are dying, so this level may simply be insufficient to trigger programmed cell death.

The death-promoting proteins Bax and BAD, which like EGL-1 contain BH3 domains, translocate to mitochondria and bind anti-apoptotic Bcl-2 family members in response to apoptotic signals (*30*). If and how this translocation promotes cell death is unknown. Our results suggest that Bax and BAD may act to release Apaf-1 or another CED-4-like protein, allowing it to activate caspase processing. Some caspase precursors, specifically procaspases-2, and –3 are present in mitochondria and upon activation translocate to nuclei (*31*). It is possible that this movement of caspases involves the translocation of a complex that includes a CED-4-like protein. By analogy, the translocation of a CED-4 CED-3 complex from mitochondria to the nuclear envelope could provide access for the active caspase to both the nucleus and the cytosol, thereby fulfilling the roles of the multiple, differentially-localized mammalian caspases.

The release of CED-4 from mitochondria resulted in the translocation of CED-4 to another distinct subcellular compartment rather than in the dispersal of CED-4 throughout the cell. This result, combined with our finding that the CED-4(P23L) mutant protein was diffusely cytoplasmic, suggests that CED-4 is recruited to nuclear membranes, possibly by interacting with another protein or protein complex. The identification of such a CED-4 receptor should help us understand the mechanism of action of CED-4 in the execution of programmed cell death.

## REFERENCES AND NOTES


1. M. D. Jacobson, M. Weil and M. C. Raff, *Cell* **88**, 347-54. (1997).

2. C. B. Thompson, *Science* **267**, 1456-62. (1995).

3. M. M. Metzstein, G. M. Stanfield and H. R. Horvitz, *Trends Genet.* **14**, 410-6 (1998).

4. M. O. Hengartner and H. R. Horvitz, *Cell* **76**, 665-76 (1994).

5. B. Conradt and H. R. Horvitz, *Cell* **93**, 519-29 (1998).

6. J. Yuan *et al.*, *Cell* **75**, 641-52 (1993).

7. H. Zou *et al.*, *Cell* **90**, 405-13 (1997).

8. D. Wu, H. D. Wallen and G. Nunez, *Science* **275**, 1126-9 (1997); M. Irmler *et al.*, *FEBS Lett.* **406**, 189-90 (1997); A. M. Chinnaiyan *et al.*, *Science* **275**, 1122-6. (1997); M. S. Spector *et al.*, *Nature* **385**, 653-6 (1997).

9. L. del Peso, V. M. Gonzalez and G. Nunez, *J. Biol. Chem.* **273**, 33495-500. (1998).

10. S. Seshagiri and L. K. Miller, *Curr. Biol.* **7**, 455-60 (1997).


11. A partial *ced-9* cDNA was cloned into vector pET19b to generate a His-10-CED-9 fusion protein lacking the C-terminal 29 amino acids of CED-9. The fusion protein was purified on $Ni^{2+}$-nitrilotriacetic acid-agarose (Qiagen) according to the manufacturer's instructions and injected with RIBI adjuvant into rabbits. The antiserum was affinity-purified against His-10-CED-9 immobilized on nitrocellulose. For the generation of CED-4 antibodies, full length *ced-4S* cDNA was cloned into pXHA [S. J. Elledge *et al.*, *Proc. Natl. Acad. Sci. U. S. A.* **89**, 2907-11 (1992)]. The hemagglutinin-CED-4 fusion was purified from inclusion bodies of *Escherichia coli* and injected into rabbits and rats. The rabbit antisera was used without further purification, and rat antiserum was affinity-purified against glutathione-S-transferase-CED-4 immobilized on nitrocellulose. Embyros were collected by bleaching mixed-stage worms in a 0.8 N NaOH, 8% hypochlorite solution. Embryos were fixed and permeabilized essentially as described [C. Guenther and G. Garriga, *Development* **122**, 3509-18 (1996)]. Embryos were incubated in a 1:100 dilution of primary antibody, washed four times, incubated for 2 hours in 1:25 dilution of secondary antibody, washed four times, washed once in phosphate-buffered saline plus 4',6'-diamidino-2-phenylindole (DAPI, 1$\mu$g/ml), and resuspended in an equal volume of VECTASHIELD mounting medium (Vector Labs). Embryos for mitochondrial colocalization experiments were collected from worms

grown in the dark on NGM agar plates containing MitoTracker Red CMXRos (2 μg/ml, Molecular Probes).

12. Supplementary data can be found in Web Figure 1 at www.sciencemag.org/feature/data/1046764.shl.

13. Mutant strains carrying the following alleles of cell-death genes were used in this study: *ced-1(e1735)*, engulfment-defective; *ced-3(n717)*, splice acceptor mutation, exon 7; *ced-9(n2812)*, Q46amber; *ced-9(n1950)*, G169E; *ced-9(n1950 n2161)*, *ced-9(n1950 n2077)*, loss-of-function mutations; *ced-9(n1653)*, Y149N; *ced-4(n1162)*, Q79ochre; *ced-4(n2860)*, E263K; *ced-4(n2879)*, E276K; *ced-4(n3040)*, P23L; *ced-4(n3043)*, D20N; *ced-4(n3100)*, S339P; *ced-4(n3141)*, R53K; *egl-1(n1084)*, G-to-A nucleotide transversion at nt +5631; *egl-1(n1084 n3082)*, *n1084* lesion plus 5-bp deletion in *egl-1* coding region.

14. M. Poot *et al.*, *J. Histochem. Cytochem.* **44**, 1363-72 (1996).

15. J. Yuan and H. R. Horvitz, *Development* **116**, 309-20 (1992).

16. D. Riemer, H. Dodemont and K. Weber, *Eur. J. Cell. Biol.* **62**, 214-23 (1993).

17. Supplementary data can be found in Web figure 2 at www.sciencemag.org/feature/data/1046764.shl.

18. Embryos for fractionation were collected as described (*11*). Embryos were resuspended in 5 volumes of cold hypotonic buffer (10 mM KCl, 1.5 mM MgCl2, 1 mM EDTA, 1 mM EGTA, 1 mM dithiothreitol, 0.1 mM phenylmethylsulfonyl fluoride, 250 mM sucrose) and homogenized in a 1-ml Dounce tissue grinder. The homogenates were spun at 40*g* briefly to remove worm debris. The supernatant was centrifuged twice at 750*g* for 10 min, and the resulting pellets were pooled as the nuclear fraction. The supernatant was further centrifuged at 100,000*g* for 1 hour. The pellet was designated the organelle and membrane fraction and the supernatant the soluble cytosolic S100 fraction. The pooled nuclear fraction was washed once with homogenization buffer. One-fifth of each fraction was used for immunoblotting analysis. Rabbit polyclonal antibody directed against human acetylated histone H4 (Upstate Biotechnology) was used as a marker for the nuclear fraction. Monoclonal anti-Ce HSP90 antibody was used as a marker for the cytosolic fraction.

19. D. D. Newmeyer, D. M. Farschon and J. C. Reed, *Cell* **79**, 353-64. (1994).

20. $P_{hsp}$*egl-1* (*5*) was injected at a concentration of 2 ng/μL, along with p76-16B [L. Bloom, H. R. Horvitz, *Proc. Natl. Acad. Sci. U. S. A.* **94**, 3414-9 (1997)] at 50 ng/μL, into a *ced-1(e1735)*; *egl-1(n1084 n3082)* *unc-76(e911)* strain as described [C. Mello, A. Fire,

*Methods Cell Biol.* **48**, 451-82 (1995)]. For immunofluorescence, mixed stage transgenic worms were incubated at 33°C for 1 hour followed by a 2-hour recovery at 20°C. Embryos were then collected as in (*11*). For analysis of cell corpses, transgenic adults were allowed to lay eggs at 20°C for 2 hours, subjected to a 1-hour heat shock at 33°C, allowed to lay eggs for an additional 2 hours at 20°C, and then removed from the plates. Hatched L1 transgenic animals were examined by Nomarski microscopy for corpses in the head.

21. E. M. Hedgecock, J. E. Sulston and J. N. Thomson, *Science* **220**, 1277-9. (1983).

22. F. Chen, B. M. Hersh, H. R. Horvitz, data not shown.

23. B. M. Hersh, B. Conradt, H. R. Horvitz, data not shown.

24. S. Ottilie *et al., Cell Death Diff.* **4**, 526-33 (1997).

25. M. Nguyen *et al., J. Biol. Chem.* **268**, 25265-8. (1993); Y. Akao *et al., Cancer Res* **54**, 2468-71 (1994); S. Krajewski *et al., Cancer Res.* **53**, 4701-4714 (1993).

26. G. Pan, K. O'Rourke and V. M. Dixit, *J. Biol. Chem.* **273**, 5841-5 (1998); Y. Hu *et al., Proc Natl Acad Sci U S A* **95**, 4386-91 (1998).

27. K. Moriishi *et al., Proc. Natl. Acad. Sci. USA* **96**, 9683-8. (1999).

28. B. Conradt and H. R. Horvitz, *Cell* **98**, 317-27. (1999).

29. D. Xue and H. R. Horvitz, *Nature* **390**, 305-8. (1997).

30. K. G. Wolter *et al., J. Cell. Biol.* **139**, 1281-92 (1997).

31. S. A. Susin *et al., J. Exp. Med.* **189**, 381-94. (1999); M. Mancini *et al., J. Cell Biol.***140**, 1485-95 (1998); B. Zhivotovsky, A. Samali, A. Gahm and S. Orrenius, *Cell Death Diff* **.6**, 644-51 (1999).

32. We thank members of the Horvitz laboratory for helpful comments and discussions concerning this manuscript. We thank Y. Yamaguchi and J. Miwa for anti-Ce HSP90 monoclonal antibody; D. Xue for generating pET19b-CED-9ΔC; B. Davies, A. Madi, S. Shaham, E. Speliotes, and G. Stanfield for *ced-4* missense mutations; B. Castor for DNA sequence determinations; and M. Boxem and S. van den Heuvel for assistance with microscopy. B. M. H. was supported by a Howard Hughes Predoctoral Fellowship. B.C. was supported by a postdoctoral fellowship from the Jane Coffin Childs Memorial Fund for Medical Research and a Leukemia Society Special Fellowship. Z. Z. was supported by a Cancer Research Fund of the Damon Runyon-Walter Winchell Foundation Fellowship (DRG 1343). H. R. H. is an Investigator of Howard Hughes Medical Institute.

## TABLES AND FIGURES

**Table 1. EGL-1 induces ectopic cell death that can be suppressed by the *ced-9* gain-of-function mutation *n1950*.**

Corpses were counted in the heads of transgenic L1 animals subjected to heat shock (*19*) and represent the mean ± SD and range observed (*n*, no. animals). The *egl-1(n1084 n3082)* allele is referred to as *egl-1(lf)*, whereas *egl-1(n3082)* indicates a transgene engineered to contain only the *n3082* 5bp deletion and not the *n1084* lesion in the *egl-1* 3' regulatory region.

| Genotype | Array | Number of corpses | Range | *N* |
|---|---|---|---|---|
| *ced-1; egl-1(lf)* | vector alone | 0.4 ± 0.6 | 0-2 | 15 |
| *ced-1; egl-1(lf)* | $P_{hsp}$*egl-1* | 45.4 ± 18.7 | 16-75 | 16 |
| *ced-1; ced-3; egl-1(lf)* | $P_{hsp}$*egl-1* | 0.5 ± 0.7 | 0-2 | 15 |
| *ced-1; ced-9(n1950); egl-1(lf)* | $P_{hsp}$*egl-1* | 1.3 ± 1.3 | 0-4 | 15 |
| *ced-1; egl-1(lf)* | $P_{hsp}$*egl-1(n3082)* | 4.4 ± 3.2 | 0-13 | 20 |

**Figure 1. CED-9 and CED-4 are localized to mitochondria in wild-type embryos.** **(A)** CED-9 expression in a wild-type embryo of approximately 30-50 cells. **(B)** Mitotracker Red localization in the same embryo as in (A). **(C)** Merged image of (A) and (B). **(D)** CED-4 expression in a wild-type embryo of approximately 200 cells **(E)** Mitotracker Red localization in embryo in (D). **(F)** Merged image of (D) and (E)

# Figure 1

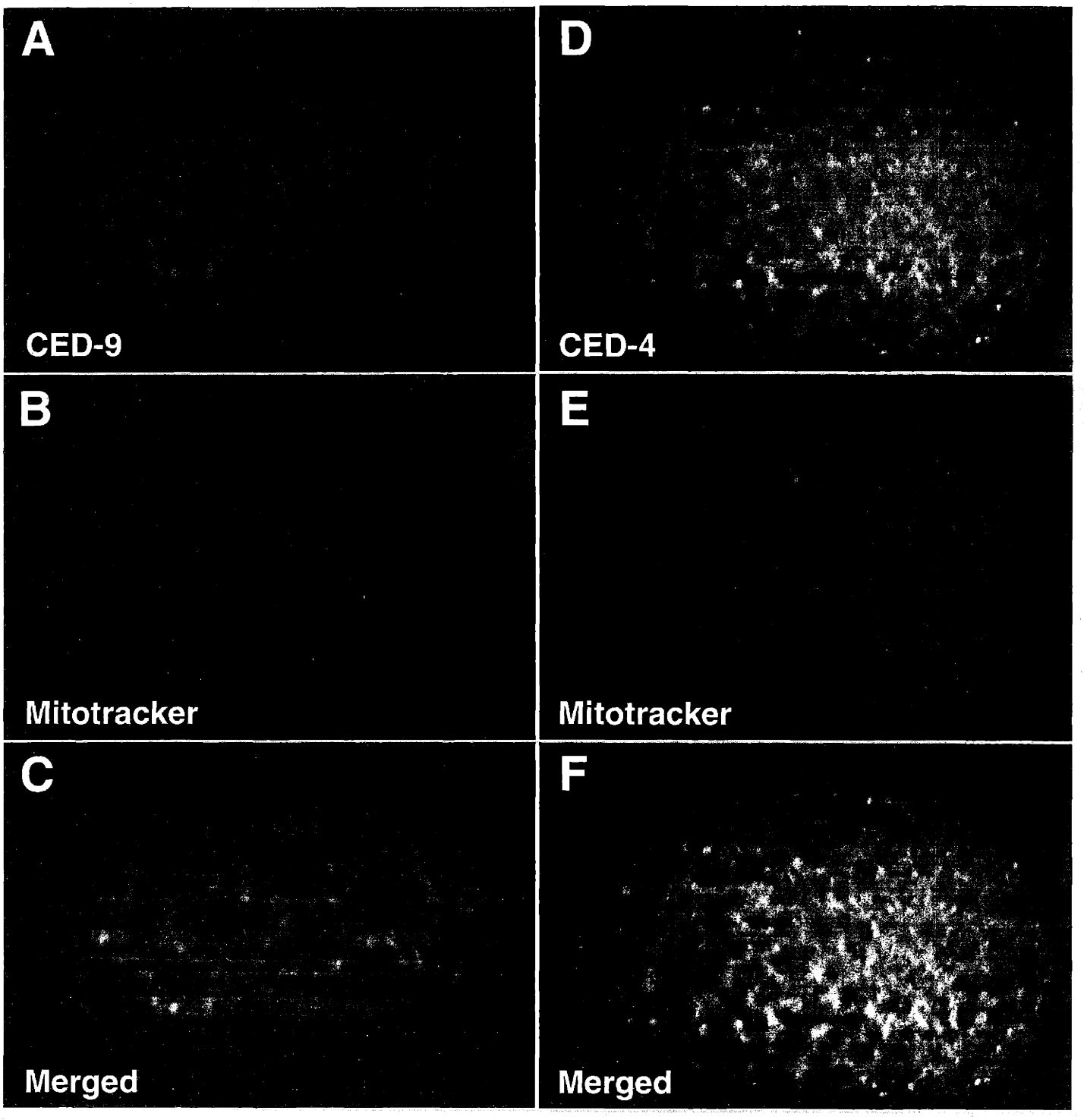

**Figure 2. CED-9 is required for the localization of CED-4 to mitochondria.**
**(A)** CED-4 expression in wild-type embryo of approximately 150 cells. **(B)** Lamin localization in same embryo as in (A). **(C)** CED-4 expression in a *ced-9(n2812); ced-3(n717)* embryo of approximately 150 cells. **(D)** Lamin staining of embryo in (F).

# Figure 2

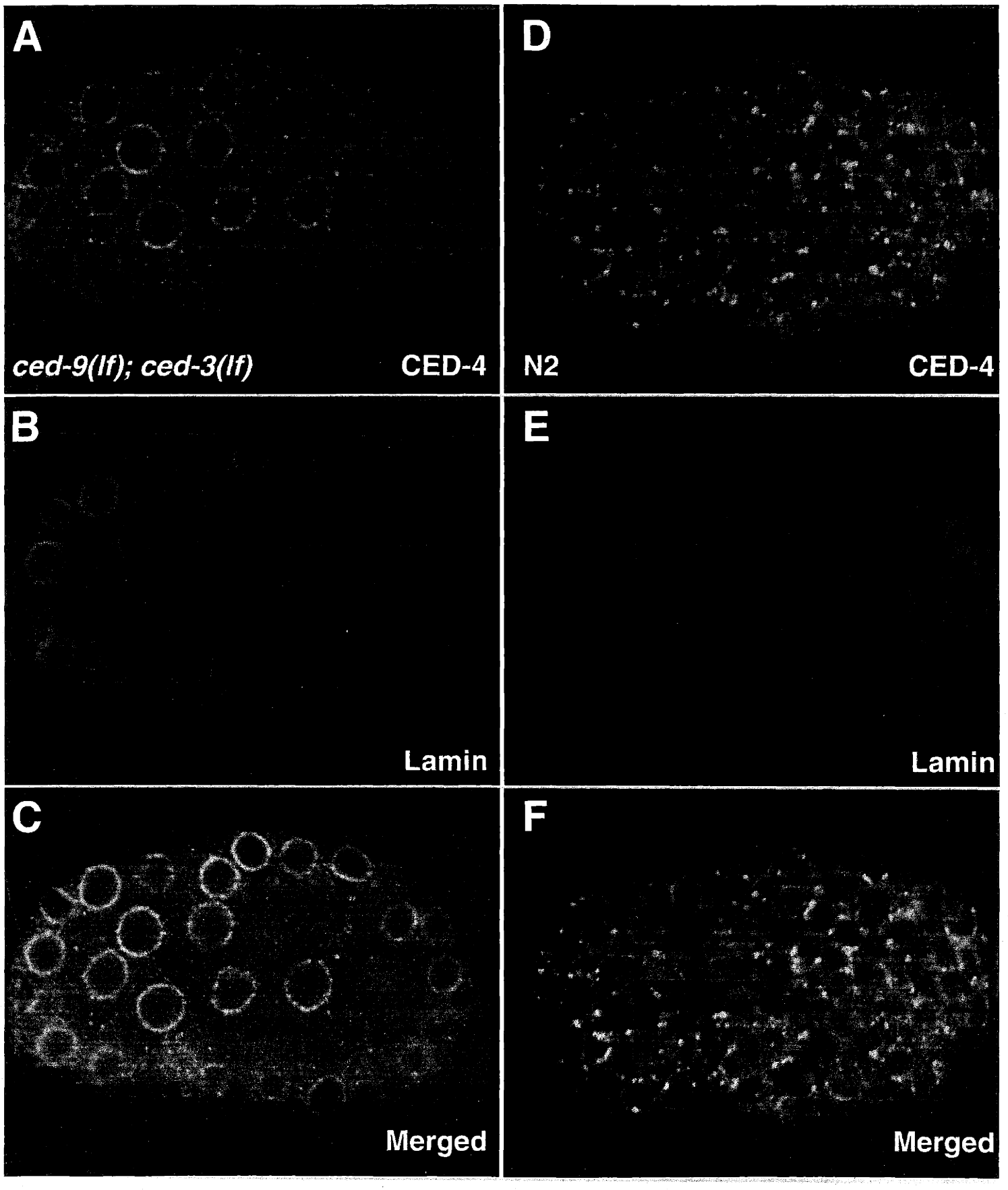
A
ced-9(lf); ced-3(lf)
CED-4
D
N2
CED-4
B
Lamin
E
Lamin
C
Merged
F
Merged

**Figure 3. CED-4 fractionates primarily with membranes and organelles from wild-type embryos and with nuclei from *ced-9(lf)* embryos.**

Western blot of subcellular fractionation (*15*) of lysates from wild-type and *ced-9(n2812); ced-3(n717)* double mutant embryos ,separated into nuclear, organelle and membrane, and cytosolic fractions. Histone H4, a nuclear fraction marker. HSP90, *C. elegans* heat-shock protein, a cytosolic marker.

# Figure 3

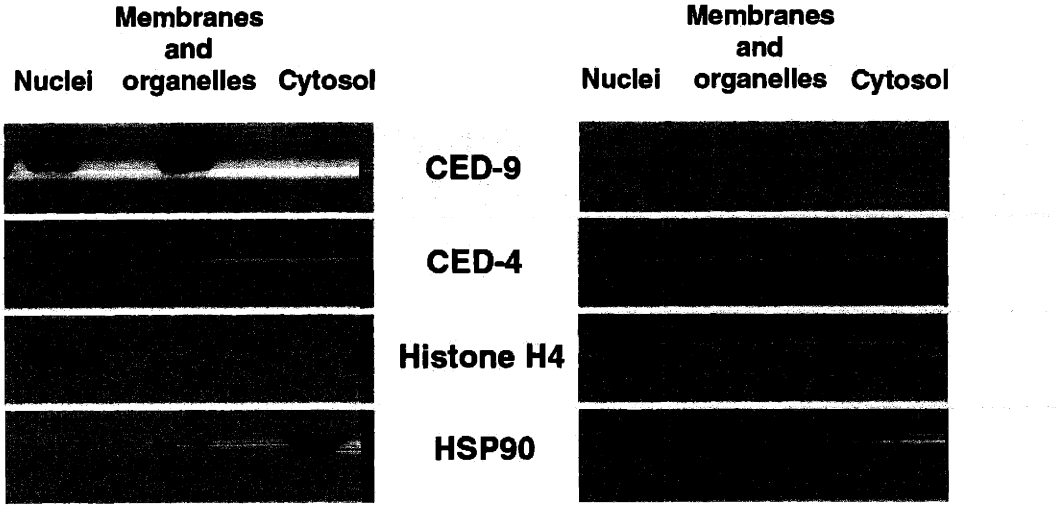


**N2** ***ced-9(lf); ced-3(lf)***

**Figure 4. Overexpression of EGL-1 induces CED-4 translocation from mitochondria to nuclear membranes in *ced-9*(+) embryos but not in *ced-9*(*n1950*) embryos.**
**(A)** CED-4 localization following heat shock in a *ced-9*(+) embryo carrying $P_{hsp}$*egl-1*. **(B)** CED-4 localization following heat shock in a *ced-9*(*n1950*) embryo carrying $P_{hsp}$*egl-1*. **(C)** CED-4 localization in a *ced-4*(*n3040*) embryo was diffusely cytoplasmic.

**Figure 4**

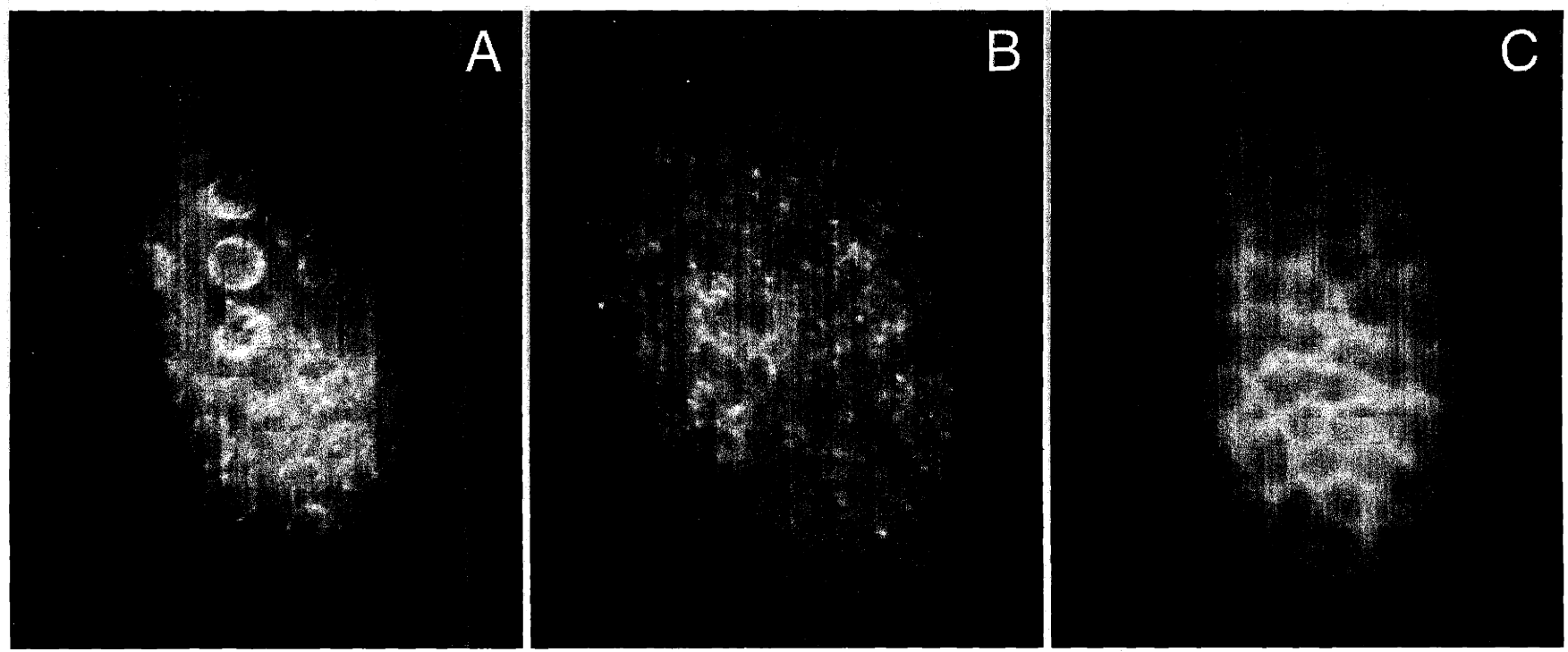

**Web Figure 1. Western blot of embryo lysates.**

CED-9 protein is present in wild-type and *ced-4* mutant worms but is absent in embryos carrying the *ced-9(n2812)* mutation. CED-4 protein is present in wild-type and *ced-9; ced-3* double mutant worms but is absent in either *ced-4* or *ced-4 ced-9* double mutant strains.

## Web Figure 1

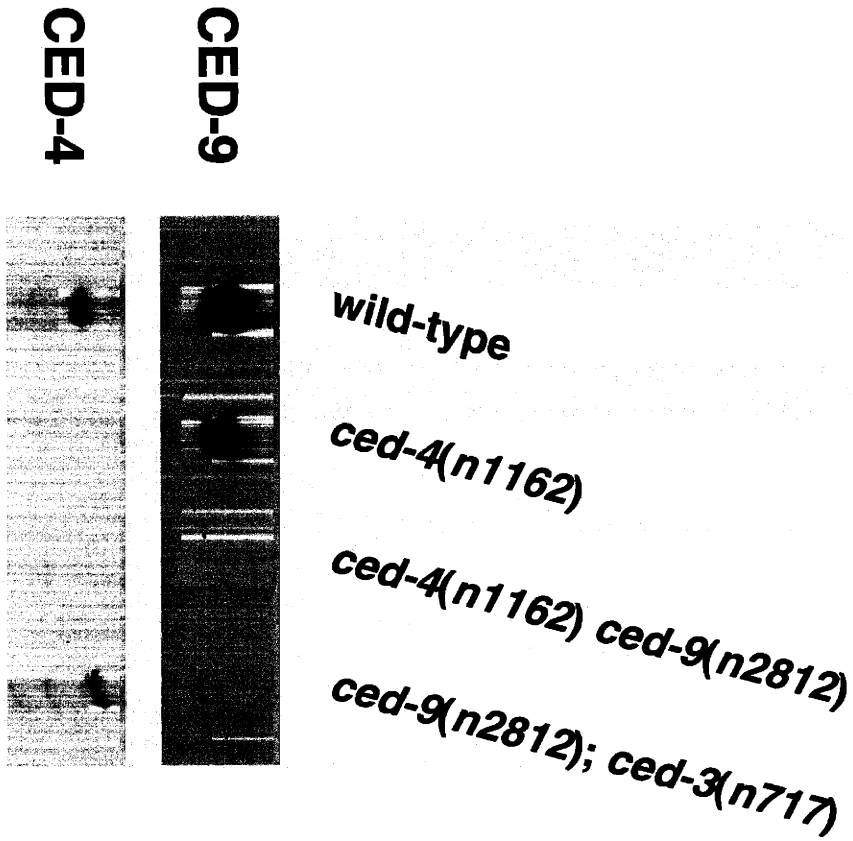
CED-4
CED-9
wild-type
ced-4(n1162)
ced-4(n1162) ced-9(n2812)
ced-9(n2812); ced-3(n717)

**Web Figure 2. Localization of mitochondria is unaffected by loss-of-function mutations in *ced-9*.**

**(A)** Mitotracker Red staining of a *ced-9*(*n2812*); *ced-3*(*n717*) mutant embryo. **(B)** CED-4 staining of same embryo, demonstrating the altered localization of CED-4 protein in the absence of CED-9. **(C)** Merged image, establishing that CED-4 and Mitotracker Red are no longer co-localized and that the observed perinuclear localization of CED-4 is not caused by a change in the morphology or localization of mitochondria.

# Web Figure 2

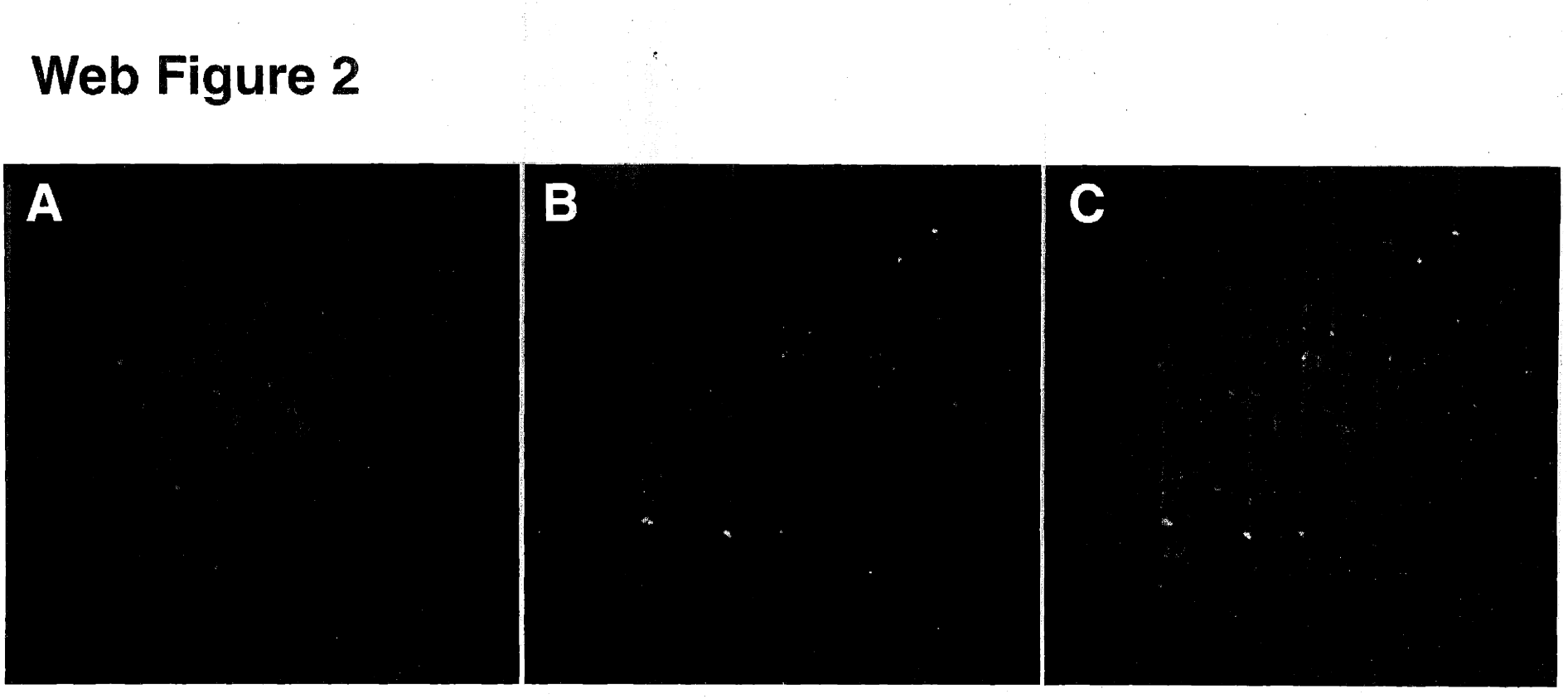

# Chapter 3

# The *C. elegans* mucolipin-like gene *cup-5* is essential for viability and regulates lysosomes in multiple cell types

Bradley M. Hersh, Erika Hartwieg, and H. Robert Horvitz

This chapter is written for submission to *Proc. Natl. Acad. Sci. USA*. Erika Hartwieg performed the electron microscopy described here.

**ABSTRACT**

The misregulation of programmed cell death, or apoptosis, can contribute to the pathogenesis of many diseases. We used Nomarski microscopy to screen for mutants containing refractile cell corpses in a *C. elegans* strain in which all programmed cell death is blocked and such corpses are absent. We isolated a mutant strain that accumulates refractile bodies resembling irregular cell corpses. We rescued this mutant phenotype with the *C. elegans* ML-IV (mucolipidosis type IV) homolog, the recently identified *cup-5* (*c*oelomocyte-*up*take defective) gene. ML-IV is a human autosomal recessive lysosomal storage disease characterized by psychomotor retardation and opthalmological abnormalities. Our null mutations in *cup-5* cause maternal-effect lethality. In addition, *cup-5* mutants contain excess lysosomes in many and possibly all cell types and contain lamellar structures similar to those observed in ML-IV cell lines. The human ML-IV gene is capable of rescuing both the maternal-effect lethality and lysosome-accumulation abnormality of *cup-5* mutants. *cup-5* mutants appear to contain excess apoptotic cells as detected by TUNEL (TdT-mediated dUTP nick-end labeling) staining. We suggest that the increased apoptosis seen in *cup-5* mutants is a secondary consequence of the lysosomal defect and that abnormalities in apoptosis may be associated with human lysosomal storage disorders.

## INTRODUCTION

Programmed cell death or apoptosis regulates cell number during metzoan development (1). The misregulation of programmed cell death, resulting in either too many or too few dying cells, contributes to the pathogenesis of many human diseases (2). For example, animal models of human retinitis pigmentosa indicate that retinal degeneration occurs by apoptotic death and that blocking this death prevents retinal degeneration (3-5). Mutations that disrupt Fas-mediated apoptosis in the immune system of mice and humans lead to lymphoproliferative disorders (6, 7). The inhibition of apoptosis caused by the misexpression of the proto-oncogene Bcl-2 is a primary cause of human follicular lymphoma (8), a cancer of the immune system.

Studies of the nematode *Caenorhabditis elegans* have played an important role in defining the components that regulate and execute programmed cell death (9). To seek new genes that can affect programmed cell death, we screened for suppressors of a gain-of-function (gf) allele of the *C. elegans* Bcl-2-like gene *ced-9*. The *ced-9* gene normally protects cells that should survive from undergoing programmed cell death (10), and the *ced-9*(gf) allele *n1950* causes all programmed cell death to be blocked (11). In this paper, we describe one *ced-9*(gf) suppressor, which proved to be a mutation in the *C. elegans* counterpart of the human mucolipidosis type IV (ML-IV) gene (12, 13) *cup-5* (coelomocyte-uptake defective) (14). We show that null mutations in *cup-5* cause maternal-effect lethality, accumulation of lysosomes, and an increase in programmed cell death, and we suggest that the pathology of human mucolipidosis type IV may involve abnormal programmed cell death.

## MATERIALS AND METHODS

### Genetics and Strains

Strains were cultured as described (15) at 20°C. The wild-type parental strain was *C. elegans* Bristol N2. Mutagenesis with ethyl methanesulfonate and genetic mapping were performed by standard methods (16). Mutations used were: linkage group I (LGI): *ced-1(e1735), sem-4(n1378)*; LGIII: *unc-36(e251), dpy-17(e164), ncl-1(e1865), sma-3(e491), ced-9(n1950), ced-9(n2812), ced-4(n1162), unc-79(e1068), qC1* [*dpy-19(e1259) glp-1(q339)*]; LGIV: *ced-3(n717), unc-31(e928), ced-5(n1812)*. We used three-factor mapping to localize *n3194* between *sma-3* and *ncl-1*: *sma-3* (10/14) *n3194* (4/14) *ncl-1*.

### Cloning and molecular characterization

Cosmids from the region between *sma-3* and *ncl-1* were injected into *unc-36 cup-5(n3194)/qC1* animals at 20 μg/ml with pRF4, which contains the *rol-6(su1006)* allele, at 80 μg/ml as a co-injection marker. Rescue of maternal-effect lethality was tested in Rol Unc animals from stably transmitting transgenic lines. cDNA clones for *cup-5* were provided by Y. Kohara (National Institute of Genetics, Japan). We determined the 5′ end of the *cup-5* message by 5′ rapid amplification of cDNA ends (5′-RACE System, Gibco-BRL).

### Heat-shock experiments

To test rescue of the *cup-5* mutant phenotype by *cup-5* and human ML-IV cDNAs, full-length cDNAs were cloned into the heat-shock vectors pPD49.78 and pPD49.83 (17). These clones were injected at 50 μg/ml each with pRF4 into *unc-36 cup-5(n3194)/qC1* animals. At least six Rol Unc animals from stable transgenic lines were used for each experiment. Animals were allowed to lay eggs at 20°C for 24 hr prior to heat shock (-HS). Adults were then transferred to new plates, incubated at 33°C for 1 hr, and allowed to lay eggs at 20°C for an additional 24 hr (+HS). Adults were removed, and the number of embryos on each plate was determined. The number of embryos that had hatched was counted one day after the removal of Rol Unc adults. The number of embryos that had reached adulthood was determined four days after removal of adults.

**TUNEL, acridine orange, and Lysotracker staining**

TUNEL staining was performed as described (18). *cup-5(n3194)* embryos for TUNEL staining were obtained from *cup-5(n3194)* hermaphrodites.

For acridine orange staining, embryos were isolated by treating adults with 0.8 M NaOH, 8% hypochlorite solution until adults had been dissolved and embryos were released. Embryos were incubated in 50 $\mu$g/ml acridine orange in embryo buffer (113 mM NaCl, 40 mM KCl, 3.4 mM $CaCl_2$, 3.4 mM $MgCl_2$, 10 mM Na-HEPES pH 7.5) for 1 hr prior to observation using epifluorescence microscopy.

For Lysotracker staining, NGM agar plates (16) were supplemented with Lysotracker Red (Molecular Probes) at 2 $\mu$M. L4 stage animals were placed on Lysotracker plates and incubated in the dark at 20°C. Embryos from these plates were observed using confocal microscopy (Zeiss LSM 510) at an excitation wavelength of 543 nm.

**Electron microscopy**

Electron microscopy was performed as described (19). L1 larvae were obtained from either *cup-5(n3264)* or *cup-5(n3194)* homozygous hermaphrodites.

## RESULTS

### Isolation of *n3194*

*ced-9(n1950)* is a gain-of-function mutation that blocks all somatic programmed cell deaths that occur during normal *C. elegans* development (11). To seek mutations that can cause cells to undergo programmed cell death even in the presence of the *ced-9(n1950)* mutation, we performed a screen for suppressors of *ced-9(n1950)*. Using Nomarski optics microscopy, we looked for cell corpses in progeny of mutagenized *ced-1(e1735) sem-4(n1378); ced-9(n1950)* animals. Mutations in the *ced-1* gene cause the persistence of unengulfed apoptotic corpses because of defects in a receptor that recognizes and promotes the engulfment of dying cells (20). Mutations in the *sem-4* gene disrupt the development of the hermaphrodite sex muscles and therefore prevent egg-laying (21), such that all progeny from a single mother can be easily screened and siblings of animals carrying homozygous lethal mutations can be obtained.

We performed two screens, of approximately 10,000 mutagenized haploid genomes for mutations with a zygotic suppression phenotype and of 6,000 haploid genomes for mutations conferring a maternal-effect suppression phenotype. From the maternal-effect screen we isolated three mutations that conferred a recessive maternal-effect lethal phenotype: *n3196*, *n3213*, and *n3194*.

The *n3196* mutation resulted in embryos containing apparently vacuolated cells, beginning at about the 50-cell stage (Figure 1A). The *n3213* mutation resulted in a similar degenerative vacuolarization defect, but the effect was limited to the posterior portion of the embryo (Figure 1B). Neither of these mutations restored the presence of refractile, unengulfed corpses as seen in *ced-1(e1735)* embryos, so they likely represent defects unrelated to the well-characterized programmed cell death pathway; *n3196* and *n3213* might affect non-apoptotic degenerative deaths.

The third mutation, *n3194*, appeared to affect programmed cell death. Embryos derived from homozygous *n3194* hermaphrodites accumulated refractile corpse-like bodies beginning at the comma stage (Figure 1C), approximately the time at which corpses begin to accumulate in *ced-1(e1735)* embryos. By the two-fold to three-fold stage of embryogenesis (Figure 1D), *n3194* embryos were filled with refractile bodies, and the embryos arrested development shortly thereafter. Rare animals that survived to hatching arrested as L1 larvae.

Using the maternal-effect lethal phenotype, we mapped the *n3194* mutation to chromosome III (data not shown). *ced-9* maps to chromosome III, and loss-of-function mutations in *ced-9* both suppress *ced-9(n1950gf)* and cause maternal-effect lethality with an accumulation of corpses (10). However, *n3194* was unlikely to be an allele of *ced-9*, since *n3194* complemented *ced-9(n2812)*, a putative null allele of *ced-9* (22). *n3194* appeared to allow cell death to occur in *ced-9(n1950)* animals, in which cells that normally die instead survive. To determine if *n3194* suppresses this effect of *ced-9(n1950)* we counted the number of cells in the anterior pharynx of homozygous *n3194 ced-9(n1950)* animals derived from *n3194 ced-9(n1950)/+ ced-9(n1950)* mothers. These animals contained 12.0 ± 1.6 extra cells in the anterior pharynx, as compared to 11.9 ± 1.1 for *ced-9(n1950gf)* animals. Thus, either *n3194* does not suppress the survival of extra cells caused by *ced-9(n1950gf)* or a maternal contribution of the *n3194* gene product is sufficient for function. As embryos derived from homozygous *n3194* mothers do not survive until cells in the pharynx can be counted, this latter possibility cannot be directly tested.

Two additional mutations that failed to complement *n3194* were identified in unrelated screens. The mutation *zu223* was isolated in a screen for mutations with a maternal-effect lethal phenotype and observed to have excess refractile corpses in arrested embryos (J. Priess, personal communication). The mutation *n3264* was isolated in a screen for mutants defective in cell-corpse engulfment (Z. Zhou and H. R. Horvitz, unpublished data). We found that *n3264* and *zu223* failed to complement *n3194* for both maternal-effect lethality and the accumulation of refractile bodies. *n3264* appears to be a partial loss-of-function allele, since unlike *zu223* or *n3194* it does not confer a maternal-effect lethal phenotype; *n3264* does cause accumulation of refractile bodies in embryos.

### *n3194* is a mutation in the *C. elegans* mucolipidosis type IV gene

We further mapped *n3194* to a region of chromosome III between *sma-3* and *ncl-1* (see Materials and Methods). We injected cosmids from this region and rescued the maternal-effect lethality conferred by *n3194* with cosmid C30C5. We subcloned this cosmid and identified an 8.6 Kb *Kpn*I-*Hpa*I rescuing fragment that contained only one complete open reading frame, R13A5.1. Deleting a portion of this reading frame while retaining the two partial open reading frames 5′ and 3′ of R13A5.1 eliminated rescuing

ability. This minimal rescuing fragment also completely rescued the accumulation of refractile corpses in *n3194* embryos.

A mutation causing inappropriate accumulation of green fluorescent protein in coelomocytes, cells of unknown function in the *C. elegans* pseudocoelom, was recently found to be a missense mutation in R13A5.1 by Fares and Greenwald (14). This mutation, *ar465*, defined the gene *cup-5*. Thus, *n3194*, *n3264*, and *zu223* are alleles of *cup-5*. *cup-5(ar465)* animals have endocytic trafficking defects, but no defects in viability.

Two classes of EST clones isolated by the *C. elegans* EST project correspond to the predicted gene R13A5.1 and differ slightly from each other, from the GENEFINDER (23) prediction for the structure of this gene as well as from the structure described by Fares and Greenwald (14). The two classes of EST clones differ in the length of exon 8. Three clones (*yk517f10*, *yk611f2*, and *yk280c8*) are in-frame with exon 9 and encode a predicted protein of 668 amino acids, which we refer to as CUP-5L (L, long). Three other clones (*yk253a6*, *yk643f6*, and *yk561c9*) extend exon 8 by four nucleotides, shifting the reading frame with respect to exon 9 and encode a predicted protein of 611 amino acids, which we refer to as CUP-5S (S, short). The two predicted proteins are identical through the first 603 amino acids. The *cup-5S* transcript corresponds to the previously reported *cup-5* sequence (14), but the longer *cup-5L* transcript was not previously reported. Neither class of cDNA contains the first exon predicted by GENEFINDER. Therefore, we performed 5′-RACE (rapid amplification of cDNA ends) analysis on mixed-stage N2 RNA to determine the starting point of the transcript. The cDNA amplified in this manner contained an SL1 leader sequence (24) followed immediately 3′ by the in-frame ATG codon at the start of the GENEFINDER predicted second exon, consistent with the starting point we observed in the longest of the EST clones.

We expressed *cup-5L* and *cup-5S* individually under the control of the *C. elegans* heat-shock promoters to test their abilities to rescue the maternal-effect lethality caused by *cup-5(n3194)*. *cup-5(n3194)* mutant animals bearing either a $P_{hsp}$*cup-5L* or a $P_{hsp}$*cup-5S* transgenic array were subjected to heat shock, and embryos derived from these animals were assayed for viability. The $P_{hsp}$*cup-5L* and $P_{hsp}$*cup-5S* constructs each effectively rescued the maternal-effect lethality (Table 1), indicating that both forms are functional. The vector alone did not rescue.

The CUP-5 protein is similar to the product of the human mucolipidosis type IV gene (12, 13) (Figure 2). Human ML-IV is a lysosomal storage disorder found most often

in Ashkenazic Jews and is characterized by lipid accumulation in lysosomes and consequent psychomotor retardation, impairment of cognitive development, corneal clouding, and retinal degeneration (25, 26). Cells derived from ML-IV patients are not defective in the lysosomal hydrolases that participate in lipid catabolism, but appear to have a block in transport or sorting of late endosome-lysosome vesicles (27, 28). CUP-5 is also similar to the predicted *Drosophila* protein CG8743 and the predicted human protein FLJ11006.

We identified mutations in the coding region of *cup-5* in all three of the alleles we studied (Figure 2). *n3194* and *zu223*, which confer a maternal-effect lethal phenotype, introduce stop codons early in the gene. The weaker allele, *n3264*, converts a conserved glycine to an aspartate. Both *zu223* and *n3194* are candidate molecular null alleles, and *cup-5(n3194)* homozygotes are similar in the penetrance of maternal-effect lethality (Table 2A) and refractility (data not shown) to *cup-5(n3194)/Df* animals. Therefore, the phenotype of *cup-5(n3194)* and *cup-5(zu223)* animals likely represents the null phenotype of this gene.

**Human ML-IV can substitute for *cup-5***

We obtained a human ML-IV (hML-IV) cDNA from G. Borsani (TIGEM Institute, Italy) and placed it under the control of the *C. elegans* heat-shock promoters. The expression of hML-IV rescued the maternal-effect lethality associated with *cup-5(n3194)*, although not as strongly as did either of the *C. elegans* cDNA clones (Table 1). Most animals that survived to hatching progressed to become healthy adults. A 5 bp frameshift introduced into the hML-IV cDNA (*Bst*EII site, nucleotide position 460) abolished rescue, demonstrating that functional ML-IV gene product is required for rescue.

***cup-5* mutants contain excess lysosomes**

As a single missense allele of *cup-5* had been previously identified on the basis of accumulated green fluorescent protein (GFP) in coelomocytes (14), and since this allele appears not to be a null allele, we tested whether the null alleles of *cup-5* we identified also conferred such a defect. A secreted GFP expressed under the control of the *myo-3* promoter normally is diffuse through the *C. elegans* pseudocoelom but accumulated in

the coelomocytes of both *cup-5(n3194)* homozygotes and *cup-5(n3264)* animals (data not shown), as it does in *cup-5(ar465)* animals (14).

We also tested whether *cup-5* mutants contain an increased number of lysosomes, as occurs in patients with ML-IV. We stained embryos with acridine orange (AO), an acidophilic dye that stains acidified lysosomal and endosomal compartments in protists, plants, insects, nematodes, and cultured mammalian cells (29), but also stains apoptotic cells in *Drosophila* and *C. elegans* (30, 31). Thus, an increase in acridine orange staining could indicate an increase in either the number of lysosomes or programmed cell deaths or both. Embryos derived from homozygous *cup-5(n3194)* mothers contained greatly increased numbers of $AO^+$ bodies compared to embryos derived from wild-type mothers (Figure 3 A,B).

To distinguish whether the $AO^+$ bodies in *cup-5* mutants represent lysosomes or corpses, we grew animals on media containing the acidophilic dye Lysotracker Red, which accumulates in highly acidified lysosomal compartments. We found that persistent cell corpses do not accumulate Lysotracker, since *ced-1* and *ced-5* mutants, both of which have persistent cell corpses (32), did not accumulate Lysotracker in corpses; both mutants displayed a distribution of Lysotracker indistinguishable from that of the wild type (Figure 3E and data not shown). In early wild-type embryos, Lysotracker had a granular cytoplasmic distribution that became restricted to intestinal granules in later embryos (Figure 3C). By contrast, all three of our *cup-5* mutants accumulated Lysotracker in most and possibly all tissues of the embryo (Figure 3D). Using polarized light microscopy, which illuminates intestinal granules in *C. elegans* embyryos and can be used to determine the extent of intestinal cells in the animal, we found that *cup-5* mutants did not have excess intestinal cells that might have been responsible for the broader distribution of Lysotracker. Furthermore, *cup-5* mutants showed normal distribution of the mitochondrial marker Mitotracker Red (33), indicating that the accumulation of Lysotracker is not a consequence of a non-specific general accumulation of dye in an unspecified intracellular compartment in these animals (data not shown). We conclude that *cup-5* mutant animals contain excess acidified intracellular compartments that most likely are lysosomes.

We analyzed the cellular ultrastructure of *cup-5* mutant animals using electron microscopy (Figure 4). *cup-5* mutants were disorganized and display irregular cellular morphologies. Specifically, *cup-5* mutant animals contained many cells with enlarged

vacuoles or lysosomes and membranous lamellar structures that are not seen in wild-type animals. We observed these structures both in the weak *cup-5(n3264)* mutant and in the strong *cup-5(n3194)* mutant. Cells derived from hML-IV patients have enlarged vacuoles and characteristic membranous cytoplasmic bodies (25, 34) that are similar to the subcellular structures present in *cup-5* mutants.

**_cup-5_ mutants display increased programmed cell death**

As the null allele *cup-5(n3194)* appears to cause the accumulation of refractile bodies similar to cell corpses, we examined the role of programmed cell death in the phenotype of *cup-5* mutant animals. The activities of *ced-3* and *ced-4* are required for essentially all programmed cell deaths in *C. elegans* (35). *ced-3* encodes a caspase (36), and *ced-4* encodes a protein similar to the human caspase activator Apaf-1 (37, 38). Introducing either a *ced-3* or *ced-4* mutation into a *cup-5* mutant background suppressed only slightly the lethality of *cup-5* mutants (Table 2A) and did not obviously suppress the accumulation of refractile bodies. Thus, *cup-5* maternal-effect lethality either is not primarily a consequence of too much programmed cell death and the refractile bodies are not cell corpses or programmed cell death is being activated independently of *ced-3* and *ced-4* in *cup-5(n3194)* animals. In addition, neither *ced-3* nor *ced-4* blocked the accumulation of Lysotracker in *cup-5* mutants (Figure 3F and data not shown), indicating that this accumulation is not dependent on *ced-4* and *ced-3*-mediated programmed cell death.

Blocking programmed cell death did slightly increase the viability of *cup-5* mutants. Compared with *cup-5(n3194)* embryos, greater numbers of both *cup-5(n3194) ced-4(n1162)* and *cup-5(n3194); ced-3(n717)* double mutants survived to hatching (Table 2A). Double mutant embryos that hatched typically did not survive to adulthood: 1/42 *cup-5(n3194); ced-3(n717)*, 7/72 *cup-5(n3194) ced-4(n1162)*, and 4/24 *cup-5(n3194)* mutants survived to adulthood. Blocking cell death by expressing the baculovirus caspase inhibitor p35 (39) similarly slightly increased viability but did not completely rescue lethality (Table 2B).

We also determined the effect of *ced-8* mutations, which cause a delay in programmed cell death (40), on *cup-5* mutants. Some of the refractile bodies in *cup-5* mutants are irregular in shape and smaller than corpses generated by programmed cell death. In *cup-5(n3194);ced-8* animals there was a delay in the appearance of the larger

but not of the smaller irregular refractile bodies in *cup-5* mutants (data not shown). This observation raises the possibility that the refractile bodies in *cup-5* mutants represent two different populations. One population may correspond to cell corpses, while the other population may represent enlarged lysosomes. Such a model is consistent with our finding (data not shown) that some, but not all, of the refractile bodies label with Lysotracker, which we showed does not label cell corpses. Thus, *cup-5* mutants may have an increase in the numbers of both lysosomes and programmed cell deaths.

To examine further whether programmed cell death was increased in *cup-5* mutants, we performed the TUNEL (TdT-mediated dUTP nick-end labeling) assay, which labels nicked DNA ends generated during programmed cell death (18). Whereas wild-type animals averaged 0.8 ± 0.9 (n=15) TUNEL$^+$ cells per embryo, *cup-5* mutants averaged 7.7 ± 4.6 (n=10) TUNEL$^+$ cells per embryo (Figure 5). We tested whether this increase in TUNEL$^+$ cells was dependent on programmed cell death by performing the TUNEL assay on *cup-5(n3194) ced-4*(lf) and *cup-5(n3194); ced-3*(lf) double mutants. In these double mutants TUNEL$^+$ cells were completely absent. Therefore, the increase in TUNEL$^+$ cells in *cup-5* mutants is dependent on *ced-3* and *ced-4*-mediated programmed cell death. We conclude that *cup-5* mutants have an increase in programmed cell death, but that this increased cell death is not primarily responsible for their lethal phenotype. Alternatively, some aspects of programmed cell death in *cup-5* mutants may be induced downstream of *ced-3* and may contribute to lethality, but such cell death apparently is not capable of generating TUNEL reactivity in the absence of *ced-3*.

## DISCUSSION

From a screen for mutations affecting programmed cell death, we isolated null alleles of the *C. elegans* homolog of the human mucolipidosis type IV gene. A recently identified missense mutation in this gene, *cup-5*, indicated that it regulates the uptake and disposal of extracellular material by coelomocytes (14), scavenger cells of poorly understood function in the *C. elegans* pseudocoelom. Our analyses have demonstrated that the function of *cup-5* is not limited to coelomocytes and that *cup-5* is likely broadly involved in lysosomal regulation in *C. elegans*. Endocytosis can transfer material from the extracellular environment to lysosomes by the fusion of lysosomes with late

endosomes, forming a hybrid organelle (41). Thus, endocytosis and proper lysosome function are closely interrelated.

*C. elegans* genes that act in receptor-mediated endocytosis were identified from screens for mutations that perturb yolk protein uptake by oocytes (42). Depletion of the *C. elegans* homolog of auxilin, a neuronal protein that acts in the uncoating of clathrin-coated vesicles, by RNA-mediated interference (RNAi) indicated that auxilin is required for endocytosis (43). Auxilin(RNAi) animals also arrest development as larvae and display necrosis of the intestine. The null phenotype of auxilin mutants is not known, and complete elimination of auxilin function may result in a more severe phenotype, potentially similar to the embryonic arrest phenotype of *cup-5* mutants. The arrest phenotypes of *cup-5* and auxilin(RNAi) individuals suggest that clonal screens for mutations that cause lethality or maternal-effect lethality and also disrupt endocytic processes in oocytes or coelomocytes could potentially isolate additional genes that act in endocytosis and intracellular endosome-lysosome trafficking.

What is the relationship between the effects of *cup-5* mutants on lysosomes and programmed cell death? The refractile bodies in *cup-5* mutants appear during development at the same time as cell corpses, but are occasionally smaller or slightly irregular in shape. We suggest that there may be two classes of refractile bodies in *cup-5* mutant animals, corresponding to enlarged lysosomes and to corpses generated by programmed cell death. Distinctions between these classes may be possible at the molecular level (e.g, Lysotracker versus TUNEL staining), but are not obvious at the level of morphological detail visible by light microscopy.

We also studied other markers of programmed cell death in *cup-5* mutants. There is an increase in the number of TUNEL-positive cells in *cup-5* mutants, and the presence of these cells is dependent on *ced-3* and *ced-4* function. These findings indicate that the increase in TUNEL staining involves the known genetic pathway for programmed cell death (9). One simple possibility is that the increased number of TUNEL-positive cells in *cup-5* mutants is a consequence of an increased number of programmed cell deaths. Alternatively, it is conceivable that the apparent increase in TUNEL-reactivity is a consequence of a decreased pace of cell death (40) or DNA degradation (18). In mice, when DNA degradation by the caspase-activated DNase CAD is blocked in thymocytes, some DNA degradation nonetheless proceeds, although at a slower rate, through the action of a lysosomal DNase in engulfing phagocytes (44). A defect in lysosomes might

affect such a pathway of DNA degradation. However, since lysosomes are not the primary site of apoptotic DNA degradation, we do not think it is likely that the increased number of TUNEL-positive cells is a consequence of defects in DNA degradation. In addition, DAPI staining of nuclei in *cup-5* mutants appeared normal (B.H. and H.R.H., unpublished observations), so there is no reason to suspect that the TUNEL-reactivity is caused by an abnormality in DNA degradation. Regardless of whether it is the rate of DNA degradation or the amount of programmed cell death that is altered in *C. elegans cup-5* mutants, some aspect of programmed cell death is clearly abnormal in these animals.

Follicular lymphoma, autoimmune disease, and retinal degeneration all involve abnormalities in apoptosis (5-8). In addition, human neurodegenerative diseases, including Alzheimer's Disease, Huntington's Disease, and amyotrophic lateral sclerosis, are associated with increased levels of apoptotic cell death (45). Our studies of the *C. elegans* homolog of the human mucolipidosis, type IV gene suggest that this disease, and by extension, other lysosomal storage disorders, may also involve abnormalities in programmed cell death. Indeed, in neuronal tissue of *Hexb*$^{-/-}$ mice, which provide a model for Sandhoff disease (46), and in spinal cord sections of Tay-Sachs and Sandhoff disease patients, apoptotic cells are present (47). Many lysosomal storage disorders seem to dramatically affect neuronal function (48). It is possible that neurons are particularly sensitive to disruptions in lysosome function. Alternatively, neurons may be more sensitive to the activation of programmed cell death. If lysosomal storage diseases indeed involve abnormalities in programmed cell death, it may be possible to alleviate aspects of these diseases by blocking the abnormal programmed cell deaths.

We have shown that null mutations in the *C. elegans* homolog of the mucolipidosis, type IV gene cause maternal-effect lethality, the accumulation of excess lysosomes, and abnormalities in programmed cell death. We suggest that abnormalities in programmed cell death may be secondary consequences of lysosomal storage disorders. *cup-5* may provide a good model for mucolipidosis type IV and may also allow a detailed genetic analysis of the mechanisms involved in the disease pathology. For example, the isolation of suppressors of the *C. elegans* maternal-effect lethal phenotype could allow the identification of additional genes that act with *cup-5*/hML-IV to regulate lysosome function and to initiate programmed cell death.

## ACKNOWLEDGMENTS

We thank Z. Zhou for the *n3264* mutation, J. Priess for the *zu223* mutation, and G. Borsani for the hML-IV cDNA. We thank C. Ceol, P. Reddien, and Z. Zhou for critical reading of the manuscript. B. M. H. was supported by a Howard Hughes Medical Institute predoctoral fellowship. H. R. H. is an Investigator of the Howard Hughes Medical Institute.

## REFERENCES


1. Jacobson, M. D., Weil, M. & Raff, M. C. (1997) *Cell* **88,** 347-54.
2. Thompson, C. B. (1995) *Science* **267,** 1456-62.
3. Chang, G. Q., Hao, Y. & Wong, F. (1993) *Neuron* **11,** 595-605.
4. Portera-Cailliau, C., Sung, C. H., Nathans, J. & Adler, R. (1994) *Proc. Natl. Acad. Sci. USA* **91,** 974-8.
5. Davidson, F. F. & Steller, H. (1998) *Nature* **391,** 587-91.
6. Rieux-Laucat, F., Le Deist, F., Hivroz, C., Roberts, I. A., Debatin, K. M., Fischer, A. & de Villartay, J. P. (1995) *Science* **268,** 1347-9.
7. Fisher, G. H., Rosenberg, F. J., Straus, S. E., Dale, J. K., Middleton, L. A., Lin, A. Y., Strober, W., Lenardo, M. J. & Puck, J. M. (1995) *Cell* **81,** 935-46.
8. Vaux, D. L., Cory, S. & Adams, J. M. (1988) *Nature* **335,** 440-2.
9. Metzstein, M. M., Stanfield, G. M. & Horvitz, H. R. (1998) *Trends Genet.* **14,** 410-6.
10. Hengartner, M. O., Ellis, R. E. & Horvitz, H. R. (1992) *Nature* **356,** 494-9.
11. Hengartner, M. O. & Horvitz, H. R. (1994) *Nature* **369,** 318-20.
12. Bargal, R. et al. (2000) *Nat. Genet.* **26,** 118-23.
13. Bassi, M. T., Manzoni, M., Monti, E., Pizzo, M. T., Ballabio, A. & Borsani, G. (2000) *Am. J. Hum. Genet.* **67,** 1110-20.
14. Fares, H. & Greenwald, I. (2001) *Nat. Genet.* **28,** 64-8.
15. Brenner, S. (1974) *Genetics* **77,** 71-94.
16. Wood, W. B. & the Community of *C. elegans* Researchers (1988) *The Nematode Caenorhabditis elegans* (Cold Spring Harbor Laboratory).
17. Fire, A., Harrison, S. W. & Dixon, D. (1990) *Gene* **93,** 189-98.
18. Wu, Y. C., Stanfield, G. M. & Horvitz, H. R. (2000) *Genes Dev.* **14,** 536-48.
19. Bargmann, C. I., Hartwieg, E. & Horvitz, H. R. (1993) *Cell* **74,** 515-27.
20. Zhou, Z., Hartwieg, E. & Horvitz, H. R. (2001) *Cell* **104,** 43-56.
21. Basson, M. & Horvitz, H. R. (1996) *Genes Dev.* **10,** 1953-65.
22. Hengartner, M. O. & Horvitz, H. R. (1994) *Cell* **76,** 665-76.
23. The *C. elegans* Genome Sequencing Consortium (1998) *Science* **282,** 2012-8.
24. Krause, M. & Hirsh, D. (1987) *Cell* **49,** 753-61.
25. Amir, N., Zlotogora, J. & Bach, G. (1987) *Pediatrics* **79,** 953-9.
26. Berman, E. R., Livni, N., Shapira, E., Merin, S. & Levij, I. S. (1974) *J. Pediatr.* **84,** 519-26.

27. Chen, C. S., Bach, G. & Pagano, R. E. (1998) *Proc. Natl. Acad. Sci. USA* **95,** 6373-8.
28. Bargal, R. & Bach, G. (1997) *J. Inherit. Metab. Dis.* **20,** 625-32.
29. Allison, A. C. & Young, M. R. (1969) in *Lysosomes in Biology and Pathology. Vol. 2,* eds. Dingle, J. T. & Fell, H. B. (North-Holland Publishing Company, Amsterdam), pp. 600-628.
30. Abrams, J. M., White, K., Fessler, L. I. & Steller, H. (1993) *Development* **117,** 29-43.
31. Gumienny, T. L., Lambie, E., Hartwieg, E., Horvitz, H. R. & Hengartner, M. O. (1999) *Development* **126,** 1011-22.
32. Ellis, R. E., Jacobson, D. M. & Horvitz, H. R. (1991) *Genetics* **129,** 79-94.
33. Chen, F., Hersh, B. M., Conradt, B., Zhou, Z., Riemer, D., Gruenbaum, Y. & Horvitz, H. R. (2000) *Science* **287,** 1485-9.
34. Schiffmann, R. et al. (1998) *Proc. Natl. Acad. Sci. USA* **95,** 1207-12.
35. Ellis, H. M. & Horvitz, H. R. (1986) *Cell* **44,** 817-29.
36. Yuan, J., Shaham, S., Ledoux, S., Ellis, H. M. & Horvitz, H. R. (1993) *Cell* **75,** 641-52.
37. Yuan, J. & Horvitz, H. R. (1992) *Development* **116,** 309-20.
38. Zou, H., Henzel, W. J., Liu, X., Lutschg, A. & Wang, X. (1997) *Cell* **90,** 405-13.
39. Sugimoto, A., Friesen, P. D. & Rothman, J. H. (1994) *EMBO J.* **13,** 2023-8.
40. Stanfield, G. M. & Horvitz, H. R. (2000) *Mol. Cell* **5,** 423-33.
41. Luzio, J. P., Rous, B. A., Bright, N. A., Pryor, P. R., Mullock, B. M. & Piper, R. C. (2000) *J. Cell. Sci.* **113,** 1515-24.
42. Grant, B. & Hirsh, D. (1999) *Mol. Biol. Cell* **10,** 4311-26.
43. Greener, T., Grant, B., Zhang, Y., Wu, X., Greene, L. E., Hirsh, D. & Eisenberg, E. (2001) *Nat. Cell Biol.* **3,** 215-9.
44. McIlroy, D., Tanaka, M., Sakahira, H., Fukuyama, H., Suzuki, M., Yamamura, K., Ohsawa, Y., Uchiyama, Y. & Nagata, S. (2000) *Genes Dev.* **14,** 549-58.
45. Nijhawan, D., Honarpour, N. & Wang, X. (2000) *Annu. Rev. Neurosci.* **23,** 73-87.
46. Kolter, T. & Sandhoff, K. (1998) *J. Inherit. Metab. Dis.* **21,** 548-63.
47. Huang, J. Q., Trasler, J. M., Igdoura, S., Michaud, J., Hanal, N. & Gravel, R. A. (1997) *Hum. Mol. Genet.* **6,** 1879-85.
48. Gieselmann, V. (1995) *Biochim. Biophys. Acta* **1270,** 103-36.

## FIGURES

**Figure 1. Mutants isolated from a screen for suppressors of *ced-9(n1950)***
**(A)** Approximately 50-cell stage embryo carrying the *n3196* mutation, which confers a maternal-effect lethal phenotype characterized by vacuolization (arrows) and degeneration of the embryo. **(B)** Two-fold stage embryo carrying the *n3213* mutation, which confers a phenotype similar to that of *n3196* embryos but is restricted to the posterior portion (bracket) of the embryo. The abnormality first appears in approximately comma-staged embryos. **(C)** Comma-stage *cup-5(n3194)* embryo derived from a homozygous *cup-5(n3194)* mother showing early appearance of refractile bodies (arrows). **(D)** *cup-5(n3194)* embryo arrested at approximately the two-fold stage filled with refractile bodies.

# Figure 1

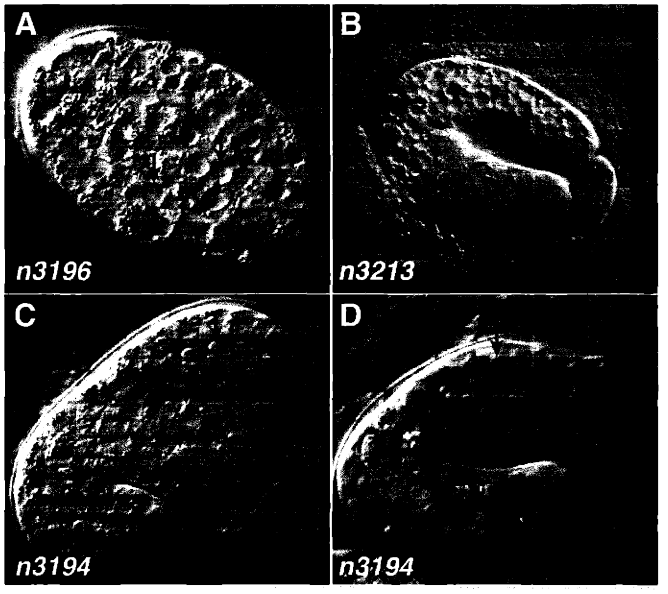

**Figure 2. CUP-5L sequence and alignment**

Alignment of CUP-5L with the product of the human ML-IV gene (12, 13) and the predicted *Drosophila* protein CG8743. Identities to the CUP-5L protein are shaded. The divergent portion of CUP-5S following amino acid 603 is indicated, and the positions of the three *cup-5* mutants alleles described in the text as well as *cup-5*(*ar465*) are shown.

# Figure 2

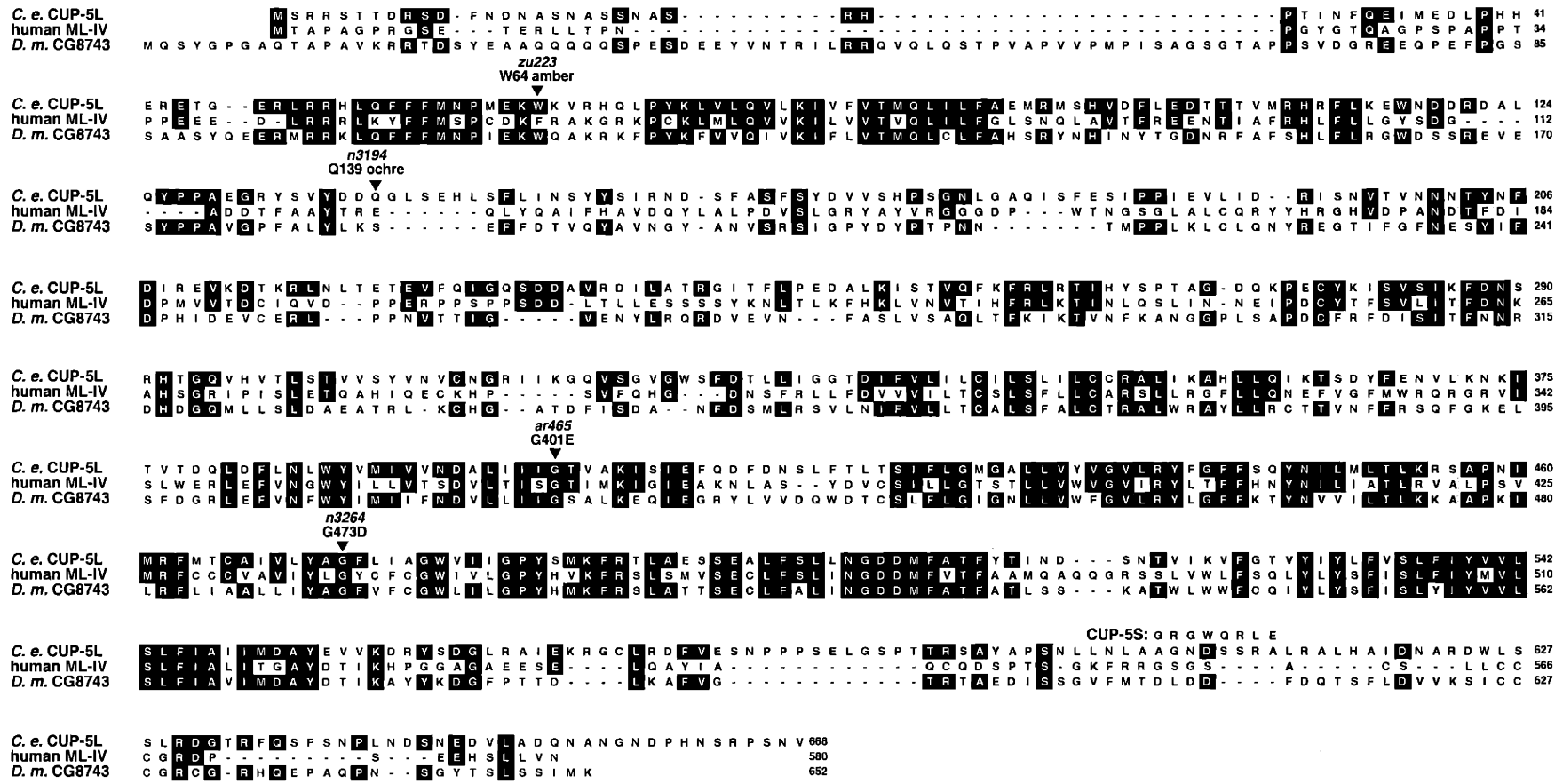
C. e. CUP-5L
human ML-IV
D. m. CG8743
zu223
W64 amber
n3194
Q139 ochre
ar465
G401E
n3264
G473D
CUP-5S: G R G W Q R L E

**Figure 3. *cup-5* mutants accumulate excess lysosomes**

**(A-B)** Acridine orange staining in embryos. **(A)** Wild-type embryo. Apoptotic corpse is indicated (arrow). **(B)** *cup-5(n3194)* embryo. Arrows indicate a few of the many additional acridine orange-positive bodies. **(C-F)** Lysotracker staining in embryos. **(C)** Late wild-type embryos with staining restricted to intestinal granules (arrow). **(D)** Increased accumulation of Lysotracker in *cup-5(n3194)* embryos. **(E)** *ced-1* embryo, which accumulates apoptotic corpses, did not accumulate Lysotracker. **(F)** *ced-4 cup-5(n3194)* embryo accumulated Lysotracker.

# Figure 3

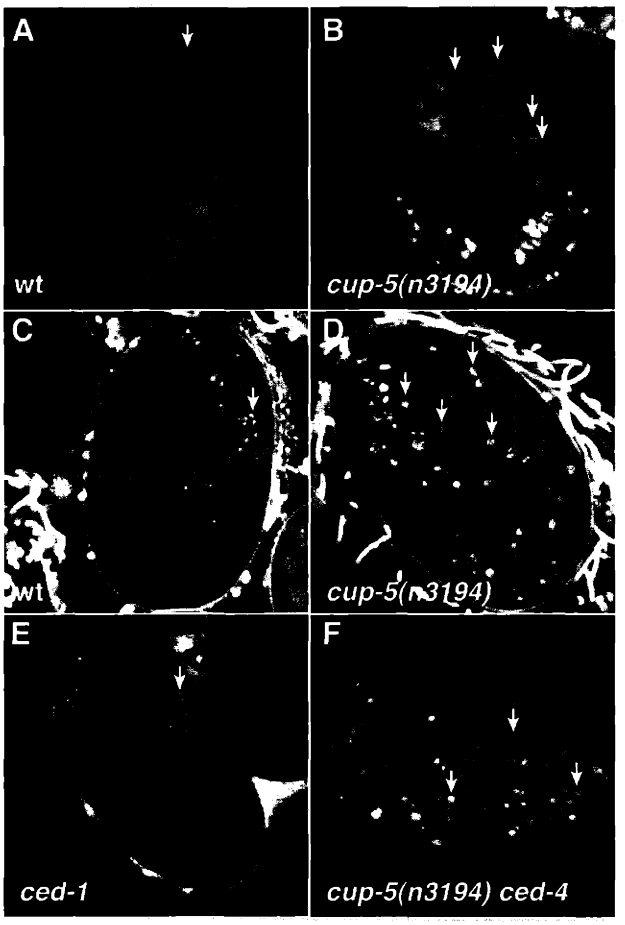

**Figure 4. Accumulation of vacuoles and lamellar material in *cup-5* mutants**
Electron micrographs of **(A)** wild-type and **(B)** *cup-5(n3194)* mutant larva at the level of the pharynx (ph). Cellular structure in the *cup-5* mutant appears disorganized. Multiple cells with enlarged vacuolar spaces (arrows) that may represent enlarged lysosomes can be seen.

# Figure 4

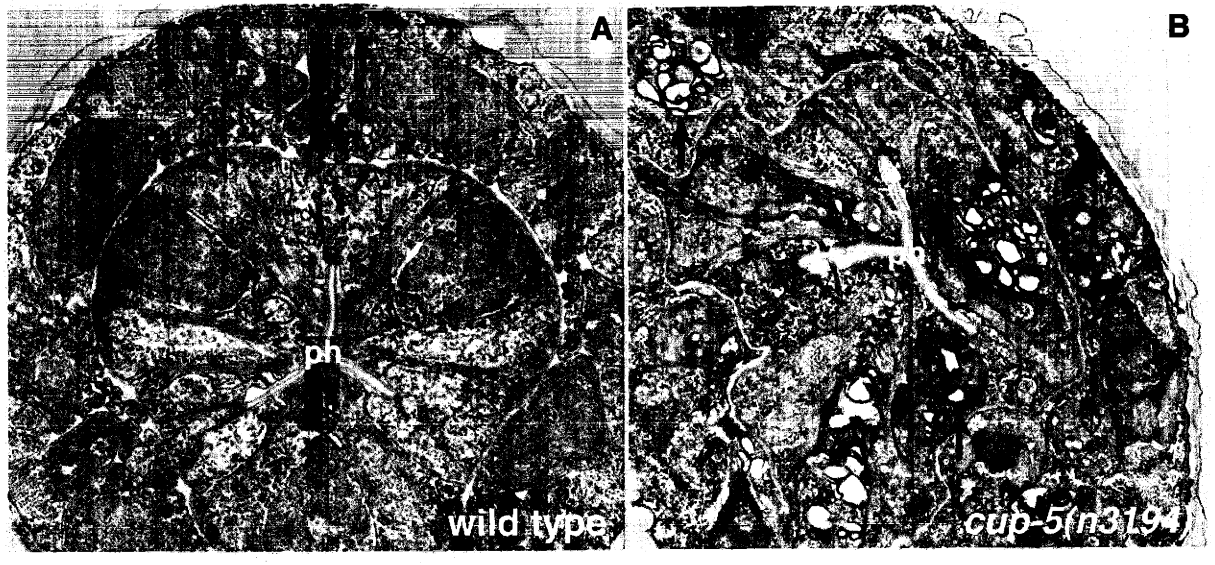

**Figure 5. Increased numbers of TUNEL-positive cells in *cup-5(n3194)* embryos**
**(A)** Wild-type embryo with very few TUNEL-positive cells (arrows). **(B,C)** *cup-5(n3194)* embryos derived from homozygous *cup-5(n3194)* animals contain many TUNEL-positive cells. **(D)** *cup-5(n3194); ced-3(n717)* embryos contain no TUNEL-positive cells.

## Figure 5

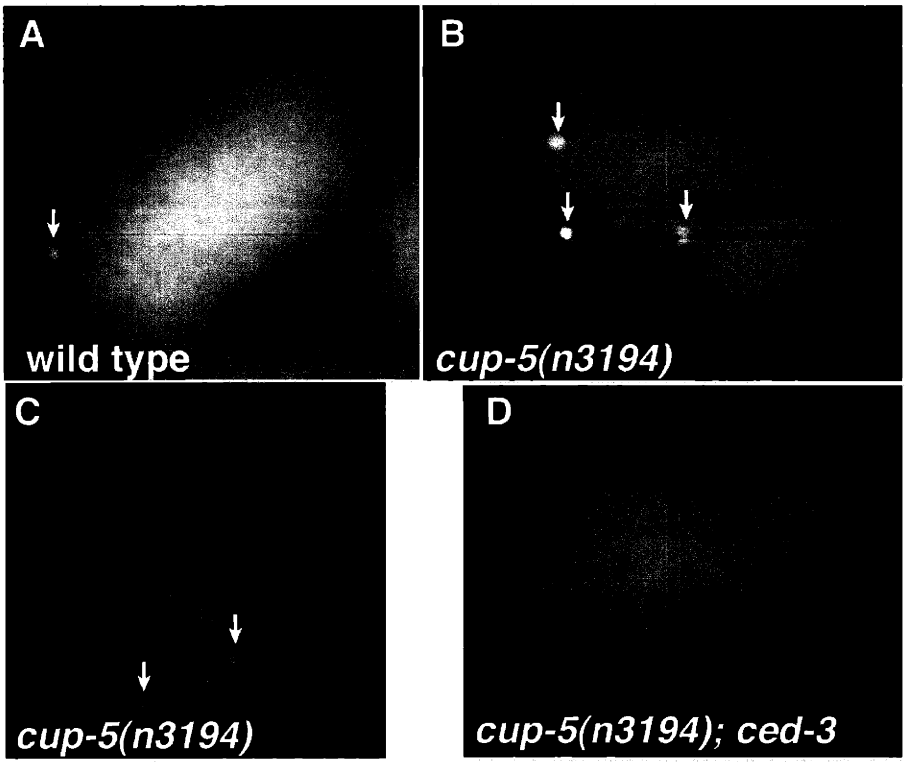

## TABLES

**Table 1. *cup-5L*, *cup-5S*, and hML-IV rescue *cup-5(n3194)* lethality**

| Transgene | Heat shock | Total # eggs laid | Total # eggs hatched | % eggs hatched | # adults |
|---|---|---|---|---|---|
| $P_{hsp}$ alone | - | 178 | 0 | 0 | 0 |
| $P_{hsp}$ alone | + | 360 | 3 | 0.8 | 1 |
| $P_{hsp}$*cup-5L* | - | 232 | 28 | 12.1 | 24 |
| $P_{hsp}$*cup-5L* | + | 301 | 127 | 42.2 | 118 |
| $P_{hsp}$*cup-5S* | - | 178 | 26 | 14.6 | 24 |
| $P_{hsp}$*cup-5S* | + | 271 | 135 | 49.8 | 121 |
| $P_{hsp}$hML-IV | - | 136 | 0 | 0 | 0 |
| $P_{hsp}$hML-IV | + | 263 | 24 | 9.1 | 21 |
| $P_{hsp}$hML-IV(fs) | - | 243 | 0 | 0 | 0 |
| $P_{hsp}$hML-IV(fs) | + | 314 | 1 | 0.3 | 0 |

Transgenic extrachromosomal arrays carried by *unc-36(e251) cup-5(n3194)/qC1* animals were tested for rescue as described in Materials and Methods. Animals were removed from Petri plates 24 h following heat-shock treatment, and the number of eggs present on each plate was counted. Hatching was assayed 2 days after heat-shock treatment, and the presence of adult animals was assayed 4 days after heat-shock treatment. At least three transgenic lines were tested for each construct. Data for a single representative line are shown here. fs, frameshift.

**Table 2. Blocking programmed cell death slightly improves *cup-5* viability**

| A. Genotype | Avg. # eggs laid | Avg. # eggs hatched | % eggs Hatched | n |
|---|---|---|---|---|
| *cup-5(n3194) unc-36* | 216 | 2.4 | 1.1 | 11 |
| *cup-5(n3194) unc-36/nDf16* | 187 | 0.2 | 0.1 | 13 |
| *cup-5(zu223) unc-36* | 206 | 0.4 | 0.2 | 7 |
| *cup-5(zu223) unc-36/nDf16* | 246 | 0.6 | 0.2 | 10 |
| *sma-3 cup-5(n3194)* | 110 | 0.6 | 0.5 | 12 |
| *unc-79 ced-4(n1162) sma-3 cup-5(n3194)* | 114 | 10 | 8.8 | 10 |
| *sma-3 cup-5(n3194); unc-31* | 56 | 0.6 | 1.1 | 10 |
| *sma-3 cup-5(n3194); unc-31 ced-3(n717)* | 64 | 7.7 | 12.1 | 9 |

| B. Transgene | Heat-shock | Total # eggs laid | Total # hatched | % hatched |
|---|---|---|---|---|
| $P_{hsp}$ p35 | - | 253 | 2 | 0.8 |
| $P_{hsp}$ p35 | + | 351 | 27 | 7.7 |
| $P_{hsp}$ p35 | + 2x | 187 | 16 | 8.6 |

A. Effects of mutations blocking programmed cell death on the viability of *cup-5* embryos. The number of eggs laid and number of eggs hatched was determined for *n* individual animals, and the mean value is indicated. % hatched was calculated by dividing the total number of eggs hatched by the total number of eggs laid for each indicated genotype. B. Effect of overexpressing the baculoviral anti-apoptotic gene p35 on the viability of *cup-5* embryos. At least ten *cup-5(n3194) unc-36(e251)* animals carrying a transgenic array of p35 were subjected to a single pulse of 33°C heat-shock (+) or two pulses of heat-shock separated by 1 hr recovery at 20°C (+ 2x). The total numbers of eggs laid and hatched were counted.

# Chapter 4

# Characterization of CED-4 interacting proteins and mechanisms of CED-4 localization

The series of experiments described here were intended to determine the mechanisms by which CED-4 protein is localized to the nuclear membrane in the absence of CED-9. Though largely unsuccessful on that account, information obtained from these experiments is presented here. Ewa Davison sequenced 11 *ced-4* alleles, Megan Higginbotham sequenced 3 alleles, the sequence of 7 alleles had been previously published, and I sequenced the remainder of the *ced-4* alleles. Zheng Zhou performed the yeast two-hybrid screen for *ced-4* interactors, isolating cDNAs for *mac-1* and *prp-1*.

## INTRODUCTION

Programmed cell death is an important process in the development and homeostasis of metazoans, and disruption of the process can contribute to disease. Investigations using the nematode *Caenorhabditis elegans* have been instrumental in establishing a genetic and molecular pathway for programmed cell death (Metzstein et al., 1998). Molecules that are critical for proper execution of cell death in the worm spurred the identification of counterparts that function in apoptosis in other experimental systems. The identification of CED-3 as a cysteine protease (Yuan et al., 1993) led to the discovery of an entire family of these caspases that function in programmed cell death and inflammatory responses (Cryns and Yuan, 1998). Apaf-1, the mammalian counterpart of the CED-4 cell death activator, was identified biochemically as an activator of caspase-3 (Zou et al., 1997). CED-9, a negative regulator of programmed cell death, and EGL-1, an upstream activator of cell death, are both members of the Bcl-2 family of apoptotic regulators (Hengartner and Horvitz, 1994).

Biochemical studies have revealed *in vitro* physical interactions between these key components of the apoptotic pathway, and it seems clear that these interactions regulate the execution of apoptosis. EGL-1 and CED-9 interact (Conradt and Horvitz, 1998), and EGL-1 can disrupt the interaction of CED-9 with CED-4 (del Peso et al., 1998). CED-4 and CED-3 also can physically interact (Chinnaiyan et al., 1997). *In vivo* work demonstrated that CED-9 and CED-4 co-localize to mitochondria and that either in the absence of CED-9 or when EGL-1 overexpression activates programmed cell death CED-4 translocates to the nuclear membrane (Chen et al., 2000). What CED-4 translocation to the nucleus accomplishes during programmed cell death and how it is achieved is still unknown. Therefore, we undertook several lines of experimentation described here to determine how CED-4 translocation is mediated, looking for requirements within CED-4 protein as well as other proteins that are necessary for CED-4 translocation.

In general, what are the components of the nuclear envelope, how are they localized to this specific structure, and could any of those components be responsible for CED-4 localization? The nuclear envelope consists of both the inner and outer nuclear membrane, as well as the pore complexes that traverse the membranes and the nuclear lamina that underlies the membrane (Gruenbaum et al., 2000). The outer

nuclear membrane is continuous with the endoplasmic reticulum and meets the inner nuclear membrane at the nuclear pore complexes. The most abundant proteins of the nuclear lamina are the lamins themselves. Lamins are type V intermediate filaments with a coiled-coil domain and a globular C-terminal tail (Stuurman et al., 1998). Vertebrates and *Drosophila* have multiple lamins, but *C. elegans* has only a single lamin gene (Riemer et al., 1993). *Drosophila* lamin is capable of binding to histones (Goldberg et al., 1999), and one of the functions of the nuclear lamina appears to be organize chromatin. Other proteins present at the nuclear envelope include nucleoporins, emerin (Nagano et al., 1996), nurim (Rolls et al., 1999), and UNC-84 (Malone et al., 1999). The emerin gene is mutated in Emery-Dreifuss muscular dystrophy (Bione et al., 1994), and mutations in A-type lamin in mice can disrupt emerin localization and cause muscular dystrophy (Sullivan et al., 1999).

Integral membrane proteins in the inner nuclear membrane appear to reach their final destination by lateral diffusion in the endoplasmic reticulum, followed by retention in the inner nuclear envelope through binding of chromatin, the lamina, or other nuclear proteins (Ellenberg et al., 1997; Östlund et al., 1999)]. Inner nuclear envelope proteins appear to form a network of interactions with one another, and lamins can interact with emerin, lamin B receptor, Man1, and lamina-associated polypeptides 1 and 2 (LAP1 and LAP2) (Gruenbaum et al., 2000). One or two domains in the N-terminus of emerin are involved in inner nuclear membrane retention, and portions of these domains are shared with LAP2 (Östlund et al., 1999). However, these domains do not appear to act in nuclear envelope targeting of LAP2, so the shared portions of the proteins do not seem to contain shared signals for retention.

Therefore, it is not possible to discern an obvious signal within CED-4 protein that would be responsible for its localization to the nuclear membrane. Since CED-4 does not seem to be an integral membrane protein, either, its localization to the nuclear membrane is likely dependent on an interaction with another protein that is a membrane resident. Through candidate gene approaches it may be possible to identify the inner nuclear membrane protein that interacts with CED-4. However, recent studies of the inner membrane have identified 19 novel proteins that had not been previously detected (Dreger et al., 2001), and as additional proteins may yet be discovered, it is not clear that assessing the role of each of these proteins in CED-4 localization is the most effective approach. We describe here experiments that attempt to address roles for

several genes in CED-4 localization—the *ced-3* gene, the lamin gene, and the *mac-1* gene identified as a CED-4 interactor. As these approaches have not identified the components required for CED-4 localization, we also propose a genetic screen to isolate genes important for CED-4 localization.

## MATERIALS AND METHODS

### Nematodes

Nematodes were cultured by standard methods (Brenner, 1974). The wild-type parental strain was Bristol N2.

The number of cells in the anterior pharynx of L3 and L4 larvae was determined as described in (Hengartner et al., 1992).

*ced-4* mutations used in this study are listed in Table 1. Other mutations used in this study: LG II: *mac-1(n3320)*, *mac-1(n3321)*; LG III: *ced-9(n1950n2161)*, *ced-9(n1653)*, *ced-9(n2812)*; LG IV: *ced-3(n717)*, *ced-3(n718)*, *ced-3(n2427)*, *ced-3(n2439)*, *ced-3(n2452)*, *ced-3(n3692)*.

### Molecular biology

Standard molecular biology procedures were followed (Sambrook et al., 1989). DNA for allele sequencing was obtained by washing *ced-4* mutant worms from plates in M9 media (Wood and *Researchers*, 1988) and incubating the worms in 2x worm lysis buffer (100 mM KCl, 20 mM Tris pH 8.2, 5 mM $MgCl_2$, 0.9% IGEPAL, 0.9% Tween-20, 0.02 % gelatin, 0.18 mg/ml proteinase K) overnight at 60°C. Proteinase K was inactivated by 20 minute incubation at 95°C. 1 $\mu$l of lysate was used for PCR amplification of *ced-4* genomic DNA. Sequencing was performed using an ABI 373A DNA sequencer.

### Antibody staining

Fixation and staining was performed essentially as described (Chen et al., 2000). Briefly, embryos were obtained by dissolving adult animals in a solution of sodium hydroxide and hypochlorite. Embryos were fixed in paraformaldehyde and methanol, washed in phosphate-buffered saline and stored at 4°C prior to staining. Polyclonal antibodies recognizing CED-4, CED-9, and lamin have been described (Chen et al., 2000). Rabbit polyclonal antibodies recognizing Ce-emerin were a gift of Y. Gruenbaum (Hebrew University, Jerusalem, Israel). Mouse monoclonal antibody Mab414 recognizing nucleoporin was purchased from Babco.

**RNA-mediated interference**

Templates for in vitro transcription reactions were made by PCR amplification of *mac-1* and *prp-1* cDNAs isolated from the yeast two-hybrid screen. In vitro-transcribed RNA was prepared and injected as described (Fire et al., 1998). RNAi of lamin was performed by growing animals on bacteria expressing dsRNA for the lamin gene (Timmons and Fire, 1998). The lamin RNAi feeding construct was a gift of Y. Gruenbaum (Hebrew University, Jerusalem, Israel). Embryos were obtained two days after the transfer of adult animals to the lamin(RNAi) plates, and were fixed and stained as described above.

**Ectopic expression**

*mac-1* and *prp-1* cDNAs were subcloned into pPD49.78 and pPD49.83 (Fire et al., 1990) to generate $P_{hsp}$*mac-1* and $P_{hsp}$*prp-1* constructs. These constructs were injected at a concentration of 100 ng/$\mu$l together with pRF4 at 80 ng/$\mu$l into N2 animals (Mello and Fire, 1995). The constructs were injected singly and in combination with each other. Expression was induced by one hour of incubation at 33°C. Animals were allowed to recover at 20°C for one hour prior to harvesting for fixation and antibody staining. To assess extra cells in the anterior pharynx, transgenic adults were heat-shocked for one hour, allowed to lay eggs at 20°C for one hour, and then removed from the plates. The number of cells in the anterior pharynx of L3/L4 larvae was determined two days later. CED-4::GFP was constructed by F. Chen (unpublished data) and consists of a PvuII-SphI genomic DNA fragment, containing 1.6 kB upstream sequence and the entire *ced-4* coding region except for the final two codons, subcloned into pPD95.77 digested with HindIII and SphI.

**Deletion library screening**

We used PCR to screen a library of chemically mutagenized nematodes and identify animals containing a deletion in *mac-1* essentially as described in (Jansen et al., 1997). The deletion library was constructed by members of the Horvitz laboratory under the direction of R. Ranganathan and P. Reddien.

## RESULTS

### Characterization of *ced-4* alleles

Various genetic screens performed in the Horvitz laboratory, including screens for suppressors of *ced-9(lf)* lethality, enhancers of the weak allele *ced-3(n2427)*, and genes required for the death of the CEM neurons (E. Speliotes, P. Reddien, H. Schwartz, and H. R. Horvitz, unpublished results), have identified numerous loss-of-function alleles of the gene *ced-4*. In total, 56 loss-of-function alleles have been identified. We have characterized the strength of many of these alleles, assessing the number of extra undead cells present in the anterior pharynx in mutant strains (Table 1). The weakest alleles result in an average of less than one extra cell per animal, whereas the strongest alleles result in animals with approximately 12 extra cells.

The molecular lesions in all 56 alleles have now been identified ((Yuan and Horvitz, 1992); E. Davison, M. Higginbotham, and B. Hersh, unpublished results; Table 1). Nineteen alleles are nonsense mutations, eleven affect splice acceptor or donor sites, one is a large deletion, and twenty-five are missense mutations.

To identify regions of CED-4 that may be necessary for its localization, either to mitochondria or to nuclear membranes, we fixed embryos from strains carrying all 25 missense mutations and stained these embryos with anti-CED-4 antibody (Chen et al., 2000). Six alleles were tested in both a *ced-9(+)* and *ced-9(lf)* background, 14 alleles were tested only in a *ced-9(+)* background, and 5 alleles were tested only in a *ced-9(lf)* background (Table 1). Six missense alleles eliminated all CED-4 staining in embryos. Of the remaining 19 alleles, two affected the localization of CED-4 protein. Both alleles, *n3040* and *n3332*, contain the same molecular change, a conversion of proline 23 to leucine. Both of these alleles cause CED-4 protein to be mislocalized to the cytoplasm, rather than the mitochondria, in the presence of CED-9. In the absence of CED-9, CED-4 protein in *ced-4(n3040)* animals is also mislocalized to the cytoplasm rather than the nuclear membrane. The effect of *ced-4(n3332)* on CED-4 localization in the absence of CED-9 has not been determined. Missense mutations in other nearby residues, including aspartate 20, threonine 15, and histidine 40, had no effect on CED-4 localization. Therefore, proline 23 does not appear to be part of a discrete N-terminal domain required for CED-4 localization. Instead, it may be required for specific

interactions that mediate localization or more generally for proper protein folding and thus localization.

To determine whether specific residues or domains are required for CED-4 localization to the nuclear membrane, CED-4 localization of the 17 alleles not yet assayed in the absence of CED-9 must be determined. In addition, truncated CED-4 proteins can be overexpressed and the localization of these forms can be determined. Initial work with truncated CED-4 has demonstrated that amino acids 1-98 are dispensible for localization of CED-4 to the nuclear membrane when overexpressed in *C. elegans* embryos (data not shown).

**CED-3 does not mediate CED-4 localization**

Because CED-3 and CED-4 are known to physically interact (Chinnaiyan et al., 1997), CED-3 is a candidate for mediating CED-4 localization. We had demonstrated that CED-4 is localized to mitochondria in *ced-3(n717)* embryos and to the nuclear membrane in *ced-9(n2812); ced-3(n717)* embryos (Chen et al., 2000). Although *ced-3(n717)* causes a strong cell death defect, it disrupts the exon 7 splice acceptor site, it is not the allele with the strongest phenotype, and thus may not reflect a complete null allele (Shaham et al., 1999). Therefore, we tested additional *ced-3* loss-of-function alleles for their effect on the localization of CED-4, both in the presence and absence of CED-9.

The *ced-3* allele *n2452* is a deletion that removes the C-terminal portion of the CED-3 molecule, including the active site cysteine. CED-4 localization remains mitochondrial in *ced-3(n2452)* embryos and at the nuclear membrane in *ced-9(n2812); ced-3(n2452)* embryos (Figure 1). However, the prodomain portion of CED-3 that is undeleted (amino acids 1-179) in this allele could potentially mediate an interaction with CED-4.

Several *ced-3* alleles affect residues in the prodomain and cause strong cell death defects: *ced-3(n718)* converts glycine 65 to arginine; *ced-3(n2439)* converts leucine 30 to phenylalanine. Neither of these alleles affected the localization of CED-4 to mitochondria or the nuclear membrane, in the presence and absence of CED-9, respectively (Figure 1).

Finally, *ced-3(n3692)*, isolated by PCR screening a library of mutagenized worms, is a 650 bp deletion, removing the promoter region, all of exon 1, and a portion of exon 2, including the first 59 amino acids of the prodomain (P. Reddien, B. Galvin, B. James,

personal communication). This deletion results in a strong cell death defect, and the elimination of the 5′ end of the gene should completely eliminate CED-3 protein. CED-4 protein is present at mitochondria in *ced-3(n3692)* embryos and at the nuclear membrane in *ced-9(n2812); ced-3(n3692)* embryos (Figure 1).

Thus, multiple lesions in the *ced-3* gene do not affect the localization of CED-4, indicating that CED-3 protein is likely not required for CED-4 localization. However, the localization of CED-3 remains unknown, and it would be interesting to determine whether CED-3 localization correlates with CED-4 localization, and if so, at which points during the initiation and execution of programmed cell death.

**Colocalization of CED-4 and nuclear membrane components**

A translational CED-4::GFP fusion protein (F. Chen, unpublished data) is localized to the nuclear membrane in punctate spots, rather than the relatively uniform distribution of lamin protein. This punctate localization suggests that CED-4 may be associated with the nuclear pore complex or other less uniformly distributed components of the nuclear membrane. In *C. elegans*, these other components include the homolog of the Emery-Dreifuss muscular dystrophy gene, emerin (*Ce-emerin*).

Double-labeling experiments with anti-CED-4 antibody and antibodies against nucleoporin or Ce-Emerin indicated that the punctate CED-4 distribution could not be specifically associated with any one nuclear membrane component (Figure 2). Despite an expectation that nuclear pores would have a discrete, punctate localization pattern, the staining pattern of all three nuclear membrane components looked similar to that observed for nuclear lamin. This result suggests that nuclear pores are very dense in *C. elegans* embryos, but also prevents the resolution of CED-4 co-localization with any one nuclear membrane component by immunofluorescence microscopy.

**Role of lamin in CED-4 localization**

To determine whether a known nuclear membrane component plays a functional role in CED-4 localization, we eliminated the function of lamin and determined the effect on CED-4 localization. We used RNA-mediated interference (RNAi) to eliminate lamin protein in both wild-type and *ced-9(n2812); ced-3(717)* embryos. Elimination of lamin caused embryonic lethality in both strains. However, CED-4 localization remained mitochondrial in wild-type (lamin RNAi) embryos and at the nuclear

membrane in *ced-9(n2812); ced-3(n717)* (lamin RNAi) embryos (Figure 3). Thus, lamin is necessary for viability, but not for localization of CED-4. In addition, lethality caused by elimination of lamin was not suppressible by blocking programmed cell death, as loss of lamin in *ced-9(lf); ced-3(lf)* embryos still resulted in embryonic arrest.

**Isolation of CED-4 interacting proteins**

To identify proteins that might interact with CED-4, either as a downstream effector or to regulate its function or localization, Zheng Zhou performed a yeast two-hybrid screen with full-length CED-4 as the bait protein. From a screen of $2.1x10^6$ transformants, she identified two specific CED-4 interacting proteins (Z. Zhou, personal communication). She isolated 3 clones of each interactor from the screen. CED-3 and CED-9, both known to physically interact with CED-4, were not identified in this screen. This absence suggests that either the screen has not been saturated for CED-4 interacting proteins, or that the library may not have equal representation of all transcripts.

One of the identified CED-4 interactors is a member of the AAA (ATPases associated with various cellular activities) ATPase family. This interactor was also identified by another group and was given the name MAC-1 (Member of the AAA ATPase family associated with CED-4) (Wu et al., 1999). The second CED-4 interactor was also identified as a putative RNA-binding protein (PRP-1) based on the presence of a KH RNA binding domain (Shtang et al., 1999), but its RNA binding properties have not been directly investigated.

**Functional characterization of CED-4 interactors**

To determine the effect of CED-4 interacting proteins on cell death and CED-4 localization, we performed both misexpression and loss-of-function analyses. First, MAC-1 and PRP-1 were overexpressed, either alone or in conjunction with one another, under the control of the heat-shock promoters in both wild-type and *ced-9(n2812); ced-3(n717)* animals. Ectopic expression of neither gene had any effect on either the number of extra cells in the anterior pharynx or the localization of CED-4 to either mitochondria or nuclear membranes (data not shown). Next, RNAi of *mac-1* and *prp-1* was performed. RNAi of *prp-1* did not produce any apparent phenotype. RNAi of *mac-1*, by

contrast, caused larval arrest at approximately the L2 stage. Therefore, we chose to study the role of *mac-1* in programmed cell death and CED-4 localization in more detail.

**Deletion of *mac-1* causes larval arrest but does not affect cell death or CED-4 localization**

To more accurately assess the effects of loss of *mac-1* function, we used PCR to screen a library of mutagenized worms for animals carrying a deletion of the *mac-1* locus. From this screen we isolated two alleles, *n3320* and *n3321*, that disrupt *mac-1*. *n3320* is a 1944 bp deletion and *n3321* is a 1404 bp deletion. Both deletions span from intron 1 to intron 2, entirely eliminating predicted exon 2 without affecting other exons (Figure 3). Because of this complete removal of exon 2, these deletions could result in aberrant splicing of exon 1 to exon 3. Such aberrant splicing, if it occurs, would produce an out-of-frame product with the first 54 amino acids of MAC-1 followed by 60 novel residues prior to the stop codon.

Homozygous *mac-1(n3320)* and *mac-1(n3321)* animals arrested as larvae, similar to the phenotype observed for *mac-1*(RNAi). These larvae grew slowly (two days after hatching, they appear to still be L1 stage larvae) and terminally arrested after 5-6 days as scrawny larvae (Figure 4). Neither the vulva nor the somatic gonad nor the germ-line of these arrested larvae showed signs of proliferation. The germ-line arrested proliferation between 4 and 20 cells, which would normally be reached during the L1 or L2 stage of larval development.

The larval lethality caused by mutations in *mac-1* was not blocked by blocking programmed cell death. Double mutant larvae, either *mac-1(lf); ced-3(n717)* or *mac-1(lf); ced-4(n1162)*, arrested with the same scrawny phenotype as *mac-1(lf)* single mutant larvae, indicating that the larval lethality is likely not due to a programmed cell death defect. *mac-1* mutants did not contain excess unengulfed corpses. Next, we tested the effect of *mac*-1 mutations on various *ced-3* and *ced-4* alleles. *mac-1* did not suppress or enhance the programmed cell death defect in either weak or strong alleles of *ced-3* and *ced-4* (Table 2).

We also tested whether *mac-1* could affect the subcellular localization of CED-4. CED-4 localized to mitochondria in *mac-1(lf)* embryos, and to the nuclear membrane in *mac-1(lf); ced-9(n2812); ced-3(n717)* embryos. Therefore, we could not discern any clear role for *mac-1* in regulating programmed cell death. Loss of *mac-1* did not cause an

increase or decrease in programmed cell death, did not cause corpses to remain unengulfed, and did not affect the localization of CED-4.

## DISCUSSION

### Role of localization in CED-4 function

In wild-type embryos, CED-4 protein is located at the mitochondria. However, when programmed cell death is ectopically activated, either by the loss of CED-9 or by the overexpression of EGL-1, CED-4 becomes localized to the nuclear membrane. Despite this correlation of CED-4 nuclear membrane localization with the activation of programmed cell death in two important cases, nuclear localization of CED-4 has not been observed in cells that normally undergo PCD in wild-type embryos. Several possibilities may explain why such localization has not been observed. One, the duration of time for which CED-4 is at the nuclear membrane before the cell activates programmed cell death and the nuclear membrane breaks down may be too short in wild-type embryos. The observation of nuclear-membrane CED-4 following activation of PCD by EGL-1 suggests that the interval between CED-4 re-localization and nuclear membrane breakdown during PCD may not be so short. However, in strains overexpressing EGL-1, *ced-1(lf)* was included in the genetic background in order to quantify the level of programmed cell death induced. Disruption of engulfment can have an effect on programmed cell death execution (Reddien et al., 2001), and it is possible that *ced-1(lf)* delays cell death enough to allow the visualization of CED-4 at the nuclear membrane.

Another possible explanation for the failure to observe CED-4 nuclear membrane localization in wild-type embryos is that the resolution of nuclear membrane staining within a background of mitochondrial staining is difficult. A potential means to address this issue is to label dying cells by another means and then determine whether such labeled cells have nuclear membrane localization of CED-4. Labeling of cells by TUNEL (terminal transferase mediated dUTP nick-end labeling) could serve this purpose (Wu et al., 2000), although by the point at which TUNEL-positive DNA ends have been generated, the cell may have passed beyond the point at which the nuclear membrane is still intact. Alternatively, dying cells express a transcriptional GFP fusion of the *egl-1* gene (Conradt and Horvitz, 1999). Since *egl-1* activation triggers

programmed cell death, expression of the GFP fusion may identify cells that are early in the process of programmed cell death, and might therefore be expected to have CED-4 at to the nuclear membrane.

Finally, the translocation of CED-4 from mitochondria to nuclear membranes during activation of programmed cell death by loss of CED-9 or overexpression of EGL-1 may not represent the normal mechanism for programmed cell death. That is, activation of CED-4 may occur by release of CED-4 from CED-9 at the mitochondria, but may not require actual localization to nuclear membranes. To test the necessity of CED-4 nuclear membrane localization for activation of PCD it may be possible to ectopically direct CED-4 to non-nuclear subcellular compartments and determine the effect on cell death. For instance, introducing a plasma membrane targeting motif (*e.g.*, CAAX motif and palmitoylation site) into CED-4 may direct the protein to the cell membrane rather than the nuclear membrane. If such a modified CED-4 is localized to the plasma membrane but is still capable of activating programmed cell death, then the release of CED-4 from CED-9 might be more critical than the nuclear membrane localization of CED-4.

**Role of *mac-1* gene in programmed cell death**

The other group that also identified the *mac-1* gene through a yeast two-hybrid screen for CED-4 interactors concluded that *mac-1* overexpression could block programmed cell death in a sensitized background (Wu et al., 1999). However, we did not observe any effect of the *mac-1* deletion on programmed cell death. Mutations in engulfment genes, which on their own have no effect on programmed cell death, are able to enhance weak *ced-3* and *ced-4* mutations (Reddien et al., 2001). Therefore, we might expect to be able to observe a weak effect of *mac-1*(lf) on programmed cell death. Since we saw no such effect, we must attempt to reconcile our findings with those of (Wu et al., 1999). Overexpression of *mac-1* in wild-type worms generated only 10 total extra cells in thirteen animals, whereas overexpression in *ced-9*(*n1950*gf)/+ progeny of wild-type mothers approximately doubled the number of extra cells. One possible explanation for this observation is that the effect is specific to the *ced-9*(*n1950*gf) allele.

**Identifying genes responsible for CED-4 localization**

These studies were initiated with the intent of identifying components involved in the localization of CED-4 to the nuclear membrane upon release from CED-9 and the mitochondria. As the approaches taken here have not yet identified such components, we must consider other means for doing so.

First, candidate gene approaches, such as those described here, have not been exhausted, and may still be able to identify components necessary for CED-4 localization. For instance, deletion of the *prp-1* gene may affect CED-4 localization or programmed cell death, even though overexpression and RNAi had no observable effects. In addition, elimination of additional components of the nuclear membrane, such as Ce-emerin, has not been assessed for effects on CED-4 localization.

Rather than relying on an approach that depends on our limited knowledge of the composition of the nuclear envelope, an unbiased genetic screen for mutations that affect CED-4 localization may prove more fruitful in identifying genes important in this process. A CED-4::GFP translational fusion is capable of rescuing the Ced phenotype of *ced-4(n1162)* animals and is localized in puncta at the nuclear membrane (F. Chen and B. Hersh, unpublished data). Using a strain in which this transgene is stably integrated, a genetic screen can be performed for mutants with disrupted CED-4::GFP localization. Since the transgene is expressed starting in embryogenesis and the GFP persists through adulthood, screening can be performed either in embryos or in adult worms via a dissecting scope equipped with GFP epifluorescence. In addition, if the screen is performed clonally, mutations in genes that have a lethal loss-of-function phenotype in addition to an effect on CED-4 localization could still be isolated. A non-clonal screen for viable adult mutants in which CED-4::GFP localization is disrupted was performed (B. Adolfsen and B. Hersh, unpublished data), and a single mutant causing spotty cytoplasmic localization of CED-4::GFP was identified from a screen of 2300 haploid genomes. This mutant has been tentatively mapped to chromosome I (M. Higginbotham and B. Hersh, unpublished data). However, the effect of this mutation on endogenous CED-4 localization has not been determined and the specificity of the effects of this mutation with regard to transgene expression and localization has not been investigated. Nevertheless, we hope that this approach may successfully identify components involved in CED-4 subcellular localization, and thereby provide insight into the molecular mechanisms of regulating programmed cell death execution.

## REFERENCES


Bione, S., Maestrini, E., Rivella, S., Mancini, M., Regis, S., Romeo, G., and Toniolo, D. (1994). Identification of a novel X-linked gene responsible for Emery-Dreifuss muscular dystrophy. Nat. Genet. *8*, 323-7.

Brenner, S. (1974). The genetics of Caenorhabditis elegans. Genetics *77*, 71-94.

Chen, F., Hersh, B. M., Conradt, B., Zhou, Z., Riemer, D., Gruenbaum, Y., and Horvitz, H. R. (2000). Translocation of *C. elegans* CED-4 to nuclear membranes during programmed cell death. Science *287*, 1485-9.

Chinnaiyan, A. M., O'Rourke, K., Lane, B. R., and Dixit, V. M. (1997). Interaction of CED-4 with CED-3 and CED-9: a molecular framework for cell death. Science *275*, 1122-6.

Conradt, B., and Horvitz, H. R. (1998). The *C. elegans* protein EGL-1 is required for programmed cell death and interacts with the Bcl-2-like protein CED-9. Cell *93*, 519-29.

Conradt, B., and Horvitz, H. R. (1999). The TRA-1A sex determination protein of *C. elegans* regulates sexually dimorphic cell deaths by repressing the *egl-1* cell death activator gene. Cell *98*, 317-27.

Cryns, V., and Yuan, J. (1998). Proteases to die for. Genes Dev. *12*, 1551-70.

del Peso, L., Gonzalez, V. M., and Nunez, G. (1998). *Caenorhabditis elegans* EGL-1 disrupts the interaction of CED-9 with CED- 4 and promotes CED-3 activation. J. Biol. Chem. *273*, 33495-500.

Dreger, M., Bengtsson, L., Schoneberg, T., Otto, H., and Hucho, F. (2001). Nuclear envelope proteomics: Novel integral membrane proteins of the inner nuclear membrane. Proc. Natl. Acad. Sci. USA *98*, 11943-8.

Ellenberg, J., Siggia, E. D., Moreira, J. E., Smith, C. L., Presley, J. F., Worman, H. J., and Lippincott-Schwartz, J. (1997). Nuclear membrane dynamics and reassembly in living cells: targeting of an inner nuclear membrane protein in interphase and mitosis. J. Cell. Biol. *138*, 1193-206.

Fire, A., Harrison, S. W., and Dixon, D. (1990). A modular set of lacZ fusion vectors for studying gene expression in Caenorhabditis elegans. Gene *93*, 189-98.

Fire, A., Xu, S., Montgomery, M. K., Kostas, S. A., Driver, S. E., and Mello, C. C. (1998). Potent and specific genetic interference by double-stranded RNA in Caenorhabditis elegans. Nature *391*, 806-11.

Goldberg, M., Harel, A., Brandeis, M., Rechsteiner, T., Richmond, T. J., Weiss, A. M., and Gruenbaum, Y. (1999). The tail domain of lamin Dm0 binds histones H2A and H2B. Proc. Natl. Acad. Sci. USA *96*, 2852-7.

Gruenbaum, Y., Wilson, K. L., Harel, A., Goldberg, M., and Cohen, M. (2000). Review: nuclear lamins--structural proteins with fundamental functions. J. Struct. Biol. *129*, 313-323.

Hengartner, M. O., Ellis, R. E., and Horvitz, H. R. (1992). *Caenorhabditis elegans* gene *ced-9* protects cells from programmed cell death. Nature *356*, 494-9.

Hengartner, M. O., and Horvitz, H. R. (1994). *C. elegans* cell survival gene *ced-9* encodes a functional homolog of the mammalian proto-oncogene *bcl-2*. Cell *76*, 665-76.

Jansen, G., Hazendonk, E., Thijssen, K. L., and Plasterk, R. H. (1997). Reverse genetics by chemical mutagenesis in Caenorhabditis elegans. Nat. Genet. *17*, 119-21.

Malone, C. J., Fixsen, W. D., Horvitz, H. R., and Han, M. (1999). UNC-84 localizes to the nuclear envelope and is required for nuclear migration and anchoring during C. elegans development. Development *126*, 3171-81.

Mello, C., and Fire, A. (1995). DNA transformation. Methods Cell Biol *48*, 451-82.

Metzstein, M. M., Stanfield, G. M., and Horvitz, H. R. (1998). Genetics of programmed cell death in *C. elegans*: past, present and future. Trends Genet. *14*, 410-6.

Nagano, A., Koga, R., Ogawa, M., Kurano, Y., Kawada, J., Okada, R., Hayashi, Y. K., Tsukahara, T., and Arahata, K. (1996). Emerin deficiency at the nuclear membrane in patients with Emery- Dreifuss muscular dystrophy. Nat. Genet. *12*, 254-9.

Östlund, C., Ellenberg, J., Hallberg, E., Lippincott-Schwartz, J., and Worman, H. J. (1999). Intracellular trafficking of emerin, the Emery-Dreifuss muscular dystrophy protein. J. Cell. Sci. *112*, 1709-19.

Reddien, P. W., Cameron, S., and Horvitz, H. R. (2001). Phagocytosis promotes programmed cell death in *C. elegans*. Nature *412*, 198-202.

Riemer, D., Dodemont, H., and Weber, K. (1993). A nuclear lamin of the nematode Caenorhabditis elegans with unusual structural features; cDNA cloning and gene organization. Eur J Cell Biol *62*, 214-23.

Rolls, M. M., Stein, P. A., Taylor, S. S., Ha, E., McKeon, F., and Rapoport, T. A. (1999). A visual screen of a GFP-fusion library identifies a new type of nuclear envelope membrane protein. J. Cell. Biol. *146*, 29-44.

Sambrook, J., Fritsch, E. F., and Maniatis, T. (1989). Molecular Cloning: A Laboratory Manual (Cold Spring Harbor, New York, Cold Spring Harbor Laboratory Press).

Shaham, S., Reddien, P. W., Davies, B., and Horvitz, H. R. (1999). Mutational analysis of the Caenorhabditis elegans cell-death gene ced-3. Genetics *153*, 1655-71.

Shtang, S., Perry, M. D., and Percy, M. E. (1999). Search for a Caenorhabditis elegans FMR1 homologue: identification of a new putative RNA-binding protein (PRP-1) that

hybridizes to the mouse FMR1 double K homology domain. Am. J. Med. Genet. *84*, 283-5.

Stuurman, N., Heins, S., and Aebi, U. (1998). Nuclear lamins: their structure, assembly, and interactions. J. Struct. Biol. *122*, 42-66.

Sullivan, T., Escalante-Alcalde, D., Bhatt, H., Anver, M., Bhat, N., Nagashima, K., Stewart, C. L., and Burke, B. (1999). Loss of A-type lamin expression compromises nuclear envelope integrity leading to muscular dystrophy. J. Cell. Biol. *147*, 913-20.

Timmons, L., and Fire, A. (1998). Specific interference by ingested dsRNA. Nature *395*, 854.

Wood, W. B., and *Researchers*, T. C. o. C. e. (1988). The Nematode *Caenorhabditis elegans*, Cold Spring Harbor Laboratory).

Wu, D., Chen, P. J., Chen, S., Hu, Y., Nunez, G., and Ellis, R. E. (1999). C. elegans MAC-1, an essential member of the AAA family of ATPases, can bind CED-4 and prevent cell death. Development *126*, 2021-31.

Wu, Y. C., Stanfield, G. M., and Horvitz, H. R. (2000). NUC-1, a caenorhabditis elegans DNase II homolog, functions in an intermediate step of DNA degradation during apoptosis. Genes Dev. *14*, 536-48.

Yuan, J., and Horvitz, H. R. (1992). The *Caenorhabditis elegans* cell death gene *ced-4* encodes a novel protein and is expressed during the period of extensive programmed cell death. Development *116*, 309-20.

Yuan, J., Shaham, S., Ledoux, S., Ellis, H. M., and Horvitz, H. R. (1993). The *C. elegans* cell death gene *ced-3* encodes a protein similar to mammalian interleukin-1 beta-converting enzyme. Cell *75*, 641-52.

Zou, H., Henzel, W. J., Liu, X., Lutschg, A., and Wang, X. (1997). Apaf-1, a human protein homologous to *C. elegans* CED-4, participates in cytochrome c-dependent activation of caspase-3. Cell *90*, 405-13.

## TABLES

### Table 1. Molecular changes in *ced-4* alleles and effects on CED-4 localization.

| Allele | Nucleotide change | Molecular change | Localization in *ced-9(+)* | Localization in *ced-9(-)* | Extra cells |
|---|---|---|---|---|---|
| *n3551* | A to C | T15P | M | | 12.4 ± 0.25 |
| *n3043* | G to A | D20N | M | N | 9.0 ± 0.70 |
| *n3040* | C to T | P23L | C | C | 11.5 ± 0.36 |
| *n3332* | C to T | P23L | C | | 9.0 ± 0.23 |
| *n3161* | G to A | E31K | M | | 9.0 ± 0.40 |
| *n3131* | C to T | H40Y | | N | |
| *n3141* | G to A | R53K | M | N | 3.0 ± 0.41 |
| *n3327* | C to T | R59 opal | none | | 11.7 ± 0.44 |
| *n2831* | C to T | R59 opal | | | |
| *n3128* | C to T | R63C | | C? | |
| *n3195* | G to A | R63H | M | | 1.0 ±0.19 |
| *n1162* | C to T | Q80 ochre | none | none | 11.8 ± 0.23 |
| *n3550* | G to A | G122E | M | | 11.4 ± 0.31 |
| *n2274* | C to T | R139 opal | | | |
| *n3158* | C to T | S163F | M | | 6.0 ± 0.37 |
| *n3455* | G to A | G164R | none | | 10.9 ± 0.34 |
| *n2423* | G to A | G164E | none | | 10.3 ± 0.41 |
| *n3532* | C to T | Q171 ochre | none | | 12.2 ± 0.28 |
| *n3572* | G to A | splice donor, intron 2 | none | | 11.0 ± 0.28 |
| *n3620* | G to A | splice donor, intron 2 | none | | 11.1 ± 0.34 |
| *n3120* | G to A | splice donor, intron 2 | | none | |
| *n1920* | G to A | splice donor, intron 3 | | | |
| *n2247* | G to A | splice donor, intron 3 | | | |
| *n2273* | G to A | splice acceptor, intron 3 | none | | 3.7 ± 0.51 |
| *n3108* | G to A | S213N | | none (w/ *n2273*) | |
| *n2723* | G to A | splice donor, intron 4 | | | |
| *n3339* | C to T | P242L | M | | 9.1 ± 0.46 |
| *n1948* | T to A | I258N | M* | | 9.1 ± 0.39 |
| *n1947* | C to T | Q262 amber | | | |
| *n2860* | G to A | E263K | M | N | 0.4 ± 0.15 |
| *n3457* | T to C | C268R | M | | 9.9 ± 0.32 |
| *n2879* | G to A | E276K | M | N | 0.4 ± 0.13 |
| *n3617* | C to T | Q283 ochre | none | | 11.5 ± 0.36 |
| *n3100* | T to C | S339P | M | N | 0.4 ± 0.18 |
| *n3362* | G to A | splice donor, intron 5 | none | | 9.4 ± 0.36 |
| *n3365* | G to A | splice donor, intron 5 | none | | 9.7 ± 0.38 |
| *n3323* | G to A | splice acceptor, intron 5 | none | | 11.2 ± 0.43 |
| *n2456* | C to T | Q379 ochre | | | |
| *n3456* | C to T | Q379 ochre | none | | 11.8 ± 0.37 |
| *n3533* | C to T | Q379 ochre | none | | 11.5 ± 0.31 |
| *n3459* | G to A | C381Y | M | | 12.8 ± 0.27 |
| *n3312* | G to A | A394T | M | | 2.0 ± 0.25 |
| *n1894* | G to A | W410 opal | | | |
| *n3084* | G to A | W410 opal | | | |
| *n3107* | G to A | E429K | | none (w/ *n2273*) | |
| *n3613* | C to T | S438S | none | | 10.7 ± 0.36 |
| *n3573* | G to A | splice acceptor, intron 6 | none | | 11.0 ± 0.37 |

| Allele | Nucleotide change | Molecular change | Localization in *ced-9(+)* | Localization in *ced-9(-)* | Extra cells |
|---|---|---|---|---|---|
| *n3153* | C to T | R448 opal | | | |
| *n3460* | C to T | R448 opal | none | | 11.6 ± 0.27 |
| *n3621* | C to T | R448 opal | none | | 12.4 ± 0.27 |
| *n3111* | G to A | G476E | | none (w/ *n2273*) | |
| *n3003* | C to T | Q504 ochre | | | |
| *n3009* | C to T | Q504 ochre | | | |
| *n3129* | C to T | Q534 ochre | | none | |
| *n3122* | C to T | Q537 amber | | none | |
| *n2925* | | large deletion | | | |

*ced-4* alleles are sorted by position in the gene. Shaded entries represent missense alleles. Number of extra cells was determined in the anterior pharynx for *ced-4* alleles in a *ced-9*(+) background. Where *ced-4* alleles have not been separated from *ced-9*(lf) mutations, no value for extra cells is presented. The average value for at least 15 animals and standard error of the mean (SEM) is indicated. Three alleles (*n3107, n3108, n3111*) were isolated in *ced-4*(*n2273*) *ced-9*(*n1653*) animals (E. Speliotes, unpublished data), and CED-4 localization was determined in this genetic background. Four alleles (*n3120, n3122, n3128, n3129*) were isolated in *ced-9*(*n1950n2161*); *ced-8*(*n1891*) animals (E. Speliotes, unpublished data), and CED-4 localization was determined in a *ced-9*(*n1950n2161*) genetic background. CED-4 localization in other *ced-4; ced-9* double mutants was determined using the *ced-9*(*n2812*) allele. While most *ced-4*(*n1948*) embryos displayed mitochondrial CED-4 localization (listed as M*), some embryos displayed a mottled distribution of CED-4. The *ced-4*(*n1948*) strain produces a significant number of dead embryos, perhaps due to a lethal mutation carried by the strain, and it is probable that these embryos are the source of the difference in CED-4 distribution in this strain. CED-4 expression in *ced-4*(*n3128*) is weak and may be cytoplasmic (C?), but the low intensity of staining makes this assessment uncertain.

**Table 2. *mac-1*(lf) does not affect programmed cell death in the anterior pharynx.**

| Genotype | **Avg. # extra cells** |
|---|---|
| *mac-1(n3320)* | 0.0 (n=6) |
| *mac-1(n3321)* | 0.0 (n=6) |
| *ced-3(n717)* | 11.0 ± 0.63 (n=10) |
| *mac-1(n3320); ced-3(n717)* | 10.4 ± 0.31 (n=10) |
| *mac-1(n3321); ced-3(n717)* | 10.8 ± 0.58 (n=5) |
| *ced-3(n2427)* | 1.2 ± 0.13 (n=25) |
| *mac-1(n3320); ced-3(n2427)* | 1.2 ± 0.17 (n=15) |
| *mac-1(n3321); ced-3(n2427)* | 1.5 ± 0.27 (n=17) |
| *ced-4(n1162)* | 11.3 ± 0.15 (n=10) |
| *mac-1(n3320); ced-4(n1162)* | 10.5 ± 0.29 (n=4) |
| *mac-1(n3321); ced-4(n1162)* | 10.2 ± 0.52 (n=9) |
| *ced-4(n3312)* | 1.5 ± 0.24 (n=15) |
| *mac-1(n3320); ced-4(n3312)* | 1.2 ± 0.15 (n=21) |
| *mac-1(n3321); ced-4(n3312)* | 1.2 ± 0.16 (n=16) |

Number of extra cells in *n* animals was determined, and average number of extra cells ± SEM is shown.

FIGURES

**Figure 1. Neither *ced-3* catalytic activity nor prodomain function are required for CED-4 localization.**

Confocal microscope images of embryos stained with anti-CED-4 primary antibody. **(A)** *ced-3(n2452)* embryo **(B)** *ced-9(n2812); ced-3(nn2452)* **(C)** *ced-3(n718)* **(D)** *ced-9(n2812); ced-3(n718)* **(E)** *ced-3(n2439)* **(F)** *ced-9(n1950n2161); ced-3(n2439)* **(G)** *ced-3(n3692)* **(H)** *ced-9(n2812); ced-3(n3692).*

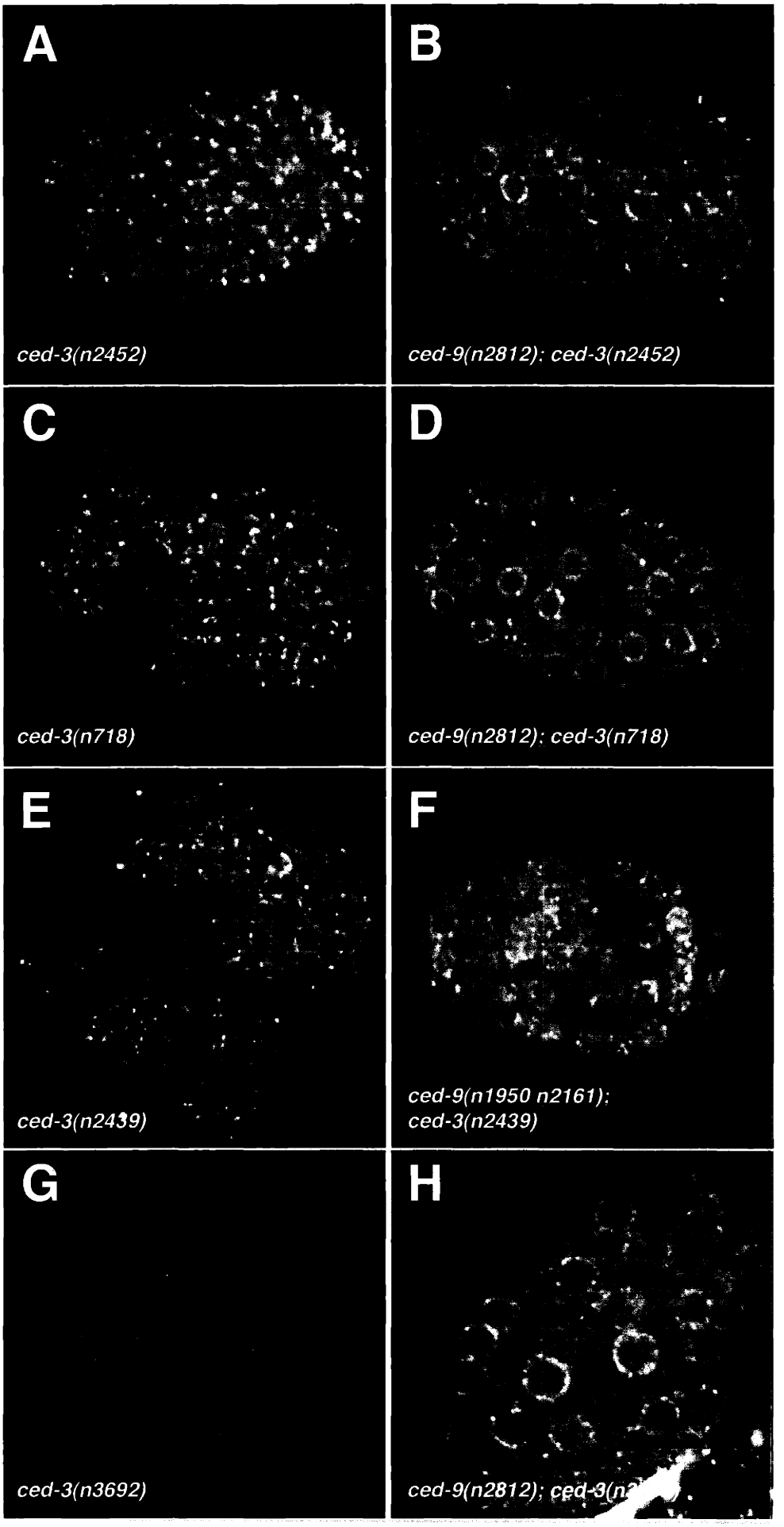
A
ced-3(n2452)
B
ced-9(n2812); ced-3(n2452)
C
ced-3(n718)
D
ced-9(n2812); ced-3(n718)
E
ced-3(n2439)
F
ced-9(n1950 n2161);
ced-3(n2439)
G
ced-3(n3692)
H
ced-9(n2812); ced-3(n

**Figure 2. Co-localization of CED-4 protein with nucleoporin and Ce-Emerin.**
**(A)** Embryo stained with rat anti-CED-4 antibody **(B)** Same embryo stained with monoclonal antibody Mab414 recognizing nucleoporin **(C)** Merged image of (A) and (B) **(D)** Embryo stained with rat anti-CED-4 antibody and **(E)** rabbit anti-Emerin antibody. **(F)** Merged image of (D) and (E).

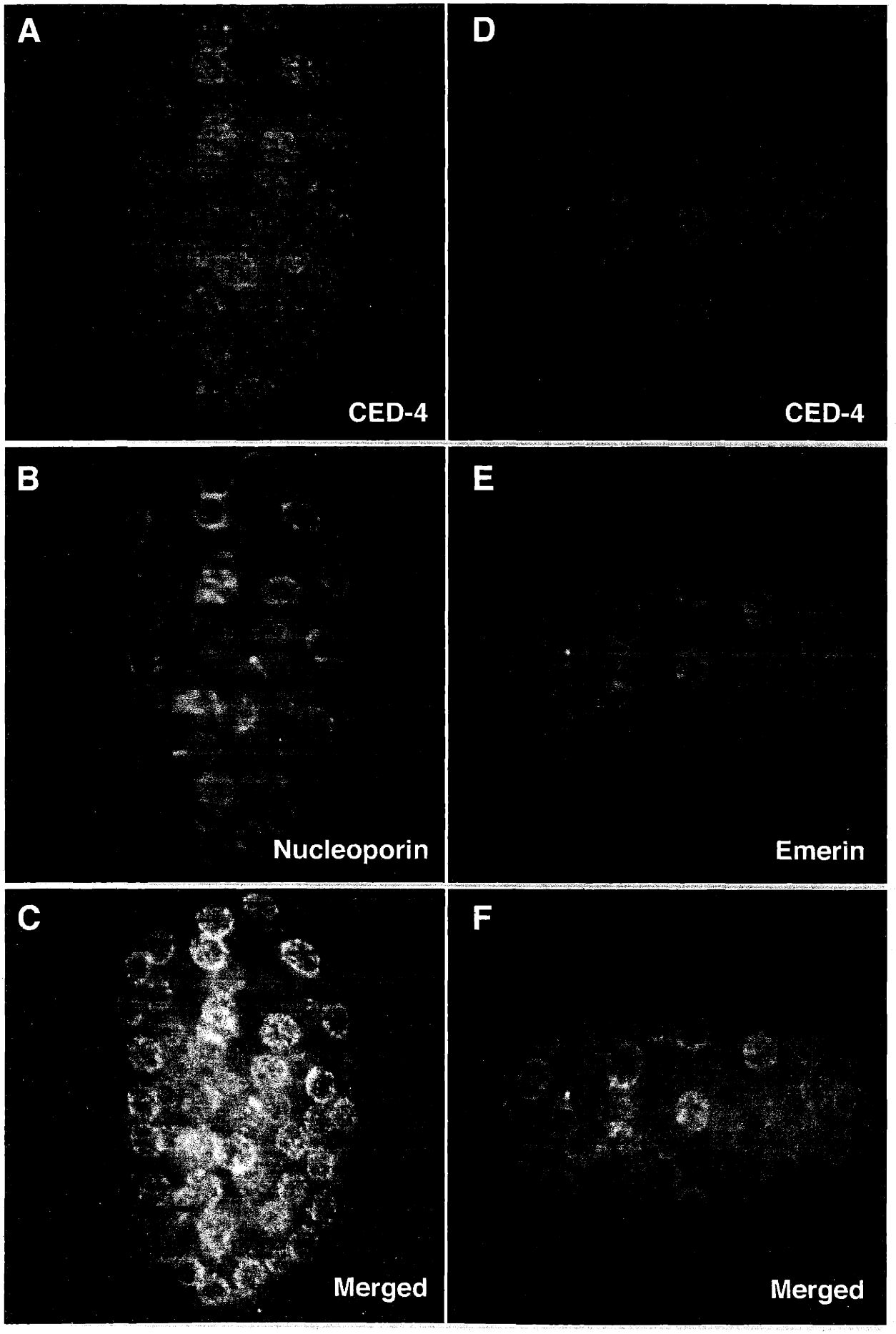
A
CED-4
D
CED-4
B
Nucleoporin
E
Emerin
C
Merged
F
Merged

**Figure 3. Lamin RNAi does not disrupt CED-4 localization**

**(A)** N2 embryo treated with lamin RNAi and stained with anti-CED-4 antibody. CED-4 localization remains mitochondrial. **(B)** *ced-9(n2812); ced-3(n717)* embryo treated with lamin RNAi and stained with anti-CED-4 antibody. CED-4 is still present at the nuclear membrane.

## Figure 3

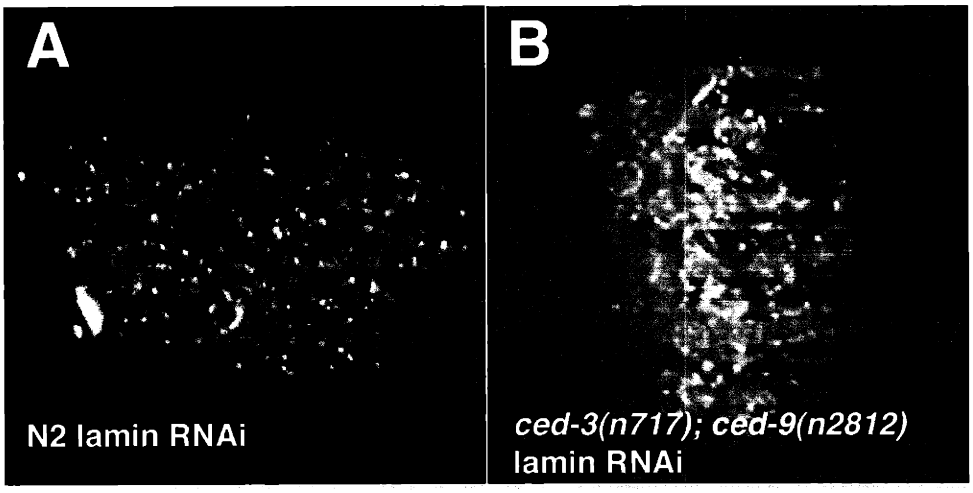

**Figure 4. Structure of and deletions in the *mac-1* gene.**

Gene structure for *mac-1*. Exons are indicated by boxes. Shaded portions represent the two conserved ATPase domains of *mac-1*. Primers used for deletion screening are indicated (L, R). The extent of the two deletion alleles, *n3320* and *n3321*, is shown. Both remove identical portions of the predicted protein. If aberrant splicing between exon 1 and exon 3 were to occur in the deletion alleles, the resulting protein would contain the first 54 amino acids of MAC-1 followed by 60 novel amino acids.

## Figure 4

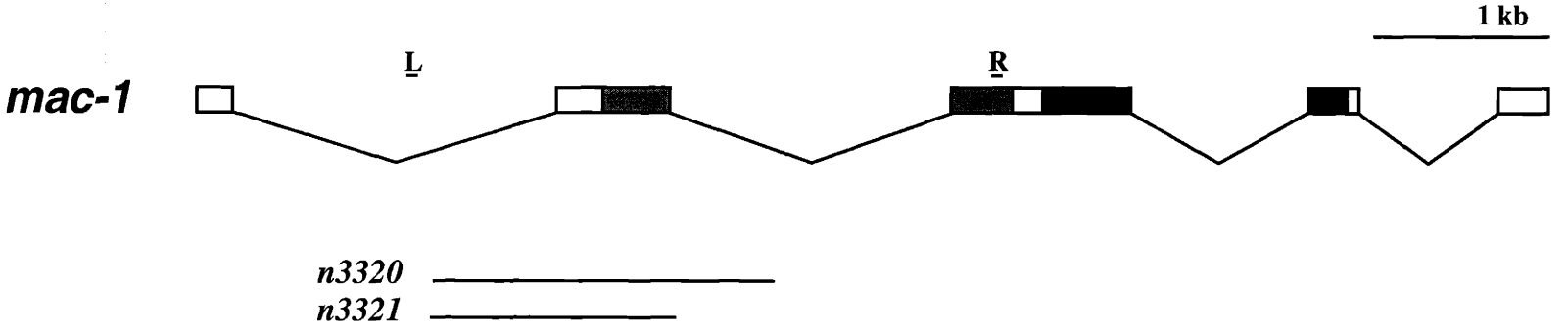

**Figure 5. Nomarksi images of *mac-1* animals**

**(A)** Two-day post-hatching *mac-1(n3320)* animal. The four-cell gonad is indicated with a bracket. **(B)** Seven-day post-hatching *mac-1(n3321)* animal. The position of the gonad is indicated with a bracket. The somatic gonad and germline are underdeveloped. The vulva is completely absent, and vulval precursor cells have not undergone their L3 stage divisions.

**Figure 5**

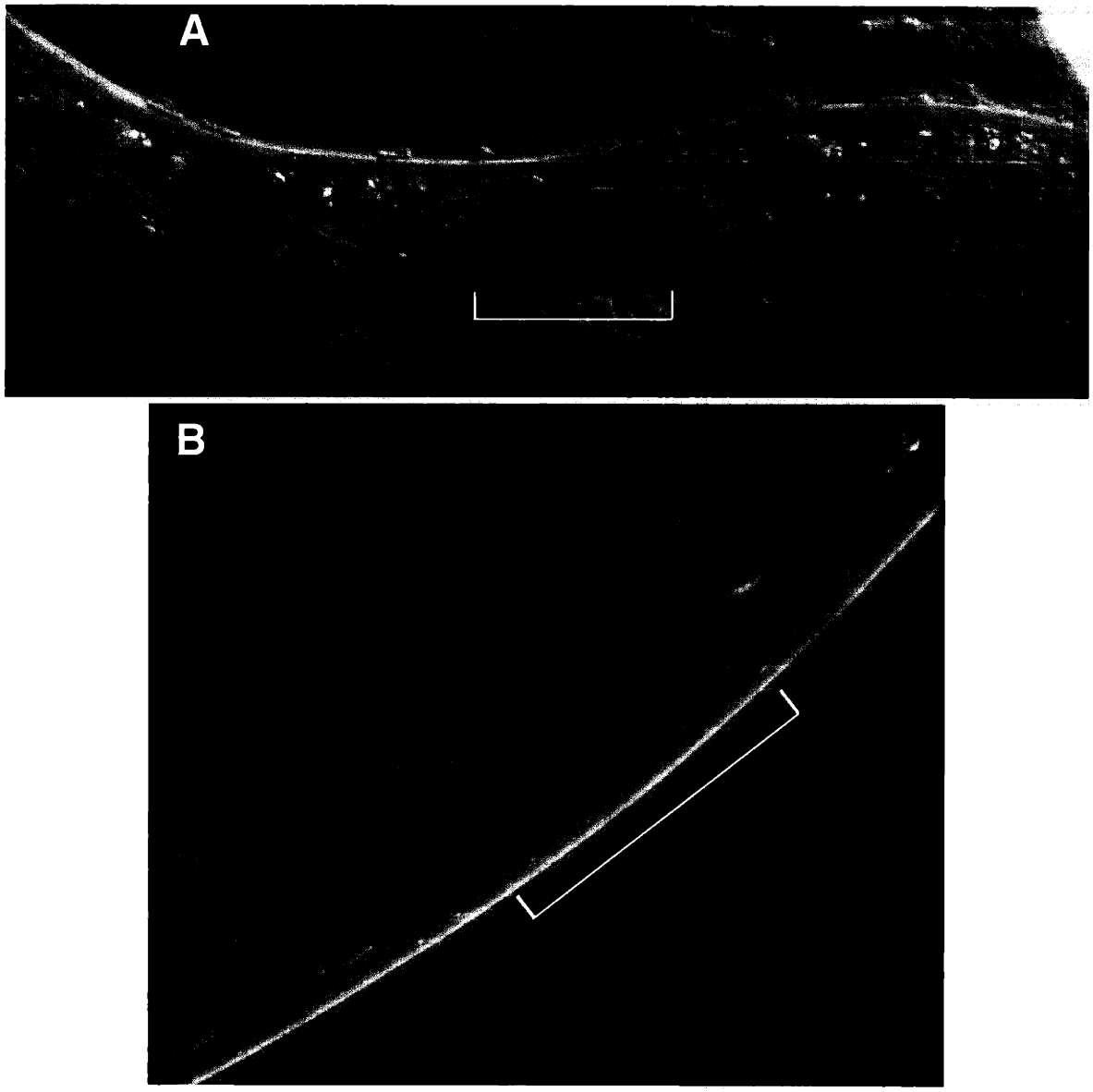

# Appendix I

# Additional Experiments and Results

## CHARACTERIZATION OF NEW *CED-9* ALLELES

The Bcl-2 family member *ced-9* acts in *C. elegans* to primarily prevent inappropriate programmed cell death, and strong loss-of-function mutations in *ced-9* result in ectopic programmed cell death, partial sterility, and maternal-effect lethality (Hengartner et al., 1992). However, like the diverse Bcl-2 family, which contains both pro- and anti-apoptotic members, *ced-9* also appears to possess a pro-apoptotic function in addition to its widely recognized protective role. The basis for this proposed pro-apoptotic function is the ability of *ced-9* loss-of-function mutations to enhance the cell death defect of weak mutations in the *ced-3* caspase (Hengartner and Horvitz, 1994). Animals bearing the allele *ced-3(n2427)* contain an average of 2.8 extra cells in the anterior pharynx. Double mutant animals of the genotype *ced-9(n2812); ced-3(n2427)* contain an average of 7.7 extra cells in the anterior pharynx (Hengartner and Horvitz, 1994). As the cell death defect is greater (*i.e.*, there are more surviving cells) in the absence of *ced-9*, this result indicates that *ced-9* must be contributing to the killing process. One proposed mechanism for the killing function of *ced-9* is that *ced-9* can inhibit the activity of *ced-4L*, an alternatively spliced variant of *ced-4* containing 72 extra base pairs and capable of preventing programmed cell death when overexpressed (Shaham and Horvitz, 1996).

A screen for mutations that enhance the cell death defect in the ventral cord of *ced-3(n2427)* animals identified mutations in the engulfment genes (Reddien et al., 2001), as well as three new alleles of *ced-9* (Reddien and Horvitz, unpublished results). As these alleles were derived from an unbiased screen for enhancers of the weak *ced-3* allele, it is possible that these new mutations in the *ced-9* gene could disrupt the killing activity without having any effect on the protective function. Therefore, we identified the molecular lesions in the new alleles of *ced-9*, attempted to isolate the new alleles away from the *ced-3(n2427)* mutation, and determined the affect of these mutations on the localization of CED-4 protein.

Sequencing of the three *ced-9* alleles (*n3377, n3400, n3407*) identified molecular changes in all three alleles (Figure 1). *ced-9(n3377)* contains a G-to-A nucleotide substitution that would convert glutamate 74 into a lysine residue. The *ced-9(n3400)* allele appeared to contain a deletion when amplified by PCR, and direct sequencing confirmed this result. The deletion eliminates 121 bp, starting in the fifth codon, and the predicted frameshifted protein product would be only 11 amino acids long. Finally,

the *ced-9(n3407)* allele contains a G-to-A nucleotide substitution that would eliminate the splice acceptor site at the beginning of exon 3. The BH1 (Bcl-2 homology) domain in *ced-9* spans exons 2 and 3, and would therefore likely be disrupted by the *ced-9(n3407)* splice acceptor mutation.

From a molecular standpoint, the *ced-9(n3400)* deletion allele might be expected to act as a null allele. However, the effect of the other two mutations on *ced-9* function is not obvious from their molecular identity. Therefore, we attempted to separate all three alleles from the *ced-3(n2427)* mutation to determine the effect of the *ced-9* mutation alone. Both *ced-9(n3400)* and *ced-9(n3407)* could only be isolated as balanced strains. Animals homozygous for these mutations appeared slightly uncoordinated (Unc) and egg-laying defective (Egl), and embryos from these Unc Egl animals arrested prior to hatching. These defects are very similar to what is observed for other *ced-9* loss-of-function alleles, including the putative null allele *ced-9(n2812)*, so these two alleles appear to affect both the protective and the killing functions of *ced-9*.

As demonstrated in Chapter 2, loss of *ced-9* results in the movement of CED-4 protein from mitochondria to the nuclear membrane. Therefore, we determined whether the new *ced-9* alleles acted in a similar manner. We fixed *ced-9; ced-3(n2427)* embryos and stained with α-CED-4 antibodies (Chen et al., 2000). CED-4 protein was observed at the nuclear membrane in embryos bearing any of the three *ced-9* mutant alleles (Figure 2), whereas *ced-3(n2427)* alone did not disrupt mitochondrial localization of CED-4. Thus, with respect to localization of CED-4, all three new *ced-9* alleles appear to behave as loss-of-function alleles.

**Figure 1. Mutations in *ced-9***

The 840 bp open reading frame of the *ced-9* gene and the predicted 280 amino acid protein product are shown, with the four Bcl-2 homology (BH) domains highlighted in color. The seven *ced-9* alleles with identified molecular changes are also shown. The three lesions identified in this study are: *n3400,* deletion; *n3377,* E74K; and *n3407,* disruption of exon 3 splice acceptor site.

# Figure 1

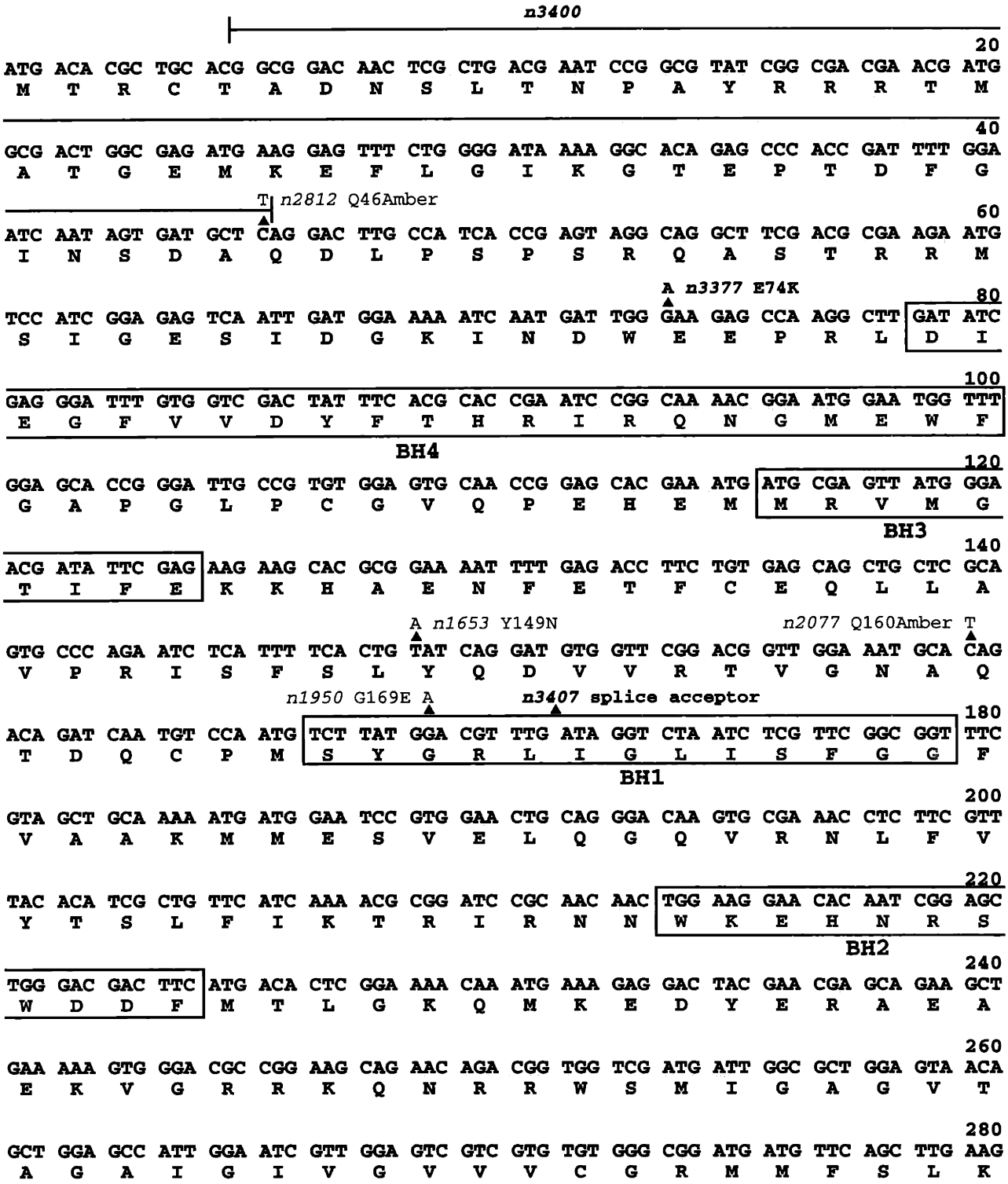
n3400
T n2812 Q46Amber
A n3377 E74K
BH4
BH3
A n1653 Y149N
n2077 Q160Amber T
n1950 G169E A
n3407 splice acceptor
BH1
BH2

**Figure 2. CED-4 localizes to the nuclear membrane in animals carrying *ced-9(n3377)*, *ced-9(n3400)*, and *ced-9(n3407)* alleles.**

**(A)** *ced-9(n3377); ced-3(n2427)* **(B)** *ced-9(n3400); ced-3(n2427)* **(C)** *ced-9(n3407); ced-3(n2427)* embryos stained with rabbit anti-CED-4 antibody.

# Figure 2

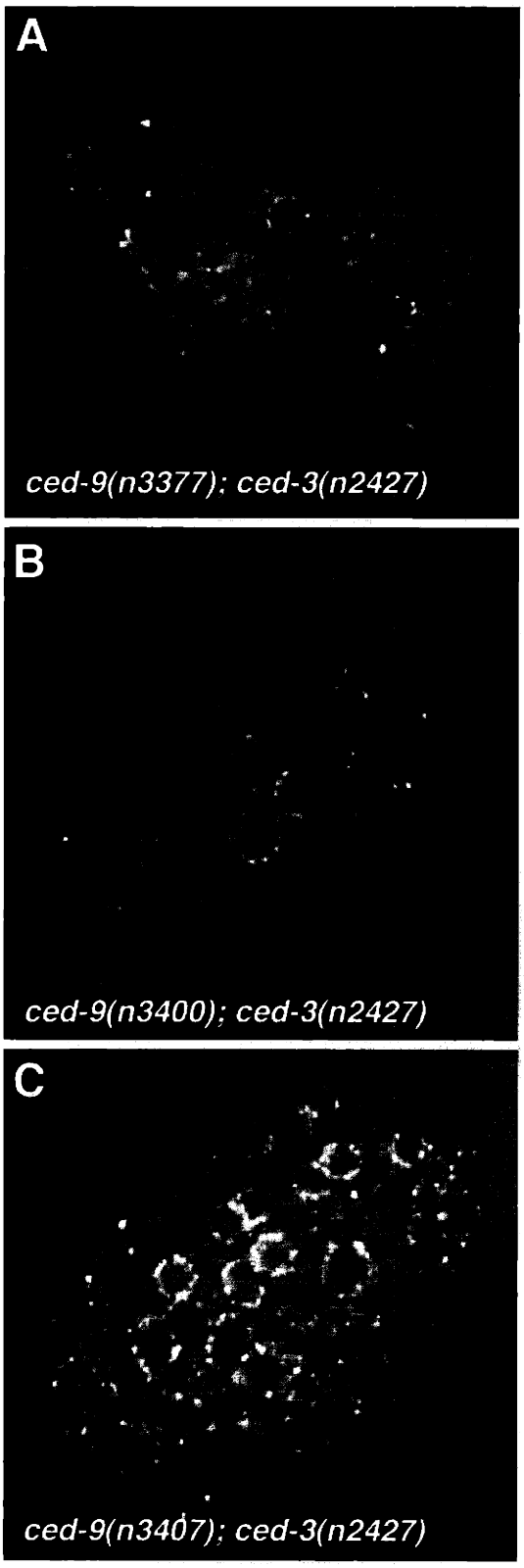
A
ced-9(n3377); ced-3(n2427)
B
ced-9(n3400); ced-3(n2427)
C
ced-9(n3407); ced-3(n2427)

## PROGRAMMED CELL DEATH IN *CED-9*(LF) EMBRYOS

Loss of protective *ced-9* function leads to maternal-effect lethality. In embryos derived from homozygous *ced-9*(*n1950 n2161*) mothers, this lethality manifests itself as an increase in programmed cell death, as numerous ectopic cell deaths are observed, even in lineages where no cells normally undergo programmed cell (Hengartner et al., 1992). However, in embryos derived from homozygous *ced-9*(*n1950 n2077*) mothers, no ectopic programmed cell deaths are observed and animals arrest much earlier in development with apparent defects in cytokinesis (Hengartner et al., 1992). A similar early arrest phenotype is observed in embryos derived from homozygous *ced-9*(*n2812*) mothers (Table 1 and Figure 3). However, blocking programmed cell death by mutations in *ced-3* or *ced-4* completely suppresses *ced-9* defects, including the early arrest defects in the stronger alleles. Therefore, either the cytokinetic defect is due to a cell death defect, possibly in the maternal germline, or *ced-9*, *ced-3*, and *ced-4* act in a non-death process during early development.

To address this issue, we generated embryos derived from *ced-9*(*n2812*) mothers with varying doses of the programmed cell death machinery and determined the arrest point of these embryos and whether they contained cell corpses (Table 1 and Figure 3). *ced-9*(*n2812*) embryos arrested early in development and this early arrest could be suppressed by mutations in *ced-3* or *ced-4* but not by mutations in *egl-1*. Arrested embryos did not contain programmed cell death corpses, as is observed in *ced-9*(*n1950 n2077*) embryos. By contrast, *ced-9*(*n2812*) embryos derived from homozygous *ced-9*(*n2812*) mothers but heterozygous for either *ced-3* or *ced-4* mutations or both were capable of developing past the early arrest stage, but only if the mother also carried the *ced-3* or *ced-4* mutation (Fig. 3 C,D). That is, if there was no cell death in the maternal germline, embryos developed past the early arrest. Embryos heterozygous for *ced-3* or *ced-4* derived from a male arrested early (Fig. 3 F, G), just as did *ced-9*(*n2812*) homozygotes. These observations imply that a maternal block in programmed cell death is required for survival of *ced-9*(lf) embryos beyond early development. Since the zygotic cell death pathway is active and they lack *ced-9* function, they arrest later and with excess corpses. That *ced-9*(*n2812*) embryos can develop beyond early stages and can generate programmed cell death corpses suggests that early *ced-9*(lf) arrest is more likely to be the result of maternal abnormalities in germline programmed cell death than an additional requirement for *ced-9* function in an early developmental process.

## Table 1. Arrest phenotype and presence of corpses in *ced-9(n2812)* embryos

| Paternal genotype | Maternal genotype | Zygotic genotype | Stage of arrest | Corpses? |
|---|---|---|---|---|
| | *ced-9(n2812)* | *ced-9(n2812)* | ~100 cells | No |
| | *ced-9(n2812); egl-1(n1084 n3082)* | *ced-9(n2812); egl-1(n1084 n3082* | ~100 cells | No |
| | *ced-9(n2812); ced-3(n717)* | *ced-9(n2812); ced-3(n717)* | No arrest | No |
| | *ced-4(n1162) ced-9(n2812)* | *ced-4(n1162) ced-9(n2812)* | No arrest | No |
| *ced-4(n1162) ced-9(n2812)* | *ced-9(n2812); ced-3(n717)* | *ced-4(n1162) ced-9(n2812)/ + ced-9(n2812); ced-3(n717)/ +* | 2-fold | Yes |
| *ced-9(n2812)/qC1* | *ced-9(n2812); ced-3(n717)* | *ced-9(n2812); ced-3(n717)/ +* | 1.5-fold | Yes |
| *ced-9(n2812); ced-3(n717)* | *ced-9(n2812)* | *ced-9(n2812); ced-3(n717)/ +* | ~100 cells | No |
| *ced-9(n2812)/qC1* | *ced-4(n1162) ced-9(n2812)* | *ced-4(n1162) ced-9(n2812)/ + ced-9(n2812)* | Comma | Yes |
| *ced-4(n1162) ced-9(n2812)* | *ced-9(n2812)* | *ced-4(n1162) ced-9(n2812)/ + ced-9(n2812)* | ~100 cells | No |
| *ced-9(n2812)/qC1* | *ced-4(n1162) ced-9(n2812); ced-3(n717)* | *ced-4(n1162) ced-9(n2812)/ + ced-9(n2812); ced-3(n717)/ +* | Comma | Yes |

**Figure 3. *ced-9(n2812)* embryos.**

Nomarski images of arrested embryos from the matings shown in Table 1. **(A)** *ced-9(n2812)* embryo from a *ced-9(n2812)* mother **(B)** *ced-9(n2812); egl-1(n1084 n3082)* embryo **(C)** *ced-4(n1162) ced-9(n2812)/ + ced-9(n2812)* embryo derived from *ced-4(n1162) ced-9(n2812)* mother and *ced-9(n2812)/qC1* father **(D)** *ced-9(n2812); ced-3(n717)/ +* embryo derived from a *ced-9(n2812); ced-3(n717)* mother and *ced-9(n2812)/qC1* father **(E)** *ced-4(n1162) ced-9(n2812)/ + ced-9(n2812); ced-3(n717)/ +* embryo derived from *ced-4(n1162) ced-9(n2812); ced-3(n717)* mother and *ced-9(n2812)/qC1* father **(F)** *ced-4(n1162) ced-9(n2812)/ + ced-9(n2812)* embryo derived from *ced-4(n1162) ced-9(n2812)* father and *ced-9(n2812)* mother **(G)** *ced-9(n2812); ced-3(n717)/ +* embryo derived from a *ced-9(n2812); ced-3(n717)* father and *ced-9(n2812)* mother.

# Figure 3

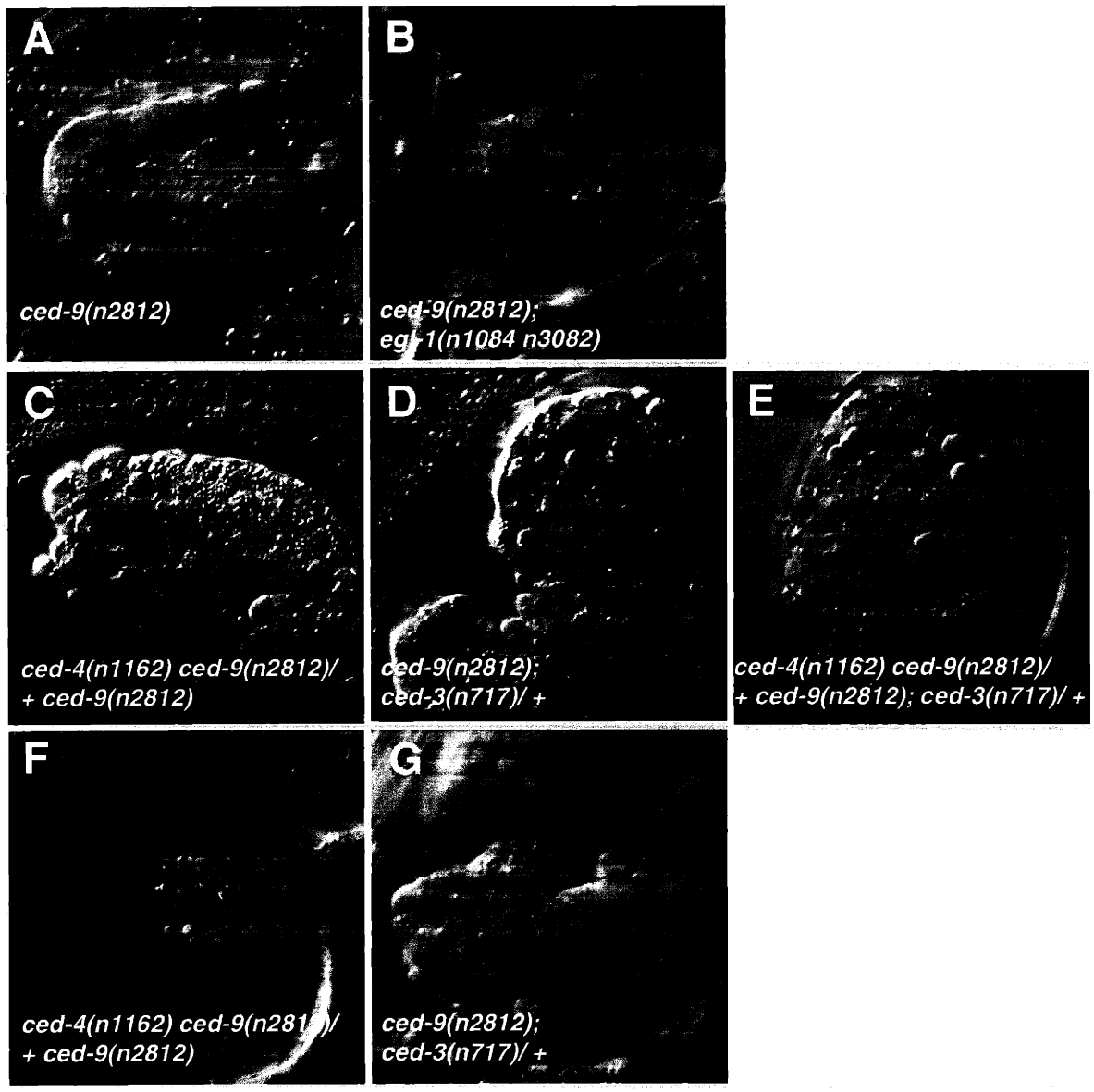
A
ced-9(n2812)
B
ced-9(n2812);
egl-1(n1084 n3082)
C
ced-4(n1162) ced-9(n2812)/
+ ced-9(n2812)
D
ced-9(n2812);
ced-3(n717)/ +
E
ced-4(n1162) ced-9(n2812)/
+ ced-9(n2812); ced-3(n717)/ +
F
ced-4(n1162) ced-9(n2812)/
+ ced-9(n2812)
G
ced-9(n2812);
ced-3(n717)/ +

## EXPRESSION AND LOCALIZATION OF CUP-5 PROTEIN

To determine the cells in which CUP-5 protein is present and where in those cells CUP-5 protein may localize, we generated fusions of the *cup-5* gene to the gene for GFP (green fluorescent protein) (Chalfie et al., 1994). A 7.6 kb AflII-KpnI genomic DNA fragment, containing 1.2 kb of sequence upstream of the EST and RACE-determined start codon and sequence encoding amino acids 1-629 of CUP-5L, was treated with Klenow DNA polymerase to blunt the ends and then cloned into GFP vectors pPD95.69 and pPD95.77 (A. Fire, unpublished) digested with MscI. Both GFP::fusion constructs were injected into *cup-5(n3194) unc-36(e251)/qC1* animals at a concentration of 50 μg/ml together with pRF4 (*rol-6* marker) at 80 μg/ml, and transgenic lines were obtained (Mello and Fire, 1995). Four lines of pPD95.69-*cup-5L* were capable of rescuing the maternal-effect lethal phenotype of *cup-5(n3194)*, and seven of eight lines of pPD95.77-*cup-5L* were likewise able to rescue.

Though the GFP moeity in pPD95.69 possesses an SV40 nuclear localization signal (NLS), no GFP expression was observed in nuclei, and the localization of both CUP-5L::GFP fusion proteins appeared identical. CUP-5L::GFP expression was most prominent in the excretory canal cell (Figure 4A), and was also observed in unidentified neurons in the head (Figure 4B) and tail, and in coelomocytes (Figure 4C). The excretory canal cell regulates osmotic balance in the worm and loss of excretory canal function appears to be responsible for *let-60*/Ras lethality in *C. elegans* (Yochem et al., 1997). CUP-5L::GFP fusions with or without the NLS were excluded from the nucleus, and appeared to be present primarily at the plasma membrane. CUP-5 protein is predicted to have at least six transmembrane domains, which would be consistent with a membrane localization.

CUP-5S::GFP is described to have a broad expression pattern in all cells of the animal, and a subcellular localization that may be consistent with lysosomal or endosomal compartments (Fares and Greenwald, 2001). Based on the different expression pattern and localization of overexpressed CUP-5S::GFP and CUP-5L::GFP fusion proteins, it is not possible to determine whether these two forms are indeed differentially expressed and localization, or whether the observed pattern of one form or the other is artifactual. To better characterize the expression and localization of CUP-5 protein, we generated rabbit polyclonal antisera directed against a peptide containing amino acids 116-133 of CUP-5. This antibody would not be able to distinguish between

CUP-5L and CUP-5S, but might provide an accurate indication of the distribution of both forms. However, the antiserum generated in this experiment produced a great deal of background staining on western blots of protein extracts from wild-type, *cup-5(n3264)*, and *cup-5(n3194)* animals (data not shown). Affinity purification against the immunizing peptide coupled to sepharose beads did not significantly reduce the background staining. Therefore, it was not possible to identify a protein band specifically recognized by the anti-peptide antisera on western blots of wild-type, but not mutant, worm extracts.

Though full-length CUP-5L protein could not be expressed as a GST fusion protein in *E. coli*, construction of additional fusion proteins may be useful for the production of CUP-5 protein for use as an antigen. Since the anti-peptide antibody did not appear to be useful for expression or localization experiments, the generation of additional antisera will be required for successful identification of the cells and subcellular compartments that contain CUP-5 protein.

**Figure 4. CUP-5L::GFP is expressed in the excretory canal cell, head neurons, and coeolomocytes.**

Confocal images **(A and B)** of CUP-5L::GFP fusion protein expression in **(A)** the excretory canal cell of two larvae and **(B)** a head neuron of an adult worm. **(C)** Epifluorescence image of CUP-5L::GFP in the midbody and posterior coelomocytes of a larva (anterior is to the left and ventral is down).

Figure 4

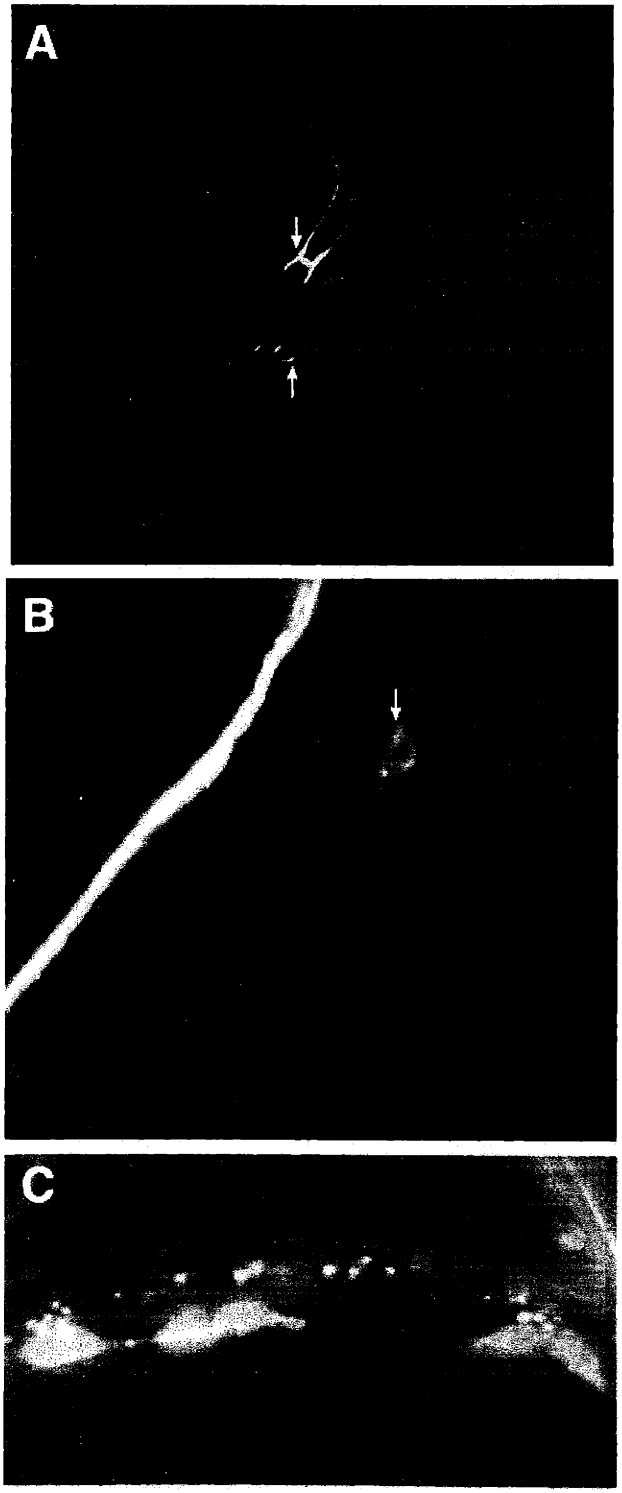

## GENETIC SCREEN FOR SUPPRESSORS OF *CUP-5(N3194)* LETHALITY

To identify additional genes that act together with *cup-5* to regulate lysosome function, we performed a genetic screen for suppressors of *cup-5(n3194)* maternal-effect lethality. The molecular lesion in *cup-5(n3194)* is a nonsense mutation converting a glutamine codon to an ochre stop codon. Mutagenized *cup-5(n3194) unc-36(e251)/qC1* animals were allowed to self-fertilize. The number of F1 non-Unc and non-Dpy animals was determined. For every F1 animal, 2 F2 Unc animals (*cup-5(n3194) unc-36(e251)* homozygotes) were transferred to individual plates, and plates were screened two days later for the presence of live progeny. From a pilot screen of approximately 700 haploid genomes, 14 candidate suppressors of *cup-5* lethality were identified. Two contained mutations unlinked to *cup-5* and conferring an Unc phenotype, and were identifiable as carriers of the *qC1* balancer chromosome. Ten candidates failed to retest and did not produce any viable progeny. A single weak suppressor produced few viable progeny and was not maintained. A single strong suppressor, *n3710*, restored viability to the strain bearing *cup-5(n3194)*. Backcrossing of this mutation to N2 wild-type animals demonstrated that *n3710* is not linked to *cup-5* on chromosome III, as 2/6 F2 Unc animals had viable progeny in the first backcross and 2/12 F2 Unc animals had viable progeny in the second backcross. The *n3710; cup-5(n3194) unc-36(e251)* strain was backcrossed to N2 a total of four times. The *n3710* mutation was introduced into a strain bearing the *cup-5(zu223)* mutation, and was capable of suppressing maternal-effect lethality in this strain. As the molecular lesion in *cup-5(zu223)* is an amber nonsense mutation, *n3710* is unlikely to be an informational suppressor capable of suppressing both an ochre and an amber nonsense mutation.

Mapping of *n3710* was attempted by two methods. The first method is the standard mapping against visible markers on each chromosome. Application of this method suggested that *n3710* was linked to chromosome IV (Table 2). However, three-factor mapping with markers on chromosome IV did not generate any recombinants that carried *n3710*, suggesting that this mutation was, in fact, unlinked to chromosome IV. The second mapping method employed snip-SNPs, single nucleotide polymorphisms that result in differences in restriction enzyme sites. Thus, both chromosomes in an animal can be followed by the presence of these polymorphisms. The *n3710; cup-5(n3194) unc-36(e251)* strain was mated to CB4856, a wild-type strain isolated from Hawaii and containing many SNPs. F2 Unc animals were transferred to

individual plates, and animals with viable progeny were presumed to carry the *n3710* suppressor mutation. Following lysis of these animals, DNA fragments containing the SNPs were amplified by PCR, and then digested with the appropriate restriction enzyme. Chromosomes linked to either *unc-36*, the selected marker in the F2 generation, or *n3710* should display only the N2 pattern of SNPs, whereas 1/4 of unlinked chromosomes should display the N2 pattern, 1/4 the CB4856 pattern, and 1/2 both N2 and CB4856 bands. As shown in Table 3, the internal control of *unc-36* gave the expected 17/17 reactions with only the N2 pattern. In this experiment, only the SNP from the chromosome II gene cluster (*pkP2107*) displayed the N2 pattern greater than 1/4 of the time. Therefore, this experiment suggested linkage of *n3710* to chromosome II, not IV. However, a marker on the far right arm of chromosome II demonstrated no linkage, and markers approximately 5 map units to the left or right of the gene cluster displayed identical linkage. Furthermore, mapping of *n3710* with respect to either *lin-31 dpy-10* or *dpy-10 rol-1* did not display any linkage to chromosome II. Thus, the two methods have given conflicting results regarding the map position of *n3710*, and neither method has generated sufficient consistent mapping data to determine an accurate position for this mutation. It is possible that *n3710* is associated with a complex chromosomal rearrangement that is confounding the mapping experiments, and might make additional mapping of this mutation equally difficult.

In an effort to identify additional suppressors of *cup-5* lethality, we generated a *cup-5* strain marked with both *unc-36* and *avr-4*, a mutation conferring ivermectin resistance. The ivermectin resistance should make screening for *cup-5* suppressors easier by allowing selection of *avr-4 cup-5 unc-36* homozygotes, rather than cumbersome identification of individual *cup-5 unc-36* homozygotes. A pilot screen of approximately 2000 haploid genomes did not identify any suppressors of *cup-5* lethality. Further screening and mapping efforts may yet successfully identify genes that act with *cup-5* to regulate lysosome function.

**Table 2. Mapping data for *n3710*, suppressor of *cup-5(n3194)* lethality**

| Chromosome | Marker | #F2 suppressed |
|---|---|---|
| I | *dpy-5* | 8/21 |
| II | *rol-6* | 5/28 |
| II | *lin-31 dpy-10* | 7/24 |
| II | *dpy-10 rol-1* | 5/23 |
| III | *unc-36* | 17/83 |
| IV | *dpy-20* | 0/19 |
| IV | *lin-1 dpy-20* | 0/10 |
| V | *dpy-11* | 11/41 |
| X | *lin-15* | 1/17 |

Mapping with visible markers was performed by mating *unc-36 cup-5(n3194)/qC1; n3710* males to hermaphrodites homozygous for the indicated visible markers. F1 animals were transferred to individual plates. Approximately one-half of F1 animals carried the *unc-36 cup-5(n3194)* chromosome. F2 Dpy Unc, Rol Unc, Muv Unc, Dpy Muv Unc, Dpy Rol Unc, or Unc animals were transferred to individual plates. Animals with viable F3 progeny were considered to be suppressed. For markers unlinked to *n3710*, 1/4 of the selected F2 animals should be suppressed. For markers linked to *n3710* less than 1/4 of the F2 animals should be suppressed.

**Table 3. SNP mapping data for *n3710***

| Chromosome | SNP marker | N2 SNP only | Heterozygous | CB4856 SNP only |
|---|---|---|---|---|
| I | *pkP1057* (0.91) | 4/18 | 12/18 | 2/18 |
| II | *pkP2107* (0.12) | 10/14 | 3/14 | 1/14 |
| II | *pkP2103* (-5.27) | 6/7 | 1/7 | 0/7 |
| II | *pkP2111* (5.50) | 7/11 | 3/11 | 1/11 |
| II | *pkP2117* (16.01) | 5/14 | 6/14 | 3/14 |
| III | *pkP3049* (-0.31) | 17/17 | 0/17 | 0/17 |
| IV | *pkP4034* (1.00) | 5/14 | 2/14 | 7/14 |
| V | *pkP5062* (0.88) | 5/18 | 7/18 | 6/18 |
| X | *pkP6110* (-0.76) | 2/18 | 10/18 | 6/18 |

SNP mapping was performed by mating CB4856 males to *unc-36 cup-5(n3194); n3710* hermaphrodites. F2 Unc animals were transferred to individual plates. F2 animals with viable progeny were selected for SNP analysis. Animals were incubated in 10 μl worm lysis buffer at 60°C for 1 hour followed by 95°C incubation for 20 minutes. One microliter of lysate was used for PCR amplification of the indicated SNP markers (map positions indicated in parentheses). Following amplification, DNA was digested with appropriate restriction enzymes to differentiate between N2 and CB4856 SNPs. Total number of animals differs between SNPs because only SNP patterns for successful amplification reactions were assessed. Markers unlinked to *cup-5(n3194)* and *n3710* should distribute as 1/4 N2 only, 1/4 CB4856 only, 1/2 heterozygous. Markers linked to *cup-5(n3194)* and *n3710* should display predominantly an N2 pattern. Chromsome III serves as an internal control for linkage to *cup-5(n3194)*. Only chromsome II SNPs display a predominance of N2 SNP DNA.

## REFERENCES


Chalfie, M., Tu, Y., Euskirchen, G., Ward, W. W., and Prasher, D. C. (1994). Green fluorescent protein as a marker for gene expression. Science *263*, 802-5.

Chen, F., Hersh, B. M., Conradt, B., Zhou, Z., Riemer, D., Gruenbaum, Y., and Horvitz, H. R. (2000). Translocation of *C. elegans* CED-4 to nuclear membranes during programmed cell death. Science *287*, 1485-9.

Fares, H., and Greenwald, I. (2001). Regulation of endocytosis by CUP-5, the *Caenorhabditis elegans* mucolipin-1 homolog. Nat. Genet. *28*, 64-8.

Hengartner, M. O., Ellis, R. E., and Horvitz, H. R. (1992). *Caenorhabditis elegans* gene *ced-9* protects cells from programmed cell death. Nature *356*, 494-9.

Hengartner, M. O., and Horvitz, H. R. (1994). Activation of *C. elegans* cell death protein CED-9 by an amino-acid substitution in a domain conserved in Bcl-2. Nature *369*, 318-20.

Mello, C., and Fire, A. (1995). DNA transformation. Methods Cell Biol *48*, 451-82.

Reddien, P. W., Cameron, S., and Horvitz, H. R. (2001). Phagocytosis promotes programmed cell death in *C. elegans*. Nature *412*, 198-202.

Shaham, S., and Horvitz, H. R. (1996). An alternatively spliced *C. elegans ced-4* RNA encodes a novel cell death inhibitor. Cell *86*, 201-8.

Yochem, J., Sundaram, M., and Han, M. (1997). Ras is required for a limited number of cell fates and not for general proliferation in *Caenorhabditis elegans*. Mol. Cell. Biol. *17*, 2716-22.